MAX-PLANCK-INSTITUT FÜR PLASMAPHYSIK

GARCHING BEI MÜNCHEN

DATA ON HEAVY ION REFLECTION

W. ECKSTEIN

IPP 9/61

Januar 1987

Die nachstehende Arbeit wurde im Rahmen des Vertrages zwischen dem Max-Planck-Institut für Plasmaphysik und der Europäischen Atomgemeinschaft über die Zusammenarbeit auf dem Gebiete der Plasmaphysik durchgeführt.

IPP 9/58 W. ECKSTEIN DATA ON HEAVY ION REFELECTION

Abstract

Backscattering of helium and heavier atoms from solid targets is investigated with the Monte-Carlo-Simulation Program TRSPlCN. Particle and energy reflection coefficients are given dependent on incident energy and angle. The report provides also data on energy and angular distributions of backscattered particles.

The report gives a collection of reflection data calculated in the last three yeary. These data are the basis for a paper publsihed in Z. Phys. B - condensed Matter 63, 471 (1986). There a description of the calculations and a discussion of the data e.g. scaling laws and a comparison with experimental data is carried out. Therefore this report provides the reader with the numerical data for the particle reflection coefficient (R_N), the energy reflection coefficient (R_E) and the relative mean energy of backscattered particles ($\overline{E}/E_o = R_E/R_N$). In addition most of the values in the tables are represented in figures some of which have appeared in the above mentioned publication. Data of energy and angular distributions shop up only in figures not in tables.

The following abbreviations are used:

Z_1, Z_2 Atomic number of the incident and target atom

M_1, M_2 Mass of the incident and target atom energy of incedent particles

ε the reduced energy of the incident particle, which is defined by

$$\varepsilon = \frac{0.8853\, a_o}{Z_1 Z_2 e^2 (Z_1^{1/2} + Z_2^{1/2})^{2/3}} \cdot \frac{M_2}{M_1 + M_2} \cdot E_o$$

where e is the elementary charge and a_o the Bohr radius

angle of incidence

R_N particle reflection coefficient, ratio of reflected to incident particles

R_E energy reflection coefficient, ratio of reflected energy to incident energy

$\overline{E}/E_o = R_E/R_N$ relative mean energy of reflected particles

ß polar emission angle of backscattered particles

azimuthal emission angle of backscattered particles

Acknowledgement

Many thanks are due to Mrs. Fritsch and Mrs. Sombach for preparing and drawing the figures.

References

/1/ W. Eckstein and J.B. Biersack, Z. Physik B 63, 471 (1986)

/2/ C. Brunnée, Z. Physik 147, 161 (1957)

/3/ J. Bøttiger and J.A. Davies, Rad. Eff. 11, 61 (1971)

/4/ J. Bøttiger, J.A. Davies, P. Sigmund and K.B. Winterbon, Rad. Eff. 11, 69 (1971)

/5/ J. Bøttiger, H. Wolder Jørgensen and K.B. Winterbon, Rad. Eff. 11, 133 (1971)

/6/ P. Sigmund, Phys. Rev. 184, 383 (1969)

Fig. 1a Particle refection coefficient, R_N, versus the reduced energy, ε, for He, C and Ne bombardment of C at normal incidence, $\alpha = 0^o$.

Fig. 1b Energy reflection coefficient, R_E, versus the reduced energy, , for He, C and Ne bombardment of C at normal incidence, $\alpha = 0^o$.

Fig. 2a Particle reflection coefficient, R_N, versus the reduced energy, ε, for He, Ne, Si and Ar bombardment of Si at normal incidence, $\alpha = 0^o$.

Fig. 2b Energy reflection coefficient, R_E, versus the reduced energy, ε, for He, Ne, Si and Ar bombardment of Si at normal incidence, $\alpha = 0^o$.

Fig. 3a Particle reflection coefficient, R_N, versus the reduced energy, ε, for He, Ne, Ar, Ni and Kr bombardment of Ni at normal incidence, $\alpha = 0^o$.

Fig. 3b Energy reflection coefficient, R_E, versus the reduced energy, ε, for He, Ne, Ar, Ni and Kr bombardment of Ni at normal incidence, $\alpha = 0^o$.

Fig. 4a Particle reflection coefficient, R_N, versus the reduced energy, ε, for He, Ne, Ar, Kr, Mo and Xe bombardment of Mo at normal incidence, $\alpha = 0^o$.

Fig. 4b Energy reflection coefficient, R_E, versus the reduced energy, ε, for He, Ne, Ar, Kr, Mo and Xe bombardment of Mo at normal incidence, $\alpha = 0^o$.

Fig. 5a Particle reflection coefficient, R_N, versus the reduced energy, ε, for He, Ne, Ar, Kr, Xe, Rn and U bombardment of U at normal incidence, $\alpha = 0^o$.

Fig. 5b Energy reflection coefficient, R_E, versus the reduced energy, ε, for He, Ne, Ar, Kr, Xe, Rn and U bombardment of U at normal incidence, $\alpha = 0^o$.

Fig. 5c The relative mean energy, $\overline{E}/E_o$, versus the reduced energy, ε, for He, Ne, Ar, Kr, Xe, Rn and U bombardment of U at normal incidence, $\alpha = 0^o$.

Fig. 6a Particle reflection coefficient, R_N, versus the mass ratio, M_2/M_1, for different reduced energies, ε, at normal incidence, $\alpha = 0^o$.

Fig. 6b Energy reflection coefficient, R_E, versus the mass ratio, M_2/M_1, for different reduced energies, ε, at normal incidence, $\alpha = 0^o$.

Fig. 7a Lines of equal particle reflection coefficients, R_N, versus the reduced energy, ε, and the mass ratio, M_2/M_1.

Fig. 7b Lines of equal energy reflection coefficents, R_E, versus the reduced energy, ε, and the mass ratio, M_2/M_1.

Fig. 8 Comparison of calculated and experimental /2,3/ data of the particle reflection coefficient, R_N, for different ion-target combinations and normal incidence, $\alpha = 0^o$.

Fig. 9 Comparison of calculated and theoretical /4/ data of the particle reflection coefficent for $\varepsilon = 0.2$ and $\alpha = 0^{o}$. The hatched area orginates from the use of different potentials in the analytical calculations /4/.

Fig. 10a Particle (R_N) and energy (R_E) reflection coefficients versus the reduced energy, ε, for a mass ratio, $M_2/M_1 = 2.4$ and normal incidence, $\alpha = 0^{o}$. The three examples chosen are the bombardment of Ti by Ne, Mo by Ar and Hg by Kr.

Fig. 10b Particle (R_N) and energy (R_E) reflection coefficients versus the reduced energy, ε, for a mass ratio, $M_2/M_1 = 1.81$ and normal incidence, $\alpha = 0^{o}$. The three examples chosen are the bombardment of Ge by Ar, Sm by Kr and U by Xe.

Fig. 10c Particle (R_N) and energy (R_E) reflection coefficients versus the reduced energy, ε, for a mass ratio, $M_2/M_1 = 0.70$ and normal incidence, $\alpha = 0^{o}$. The three examples chosen are the bombardment of Si by Ar, Ni by Kr and Zr by Xe.

Fig. 11 Particle (R_N) and energy (R_E) reflection coefficients versus the reduced energy, ε, for a mass ratio, $M_2/M_1 = 6$ and normal incidence, $\alpha = 0^{o}$. The bombardment of U by Ar and Mo by O is investigated. The influence of a binding of O to the Mo-surface is shown for different binding energies (planar surface binding potential), $E_s = 0, 4, 7.89, 12$ eV.

Fig. 12 Comparison of calculated and experimental /5/ data of the particle reflection coefficient, R_N, versus the angle of incidence, α, for 30 keV ^{24}Na and ^{42}K bombardment of Ag and Au.

Fig. 13 Comparison of calculated and theoretical /6/ data of the particle reflection coefficient, R_N, versus the angle of incidence, α, for a reduced energy, $\varepsilon = 0.0208$. Ni is bombarded by 1 keV Ne, U by 17.93 keV Kr.

Fig. 14a Particle (R_N) and energy (R_E) reflection coefficients versus the angle of incidence, α, at a fixed reduced energy, $\varepsilon = 0.1$, and mass ratio, $M_2/M_1 = 2.4$. The three examples chosen are the bombardment of Ti by Ne, Mo by Ar, and Hg by Kr.

Fig. 14b Particle (R_N) and energy (R_E) reflection coefficients versus the angle of incidence, α, at a fixed reduced energy, $\varepsilon = 10^{-2}$, and mass ratio, $M_2/M_1 = 2.4$. The three examples chosen are the bombardment of Ti by Ne, Mo by Ar, and Hg by Kr.

Fig. 14c Particle (R_N) and energy (R_E) reflection coefficients versus the angle of incidence, α, at a fixed reduced energy, $\varepsilon = 10^{-3}$, and mass ratio, $M_2/M_1 = 2.4$. The three examples chosen are the bombardment of Ti by Ne, Mo by Ar, and Hg by Kr.

Fig. 15a Angular distributions of backscattered particles versus the cosine of the polar emission angle, ß, at a fixed reduced energy, $\varepsilon = 0.1$, a mass ratio, $M_2/M_1 = 2.4$, and four angles of incidence, $\alpha = 30^o, 45^o, 60^o, 75^o$ (integrated over the azimuthal angle, φ). The three examples chosen are the bombardment of Ti by Ne, Mo by Ar, and Hg by Kr. The straight line indicates a cosine distribution.

Fig. 15b Angular distributions of backscattered particles versus the cosine of the polar emission angle, ß, at a fixed reduced energy, $\varepsilon = 10^{-2}$, a mass ratio, $M_2/M_1 = 2.4$, and four angles of incidence, $\alpha = 30^o, 45^o, 60^o, 75^o$ (integrated over the azimuthal angle, φ). The three examples chosen are the bombardment of Ti by Ne, Mo by Ar, and Hg by Kr. The straight line indicates a cosine distribution.

Fig. 15c Angular distributions of backscattered particles versus the cosine of the polar emission angle, ß, at a fixed reduced energy, $\varepsilon = 10^{-3}$, a mass ratio, $M_2/M_1 = 2.4$, and four angles of incidence, $\alpha = 30^o, 45^o, 60^o, 75^o$ (integrated over the azimuthal angle, φ). The three examples chosen are the bombardment of Ti by Ne, Mo by Ar, and Hg by Kr. The straight line indicates a cosine distribution.

Fig. 16a Complete angular distributions of backscattered particles for an angle of incidence, $\quad = 0^{o}$. Ni was bombarded by 1 keV Ar. The contour line plot shows lines of equal intensity per solid angle. The distance, c = 0.13 between adjacent contour-lines is logarithmic.

Fig. 16b Complete angular distributions of backscattered particles for an angle of incidence, $\quad = 30^{o}$. Ni was bombarded by 1 keV Ar. The contour line plot shows lines of equal intensity per solid angle. The distance, c = 0.13 between adjacent contour-lines is logarithmic.

Fig. 16c Complete angular distributions of backscattered particles for an angle of incidence, $\quad = 45^{o}$. Ni was bombarded by 1 keV Ar. The contour line plot shows lines of equal intensity per solid angle. The distance, c = 0.14, between adjacent contour-lines is logarithmic.

Fig. 16d Complete angular distributions of backscattered particles for an angle of incidence, $\quad = 60^{o}$. Ni was bombarded by 1 keV Ar. The contour line plot shows lines of equal intensity per solid angle. The distance, c = , between adjacent contour-lines is logarithmic.

Fig. 16e Complete angular distributions of backscattered particles for an angle of incidence, $\quad = 75^{o}$. Ni was bombarded by 1 keV Ar. The contour line plot shows lines of equal intensity per solid angle. The distance, c = 0.20, between adjacent contour-lines is logarithmic.

Fig. 17 Energy distributions of backscattered particles for a fixed reduced energy, $\quad = 0.1$, and normal incidence, $\quad = 0^{o}$. The four examples are

7.498 keV Ar $\longrightarrow$ Si, $\quad M_2/M_1 = 0.703$

11.71 keV Ar $\longrightarrow$ Ni, $\quad M_2/M_1 = 1.47$

16.01 keV Ar $\longrightarrow$ Mo, $\quad M_2/M_1 = 2.40$

34.27 keV Ar $\longrightarrow$ U, $\quad M_2/M_1 = 5.96$

Fig. 18 Energy distributons of backscattered particles for a fixed incident energy, E_o = 1 keV, and normal incidence, $\alpha = 0^o$. The four examples are

Ar → Si	$M_2/M_1 = 0.703$
Ar → Ni	$M_2/M_1 = 1.47$
Ar → Mo	$M_2/M_1 = 2.40$
Ar → U	$M_2/M_1 = 5.96$

Fig. 19a Energy distributions of backscattered particles for a fixed incident energy, E_o = 1 keV, and normal incidence, $\alpha = 0^o$. The three examples are

He → U	$M_2/M_1 = 59.52$
Ar → U	$M_2/M_1 = 5.96$
Xe → U	$M_2/M_1 = 1.81$

Fig. 19b Energy distributions of backscattered particles for a fixed incident energy, E_o = 1 keV, and normal incidence, $\alpha = 0^o$. The three examples are

Ne → U	$M_2/M_1 = 11.80$
Kr → U	$M_2/M_1 = 2.84$
Rn → U	$M_2/M_1 = 1.07$

Fig. 20a Energy distributions of backscattered particles for a fixed reduced energy, $\varepsilon = 0.1$, a mass ratio, $M_2/M_1 = 2.4$ and normal incidence, $\alpha = 0^o$. The three examples are the bombardment of Ti by Ne, Mo by Ar, and Hg by Kr. The upper histograms represent ratios of the energy distributions (bottom), where the Ar/Mo example was used for normalization.

Fig. 20b Energy distributions of backscattered particles for a fixed reduced energy, $\varepsilon = 10^{-2}$, a mass ratio, $M_2/M_1 = 2.4$ and normal incidence, $\alpha = 0^o$. The three examples are the bombardment of Ti by Ne, Mo by Ar, and Hg by Kr. The upper histograms represent ratios of the energy distributions (bottom), where the Ar/Mo example was used for normalization.

Fig. 20c Energy distributions of backscattered particles for a fixed reduced energy, $\varepsilon = 10^{-3}$, a mass ratio, $M_2/M_1 = 2.4$ and normal incidence, $\alpha = 0^{\circ}$. The three examples are the bombardment of Ti by Ne, Mo by Ar, and Hg by Kr. The upper histrograms represent ratios of the energy distributions (bottom), where the Ar/Mo example was used for normalization.

Fig. 21 Normalized energy distributions of backscattered particles for Ni bombarded by 1 keV Ar. The dependence of the energy distributions on the angle of incidence, α, is shown for $\alpha = 30^{\circ}$, 45°, 60°, 70°, 75°. For normal incidence, $\alpha = 0^{\circ}$, the energy distribution is similar to the distribution at $\alpha = 30^{\circ}$.

Fig. 22a Intensity distributions of backscattered particles versus the energy of the backscattered particles and the cosine of the polar emission angle, ß, in the forward direction ($-15^{\circ} < \varphi < 15^{\circ}$). Ni is bombarded by 1 keV ar at an angle of incidence, $\alpha = 0^{\circ}$. The contour plot shows lines of equal intensity per solid angle. The distance, c = 0.11, between adjacent contour lines is logarithmic.

Fig. 22b Intensity distributions of backscattered particles versus the energy of the backscattered particles and the cosine of the polar emission angle, ß, in the forward direction ($-15^{\circ} < \varphi < 15^{\circ}$). Ni is bombarded by 1 keV ar at an angle of incidence, $\alpha = 30^{\circ}$. The contour plot shows lines of equal intensity per solid angle. The distance, c = 0.11, between adjacent contour lines is logarithmic.

Fig. 22c Intensity distributions of backscattered particles versus the energy of the backscattered particles and the cosine of the polar emission angle, ß, in the forward direction ($-15^{\circ} < \varphi < 15^{\circ}$). Ni is bombarded by 1 keV ar at an angle of incidence, $\alpha = 45^{\circ}$. The contour plot shows lines of equal intensity per solid angle. The distance, c = 0.12, between adjacent contour lines is logarithmic.

Fig. 22d Intensity distributions of backscattered particles versus the energy of the backscattered particles and the cosine of the polar emission angle, ß, in the forward direction ($-15^{o} < /\varphi < 15^{o}$). Ni is bombarded by 1 keV Ar at an angle of incidence, $\alpha = 60^{o}$. The contour plot shows lines of equal intensity per solid angle. The distance, c = 0.13, between adjacent contour lines is logarithmic.

Fig. 22e Intensity distributions of backscattered particles versus the energy of the backscattered particles and the cosine of the polar emission angle, ß, in the forward direction ($-15^{o} < \varphi < 15^{o}$). Ni is bombarded by 1 keV ar at an angle of incidence, $\alpha = 75^{o}$. The contour plot shows lines of equal intensity per solid angle. The distance, c = 0.18, between adjacent contour lines is logarithmic.

Fig. 23a Intensity distributions of backscattered particles versus the relative energy of the backscattered particles and the cosine of the polar emission angle, ß, in an azimuthal direction, $15^{o} < /\varphi/ < 30^{o}$. Ni is bombarded by 1 keV Ar at an angle of incidence, $\alpha = 60^{o}$. The contour plot shows lines of equal intensity per solid angle. The distance, c = 0.11, between adjacent contour lines is logarithmic.

Fig. 23b Intensity distributions of backscattered particles versus the relative energy of the backscattered particles and the cosine of the polar emission angle, ß, in an azimuthal direction, $45^{o} < /\varphi/ < 60^{o}$. Ni is bombarded by 1 keV Ar at an angle of incidence, $\alpha = 60^{o}$. The contour plot shows lines of equal intensity per solid angle. The distance, c = 0.12, between adjacent contour lines is logarithmic.

Fig. 23c Intensity distributions of backscattered particles versus the relative energy of the backscattered particles and the cosine of the polar emission angle, ß, in an azimuthal direction, $75^{o} \leq |\varphi| \leq 90^{o}$. Ni is bombarded by 1 keV Ar at an angle of incidence, $\alpha = 60^{o}$. The contour plot shows lines of equal intensity per solid angle. The distance, c = 0.12, between adjacent contour lines is logarithmic.

Fig. 23d Intensity distributions of backscattered particles versus the relative energy of the backscattered particles and the cosine of the polar emission angle, ß, in an azimuthal direction, $105^{o} \leq |\varphi| \leq 120^{o}$. Ni is bombarded by 1 keV Ar at an angle of incidence, $\alpha = 60^{o}$. The contour plot shows lines of equal intensity per solid angle. The distance, c = 0.12, between adjacent contour lines is logarithmic.

Fig. 23e Intensity distributions of backscattered particles versus the relative energy of the backscattered particles and the cosine of the polar emission angle, ß, in an azimuthal direction, $135^{o} \leq |\varphi| \leq 150^{o}$ Ni is bombarded by 1 keV Ar at an angle of incidence, $\alpha = 60^{o}$. The contour plot shows lines of equal intensity per solid angle. The distance, c = 0.12, between adjacent contour lines is logarithmic.

Fig. 23f Intensity distributions of backscattered particles versus the relative energy of the backscattered particles and the cosine of the polar emission angle, ß, in an azimuthal direction, $135^{o} \leq |\varphi| \leq 180^{o}$ Ni is bombarded by 1 keV Ar at an angle of incidence, $\alpha = 60^{o}$. The contour plot shows lines of equal intensity per solid angle. The distance, c = 0.12, between adjacent contour lines is logarithmic.

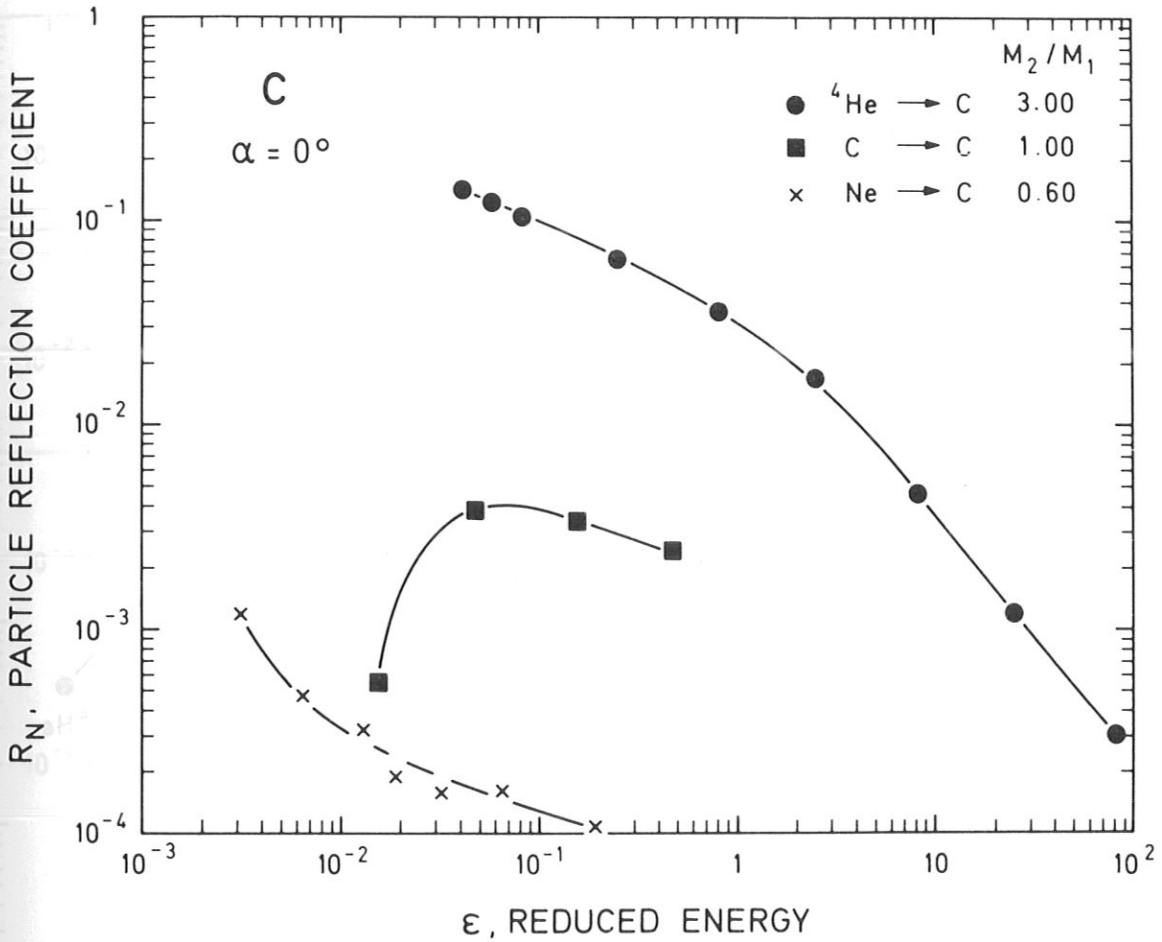

Fig. 1a Particle refection coefficient, R_N, versus the reduced energy, $\mathcal{E}$, for He, C and Ne bombardment of C at normal incidence, $\alpha = 0^{\circ}$.

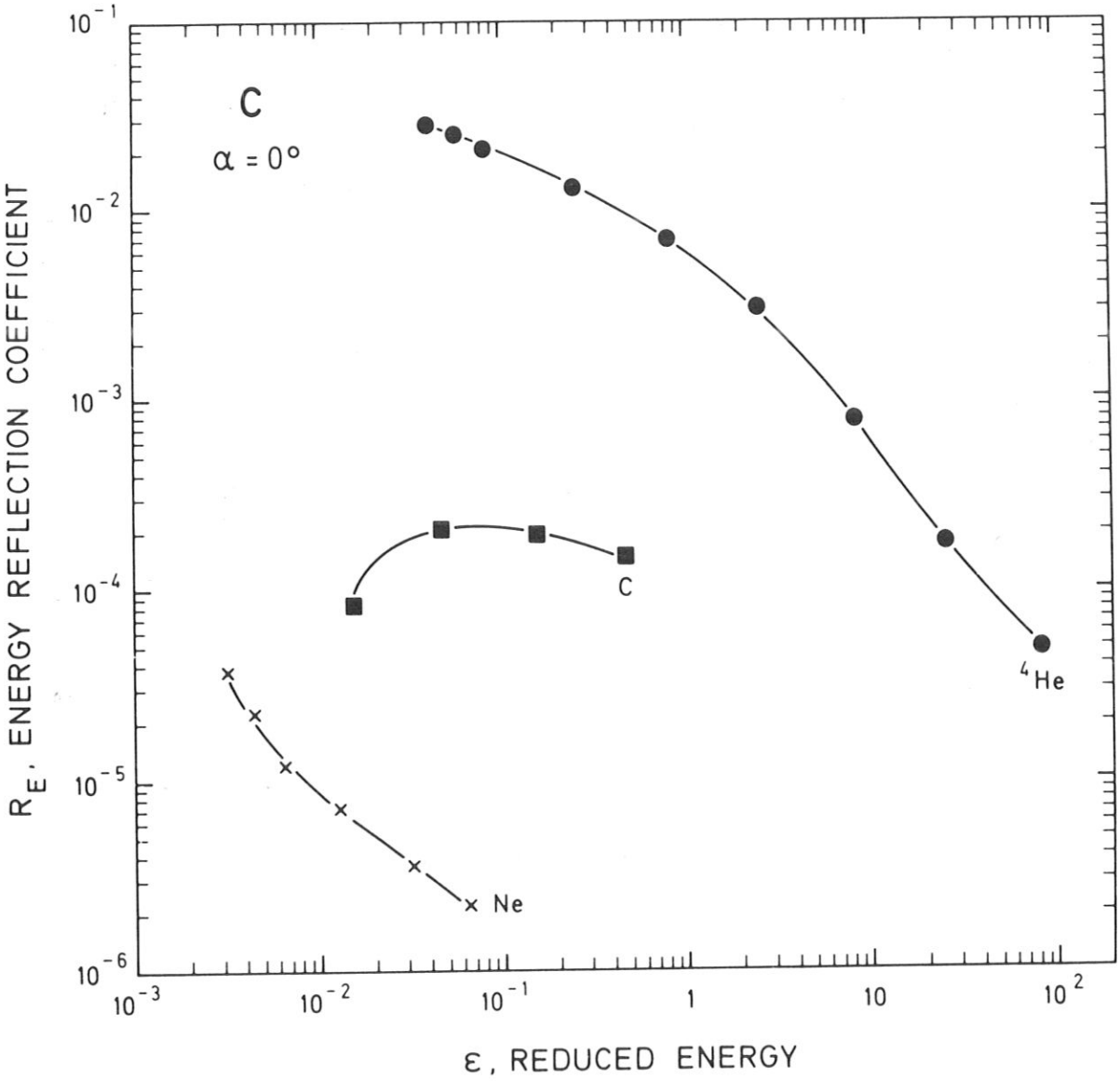

Fig. 1b Energy reflection coefficient, R_E, versus the reduced energy, ε, for He, C and Ne bombardment of C at normal incidence, $\alpha = 0^o$.

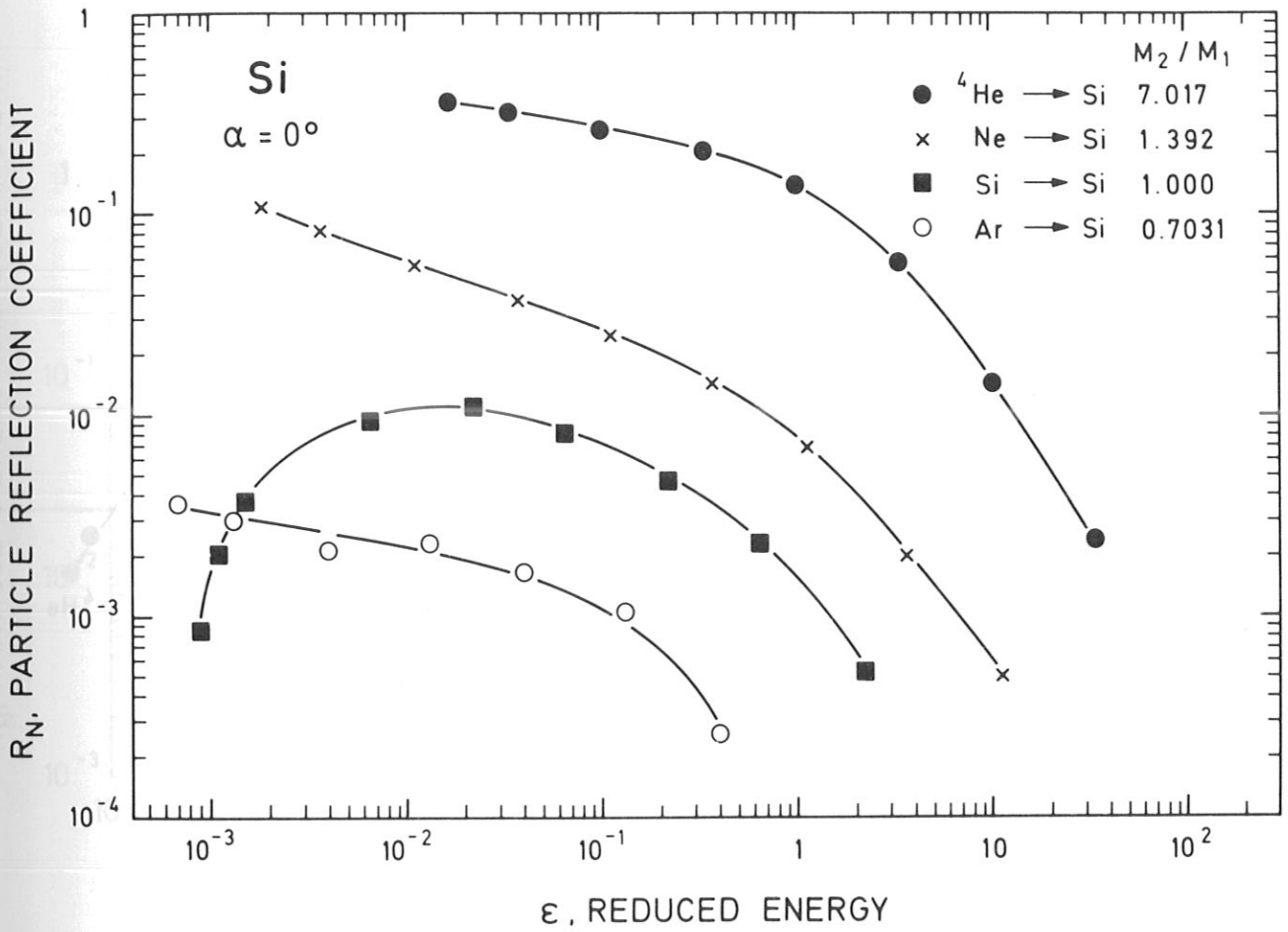

Fig. 2a Particle reflection coefficient, R_N, versus the reduced energy, ε, for He, Ne, Si and Ar bombardment of Si at normal incidence, $\alpha = 0^\circ$.

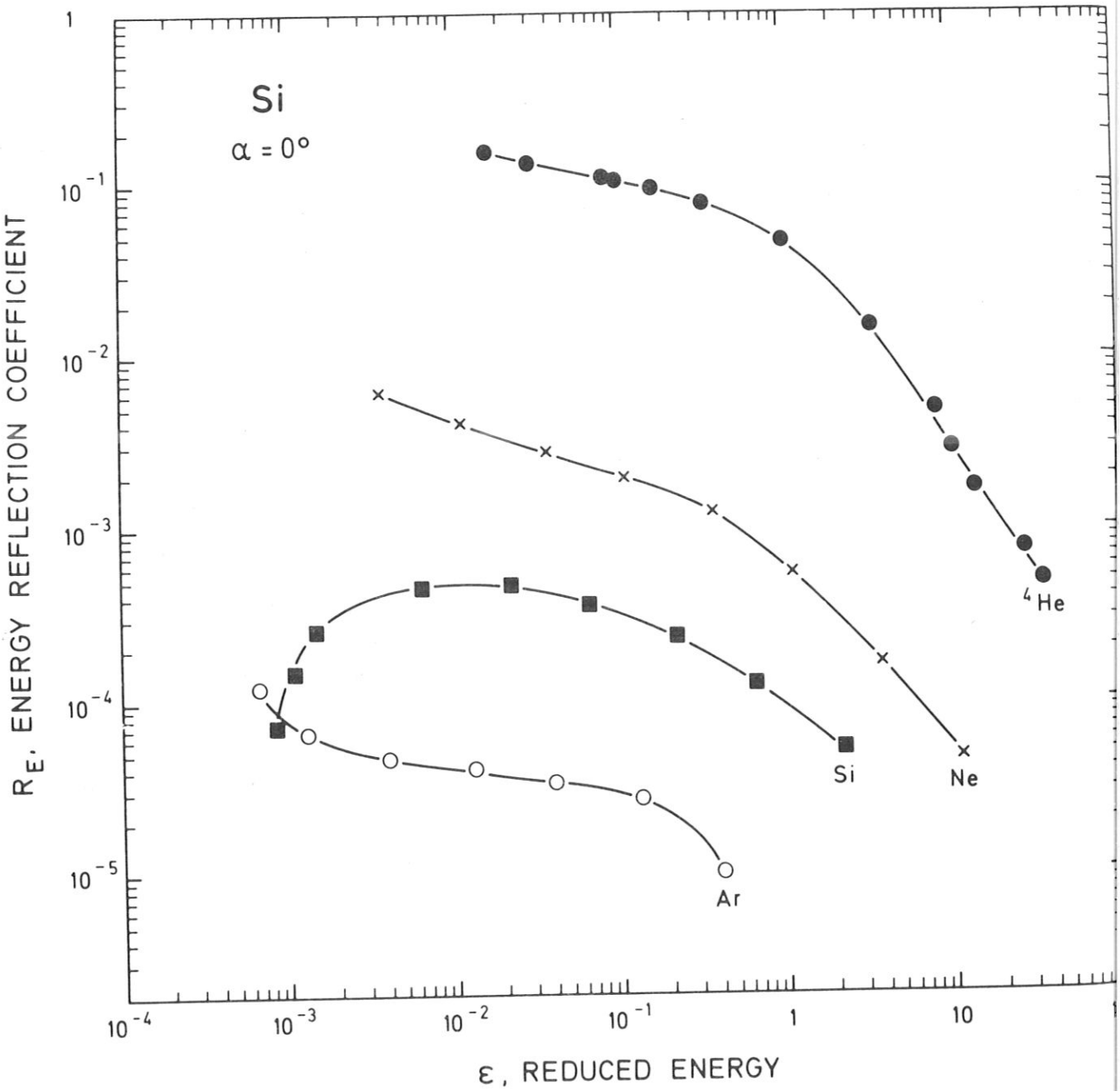

Fig. 2b Energy reflection coefficient, R_E, versus the reduced energy, ε, for He, Ne, Si and Ar bombardment of Si at normal incidence, $\alpha = 0^o$.

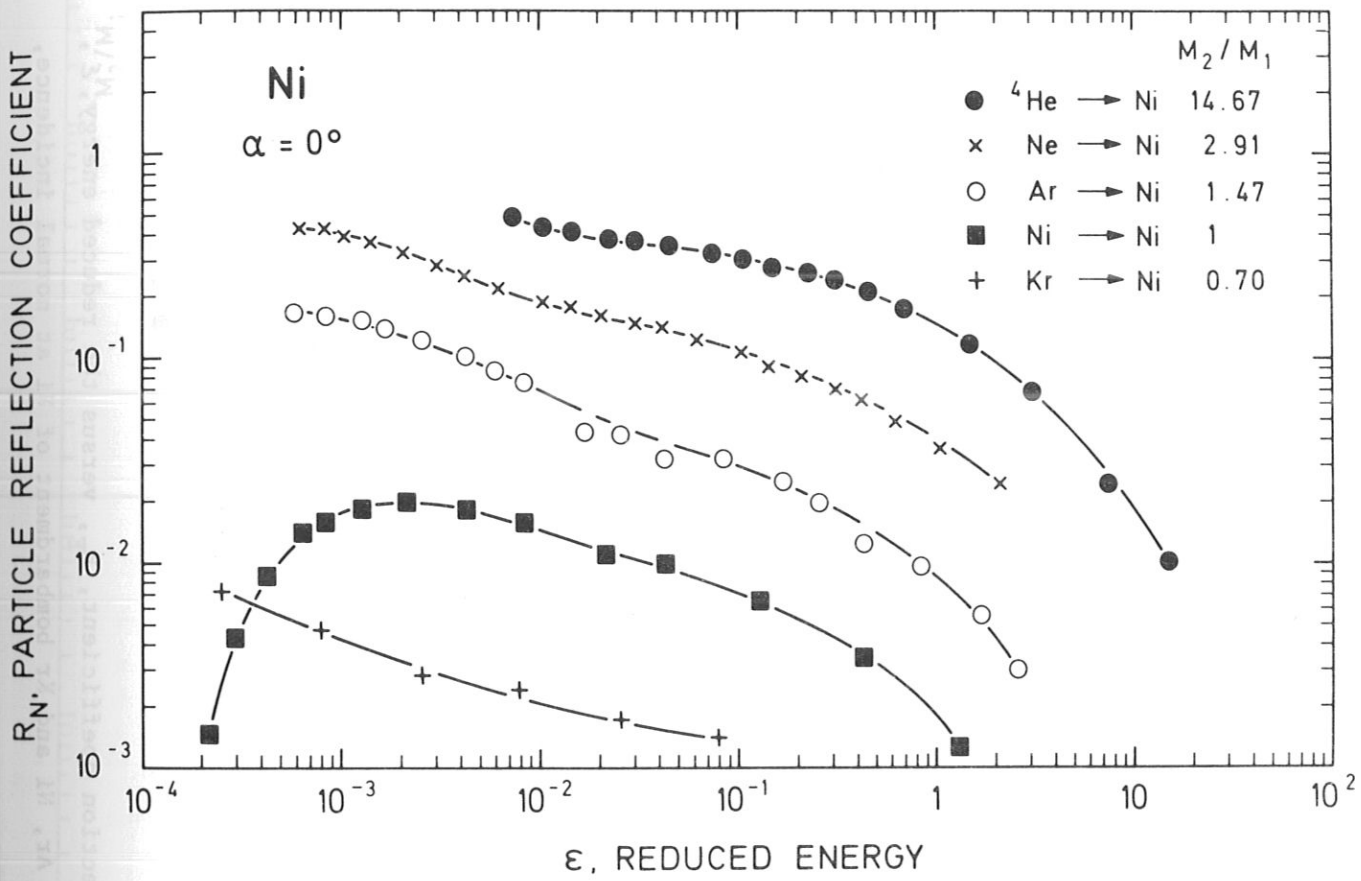

Fig. 3a Particle reflection coefficient, R_N, versus the reduced energy, ε, for He, Ne, Ar, Ni and Kr bombardment of Ni at normal incidence, $\alpha = 0^o$.

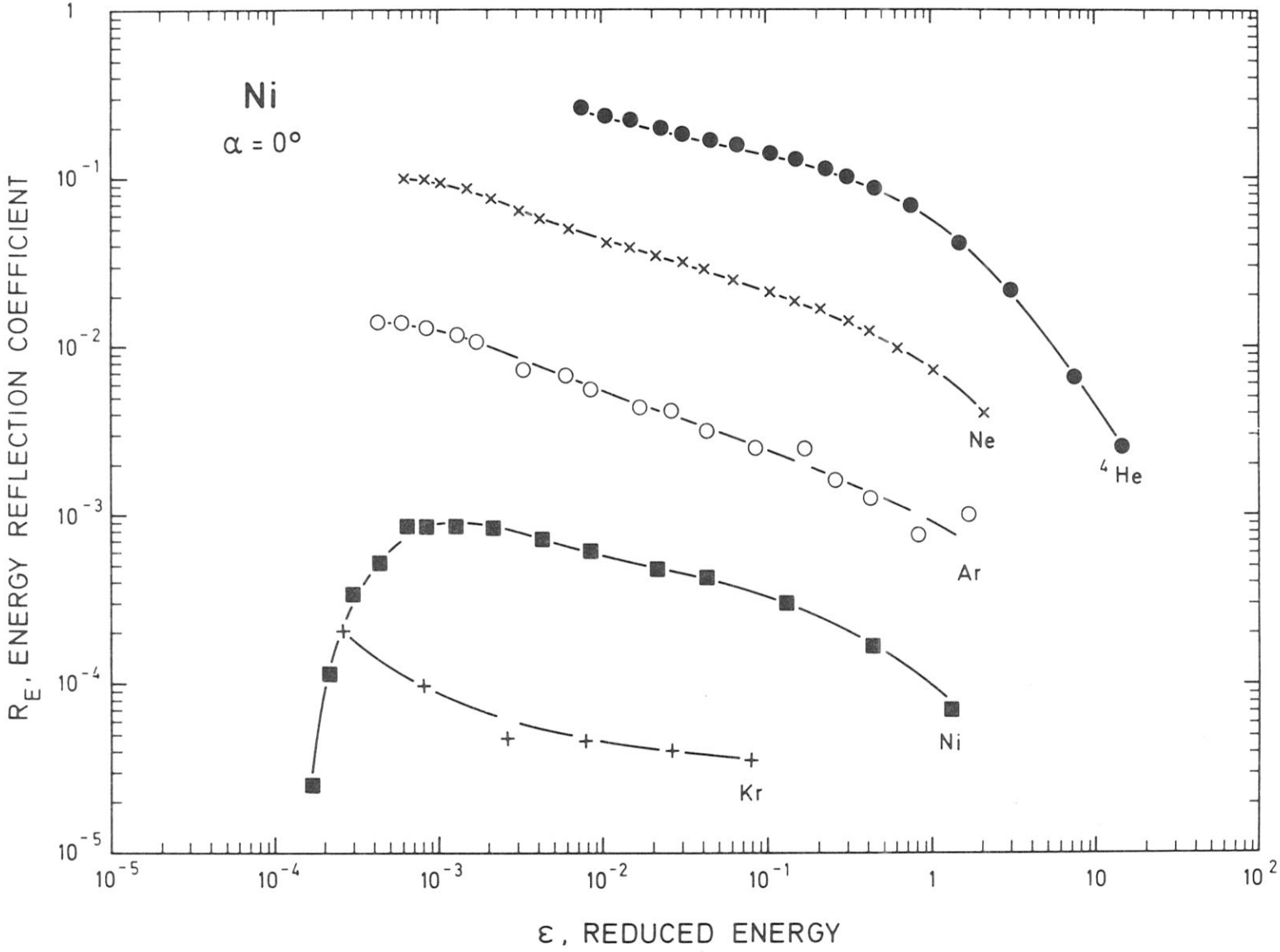

Fig. 3b Energy reflection coefficient, R_E, versus the reduced energy, ε, for He, Ne, Ar, Ni and Kr bombardment of Ni at normal incidence,

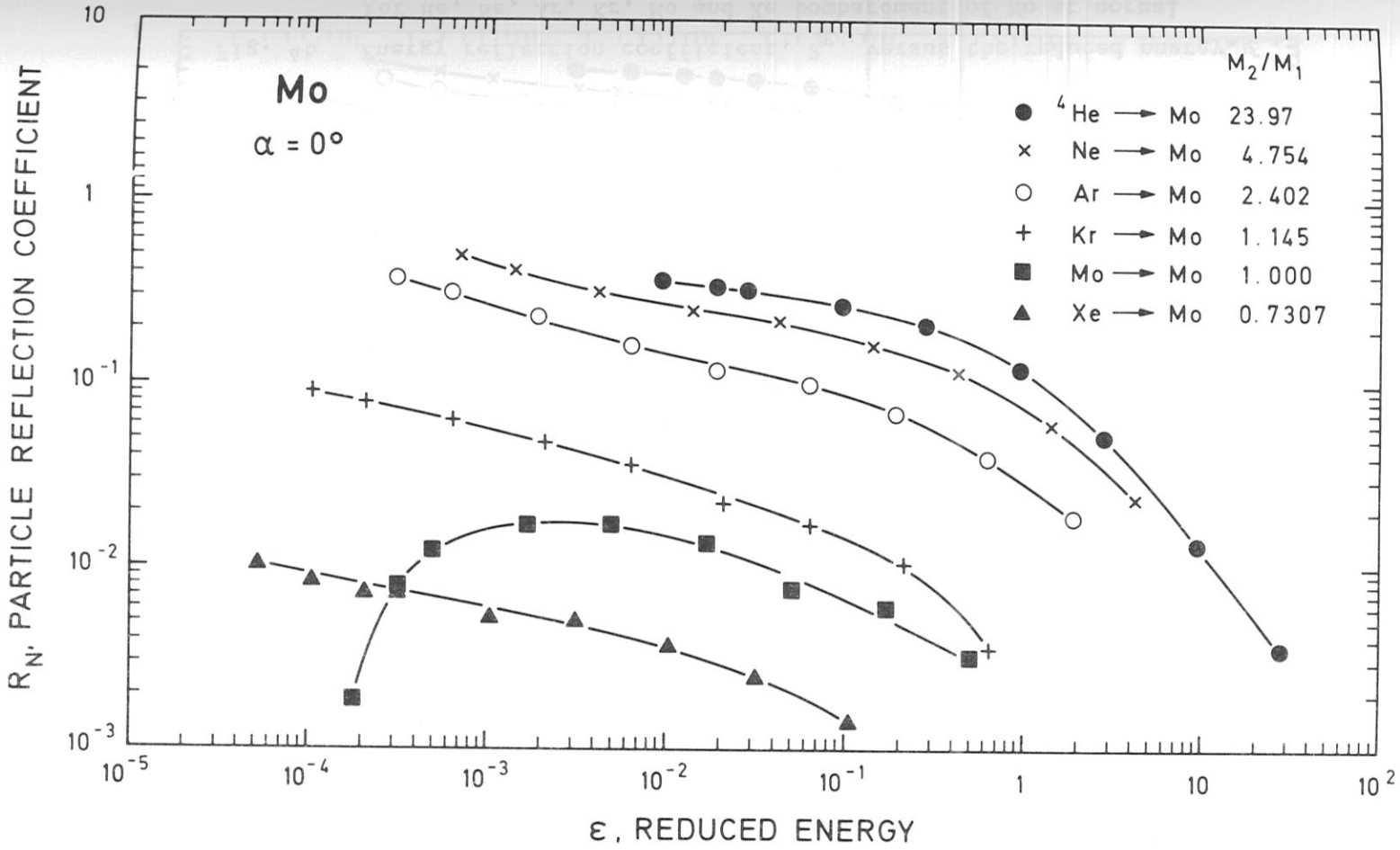

Fig. 4a Particle reflection coefficient, R_N, versus the reduced energy, ε, for He, Ne, Ar, Kr, Mo and Xe bombardment of Mo at normal incidence, $\alpha = 0^o$.

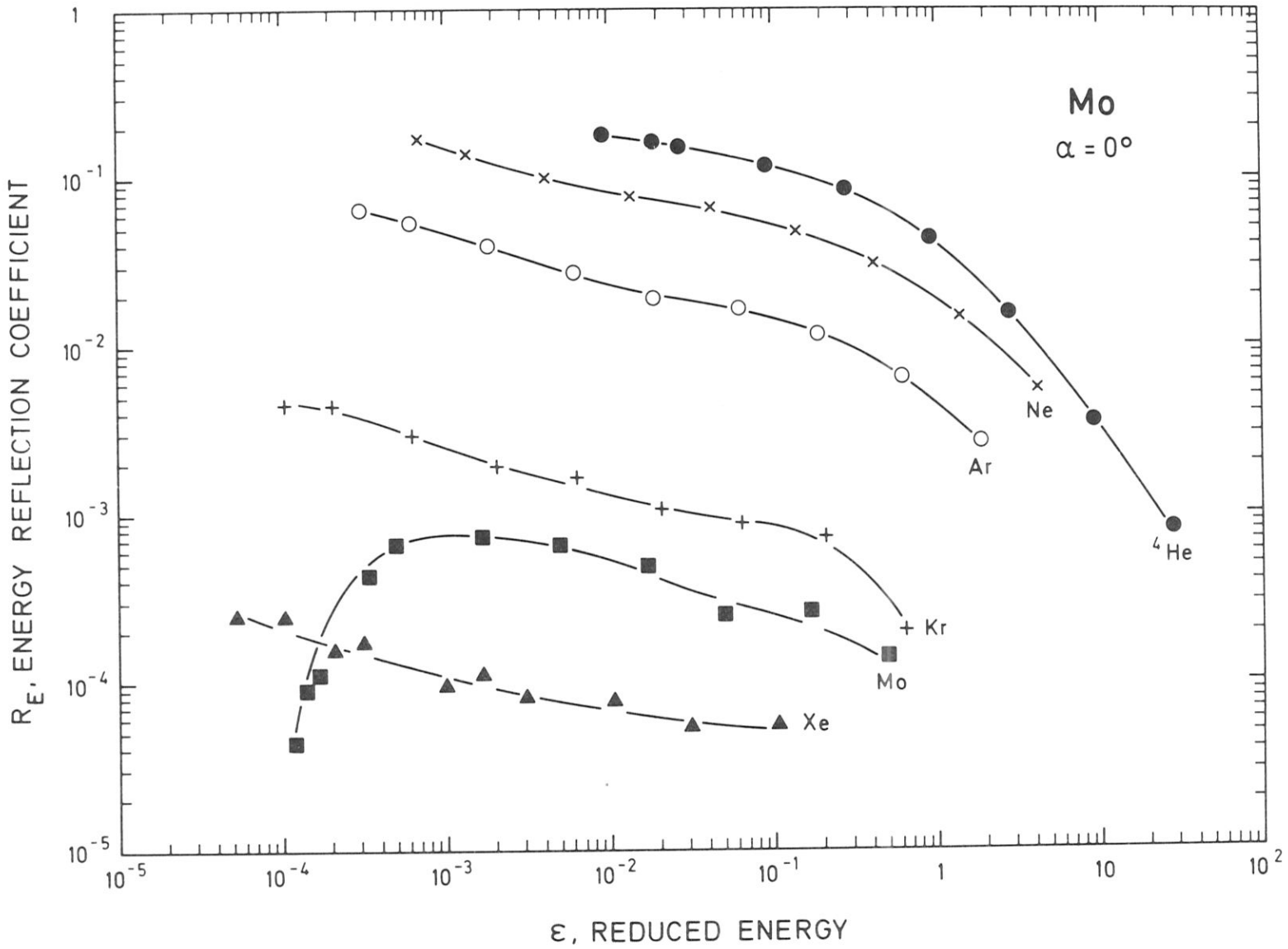

Fig. 4b Energy reflection coefficient, R_E, versus the reduced energy, ε, for He, Ne, Ar, Kr, Mo and Xe bombardment of Mo at normal

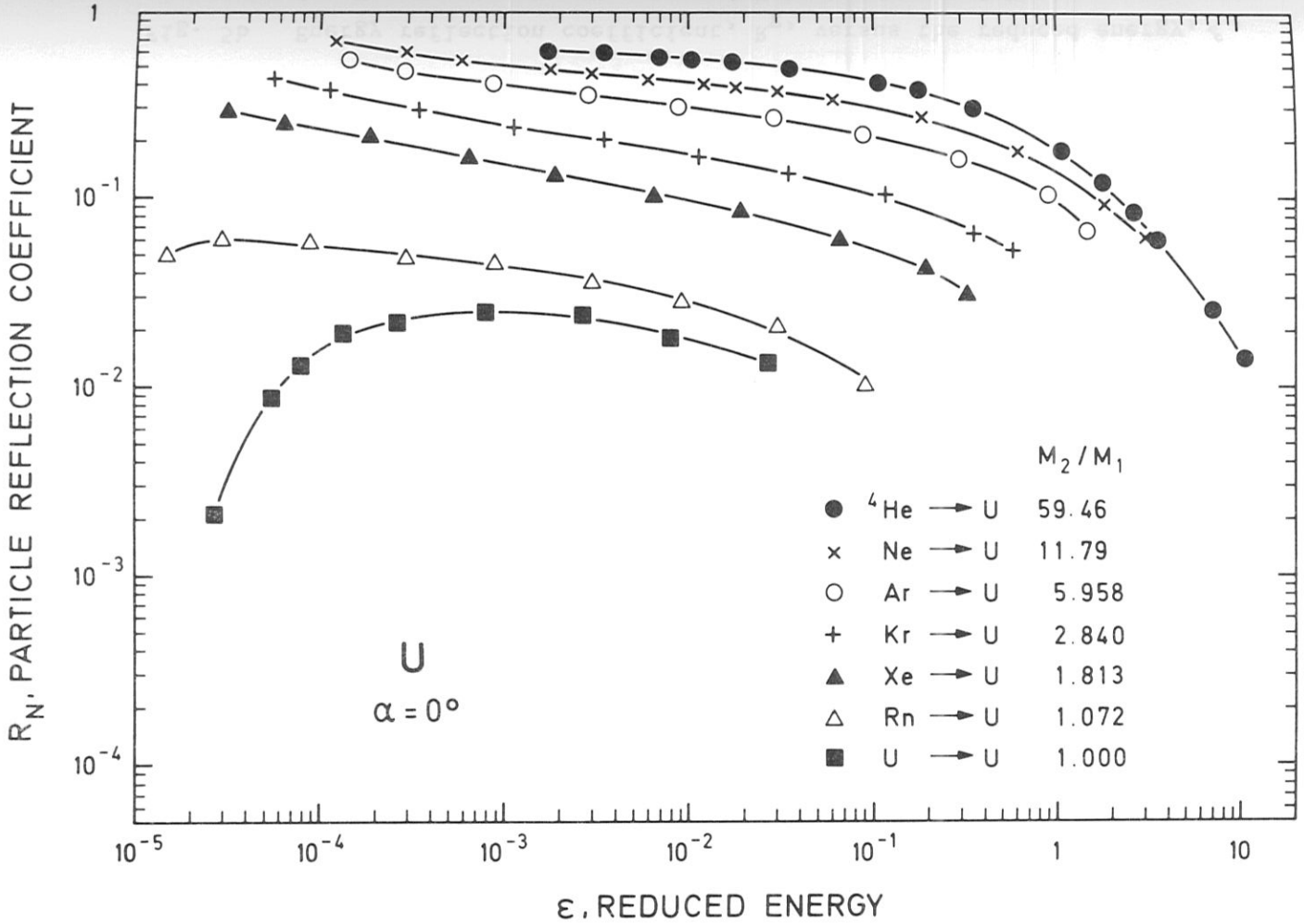

Fig. 5a Particle reflection coefficient, R_N, versus the reduced energy, ε, for He, Ne, Ar, Kr, Xe, Rn and U bombardment of U at normal incidence, $\alpha = 0^o$.

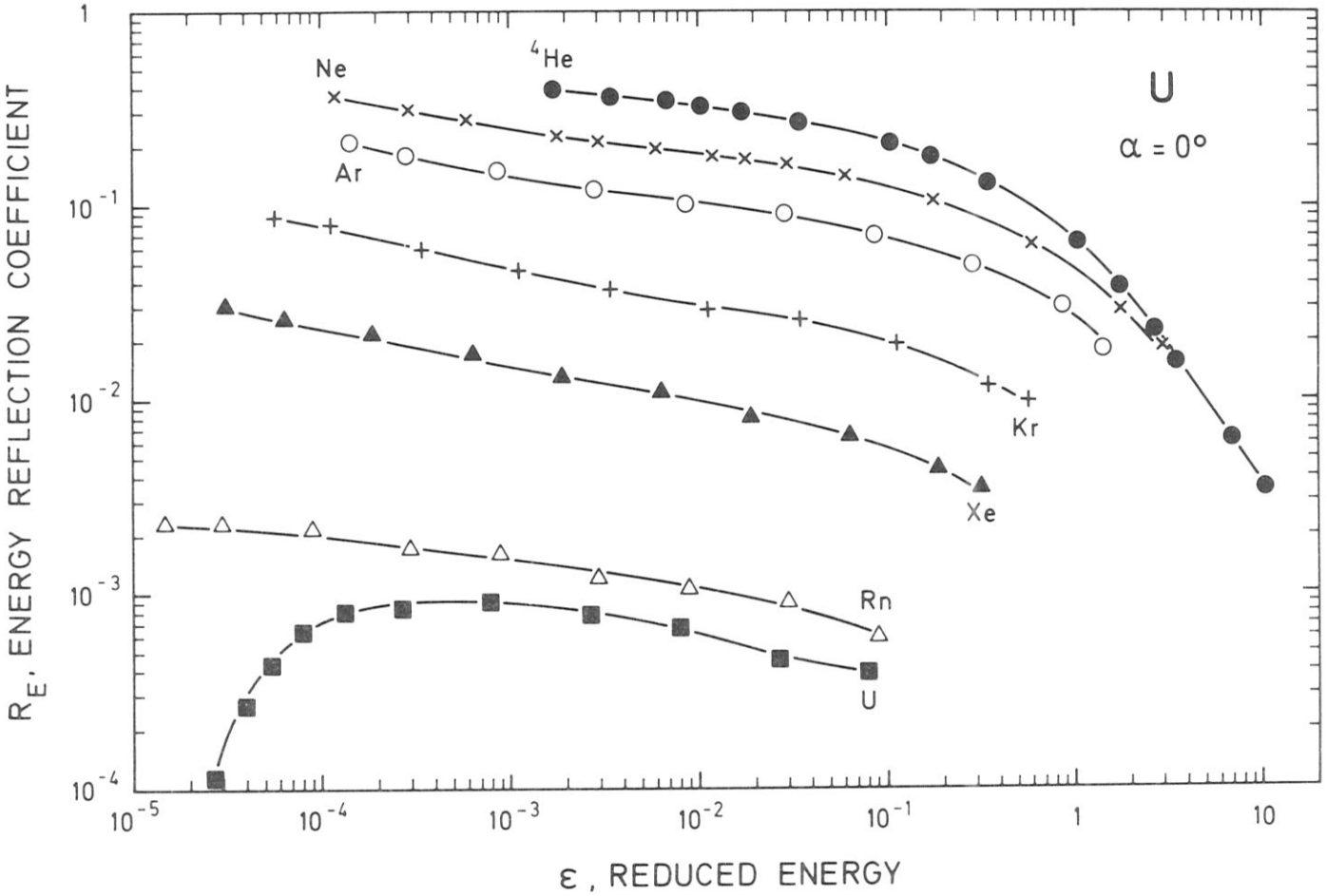

Fig. 5b Energy reflection coefficient, R_E, versus the reduced energy, ε, for He, Ne, Ar, Kr, Xe, Rn and U bombardment of U at normal

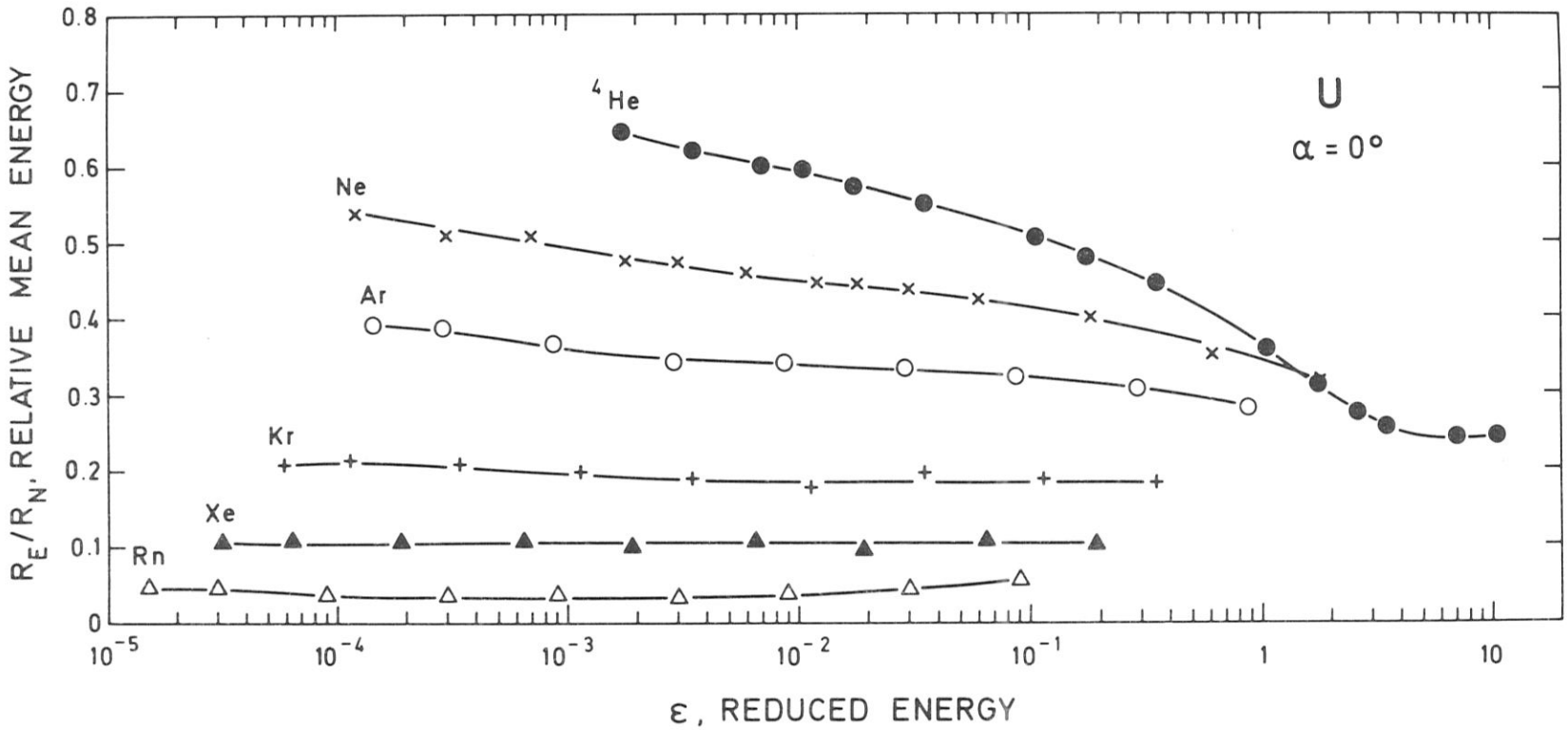

Fig. 5c The relative mean energy, $\overline{E}/E_o$, versus the reduced energy, ε, for He, Ne, Ar, Kr, Xe, Rn and U bombardment of U at normal incidence, $\alpha = 0^o$.

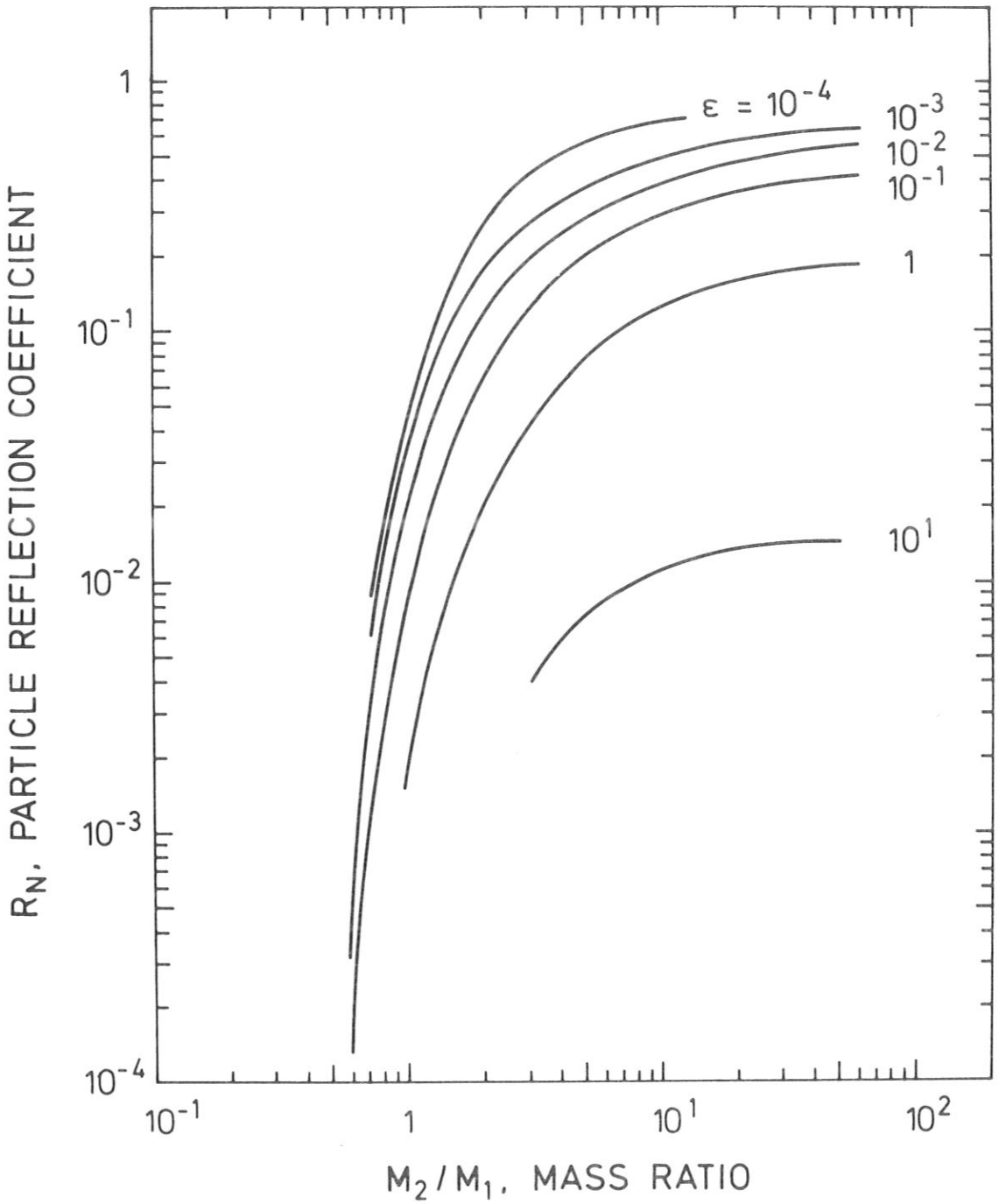

Fig. 6a Particle reflection coefficient, R_N, versus the mass ratio, M_2/M_1, for different reduced energies, ε, at normal incidence, $\alpha = 0^{\circ}$.

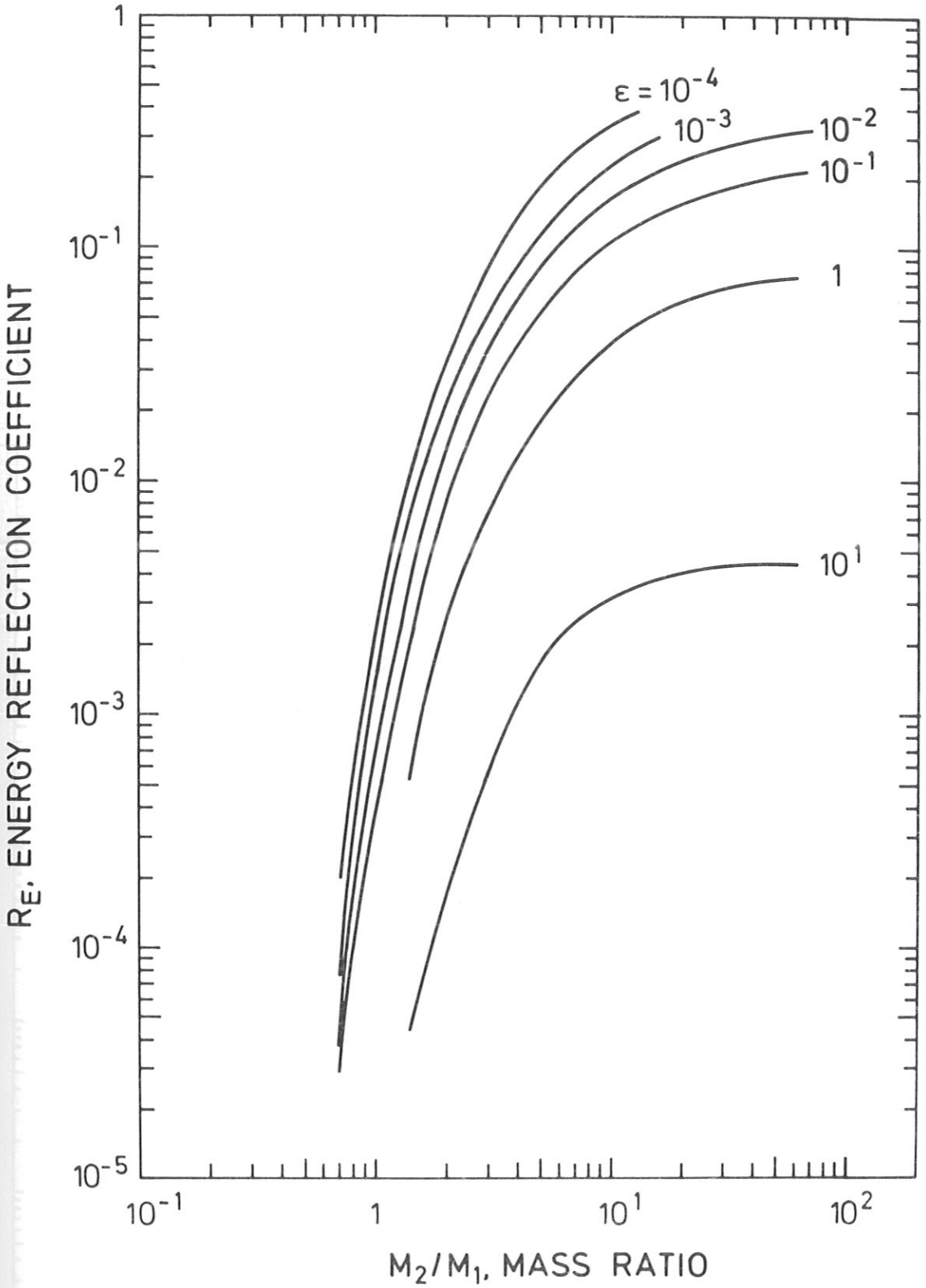

Fig. 6b Energy reflection coefficient, R_E, versus the mass ratio, M_2/M_1, for different reduced energies, ε, at normal incidence, $\alpha = 0^o$.

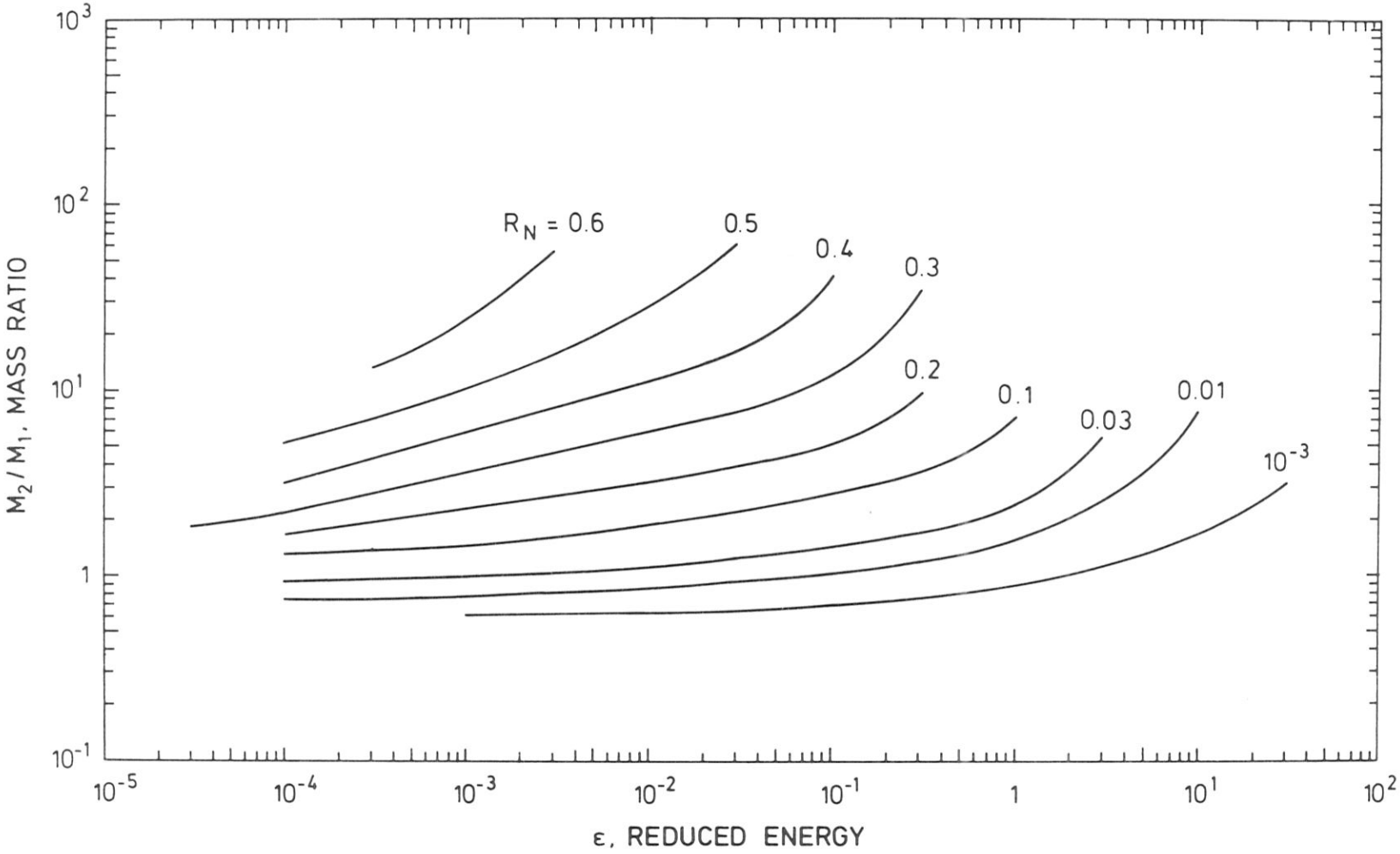

Fig. 7a Lines of equal particle reflection coefficients, R_N, versus the reduced energy, ε, and the mass ratio, M_2/M_1.

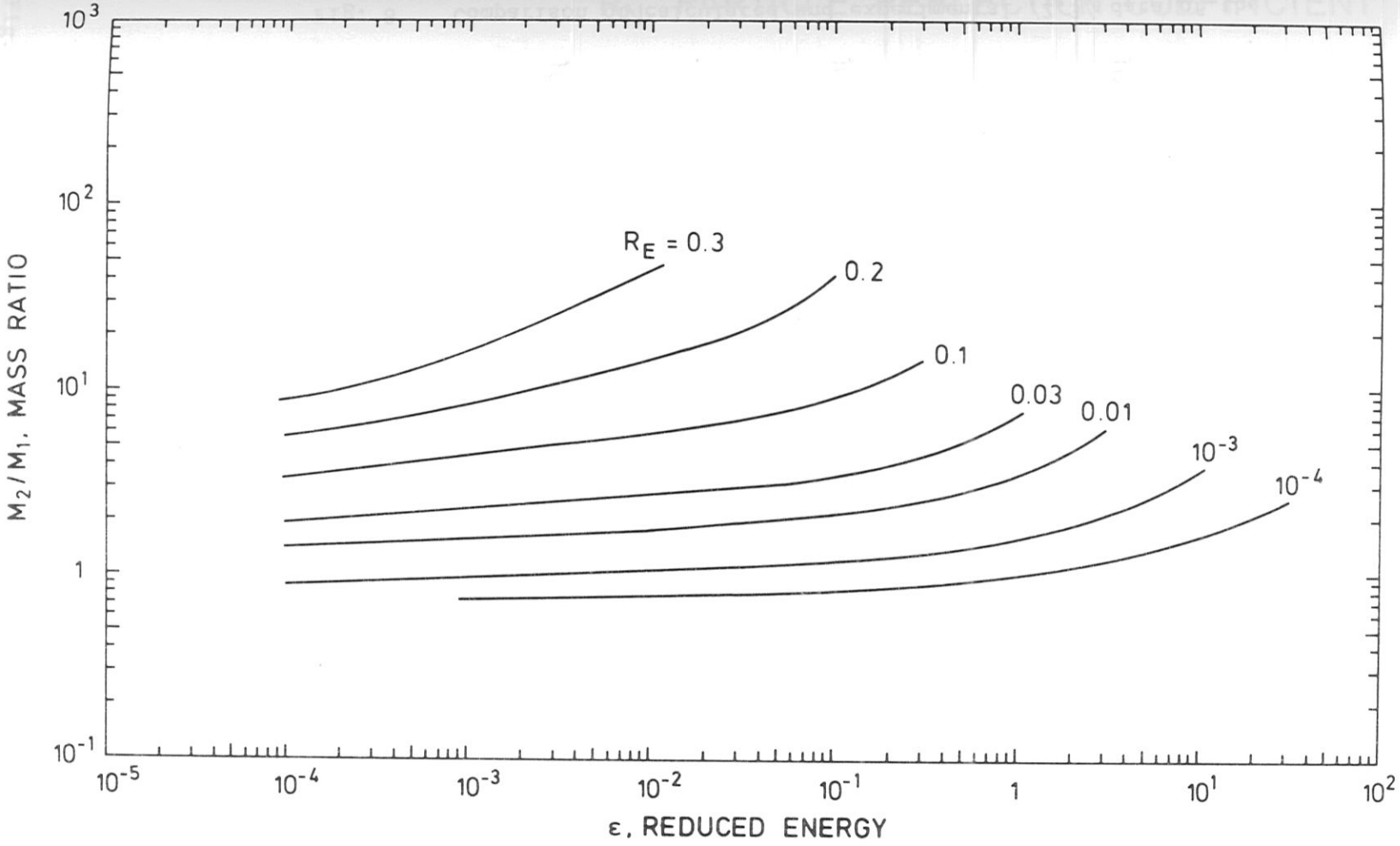

Fig. 7b Lines of equal energy reflection coefficents, R_E, versus the reduced energy, ε, and the mass ratio, M_2/M_1.

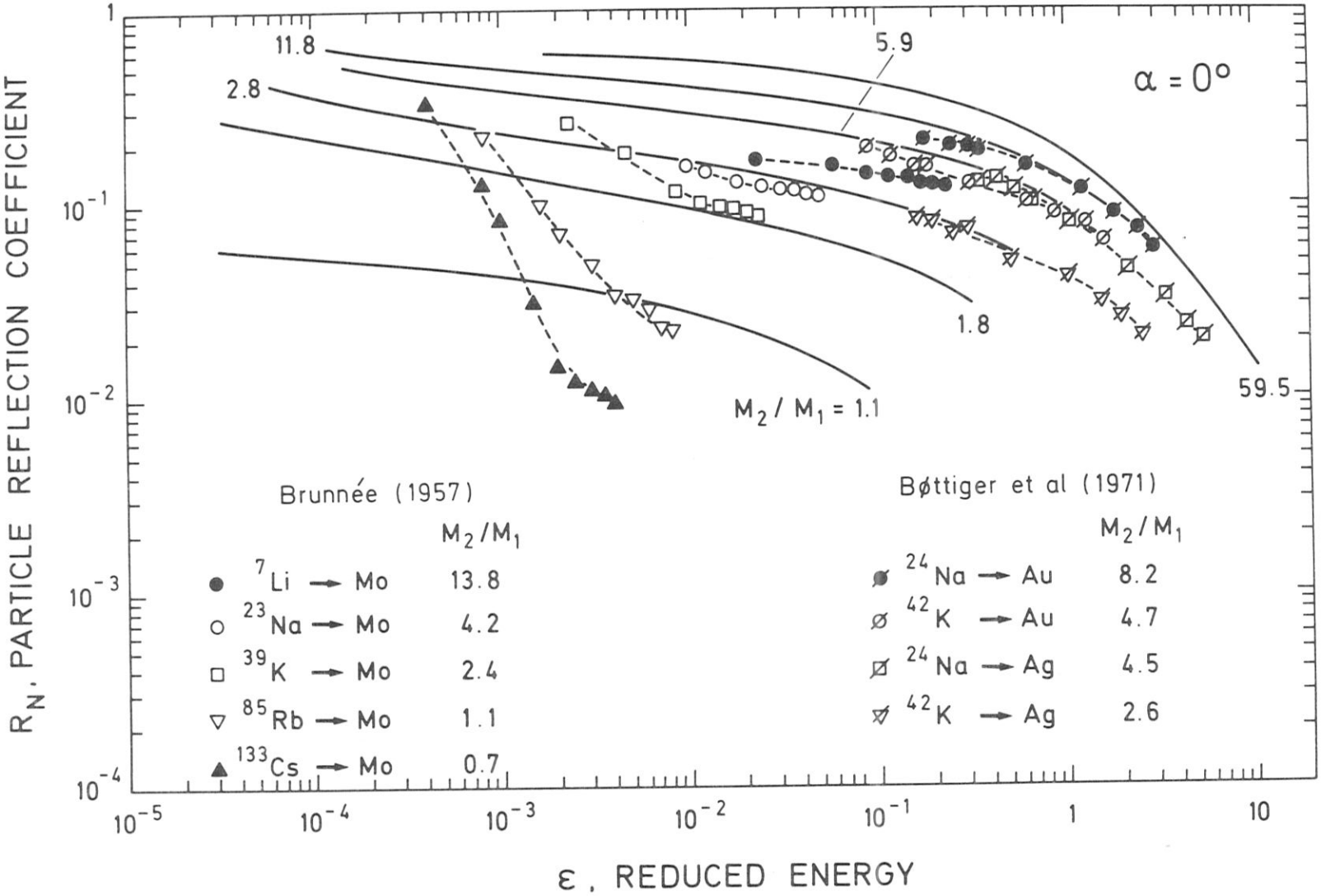

Fig. 8 Comparison of calculated and experimental /2,3/ data of the particle reflection coefficient, R_N, for different ion-target combinations and normal incidence, $\alpha = 0°$

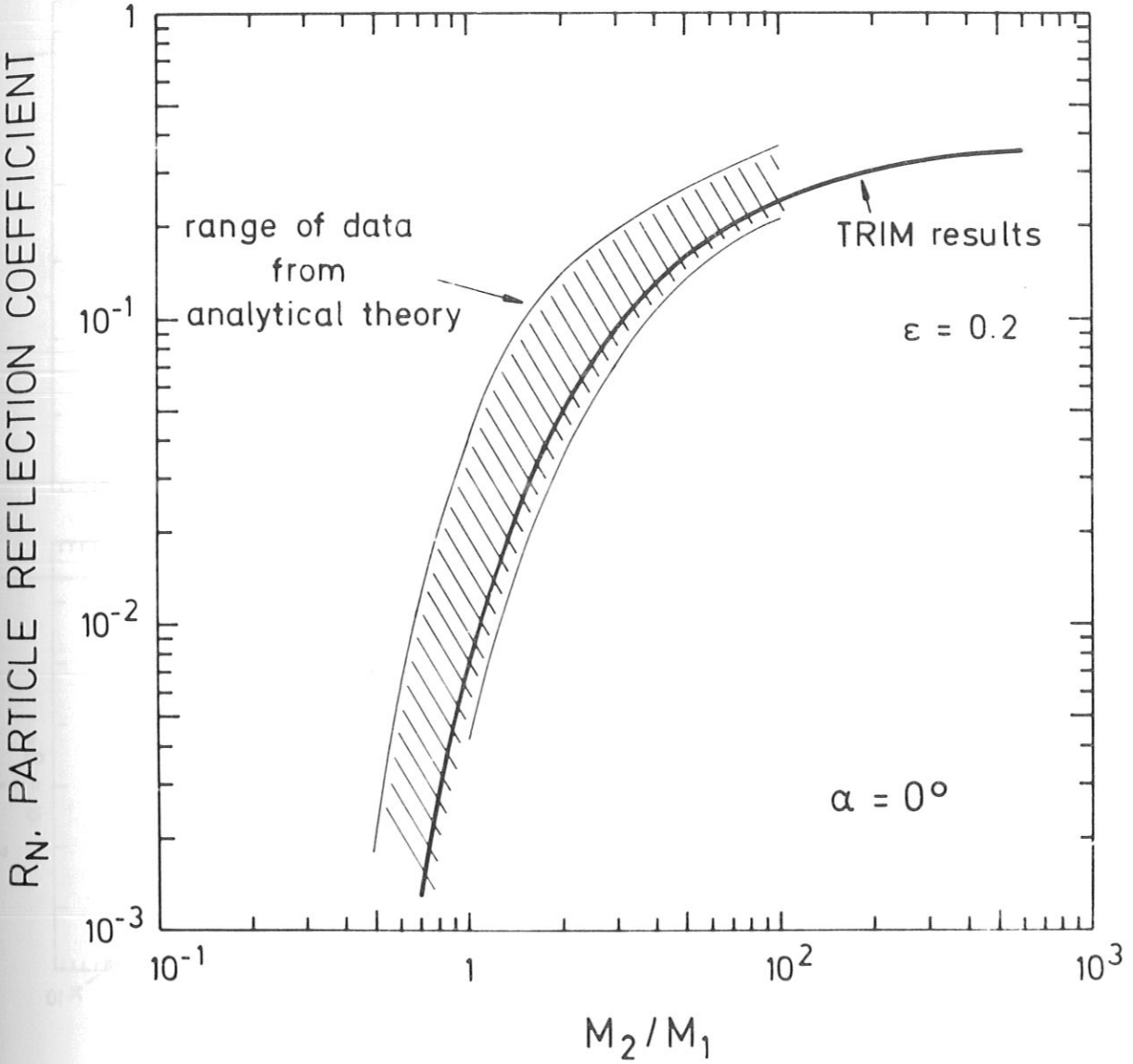

Fig. 9 Comparison of calculated and theoretical /4/ data of the particle reflection coefficent for $\varepsilon = 0.2$ and $\alpha = 0^{\circ}$. The hatched area orginates from the use of different potentials in the analytical calculations /4/.

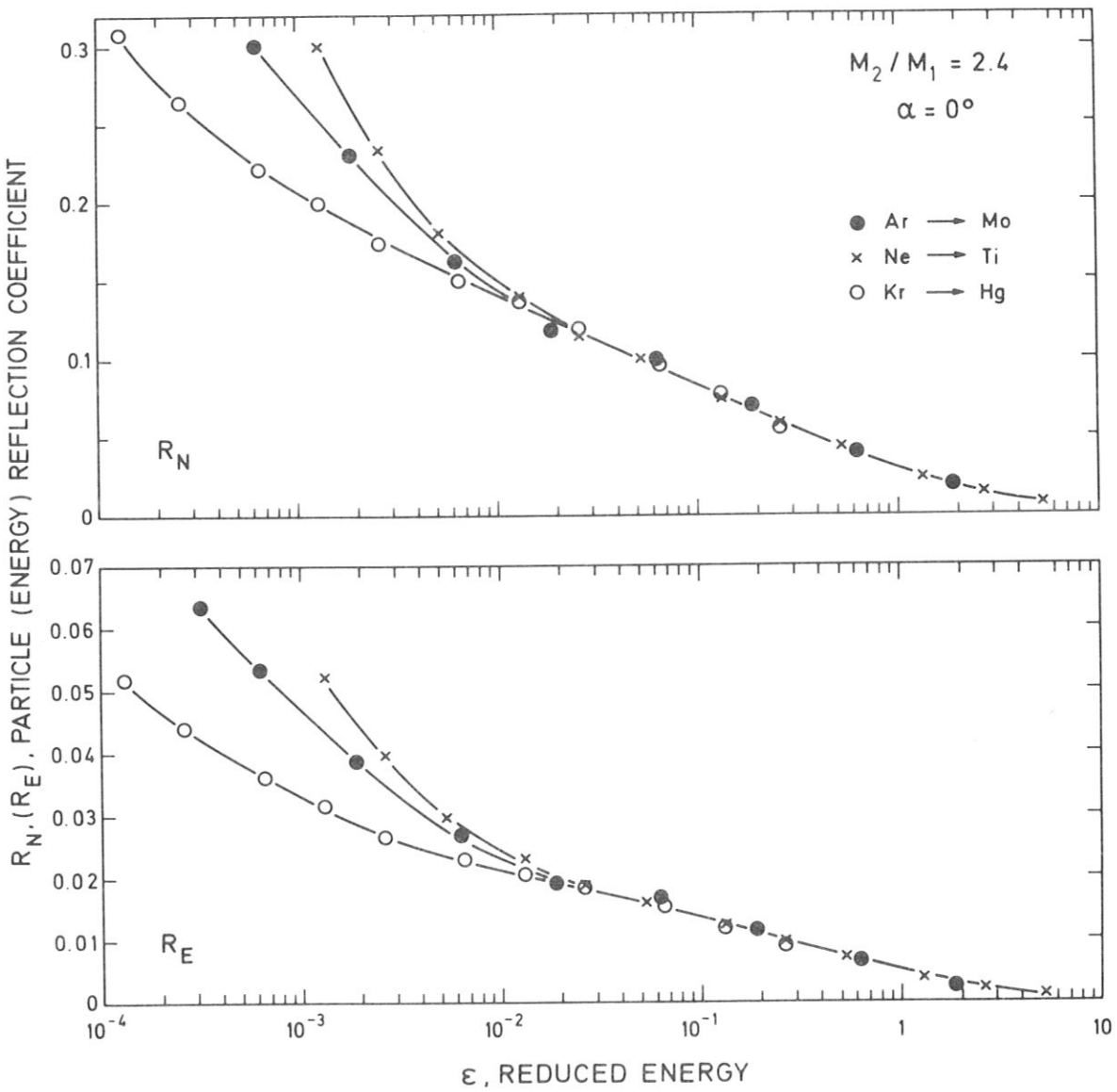

Fig. 10a Particle (R_N) and energy (R_E) reflection coefficients versus the reduced energy, ε, for a mass ratio, $M_2/M_1 = 2.4$ and normal incidence, $\alpha = 0^o$. The three examples chosen are the bombardment of Ti by Ne, Mo by Ar and Hg by Kr.

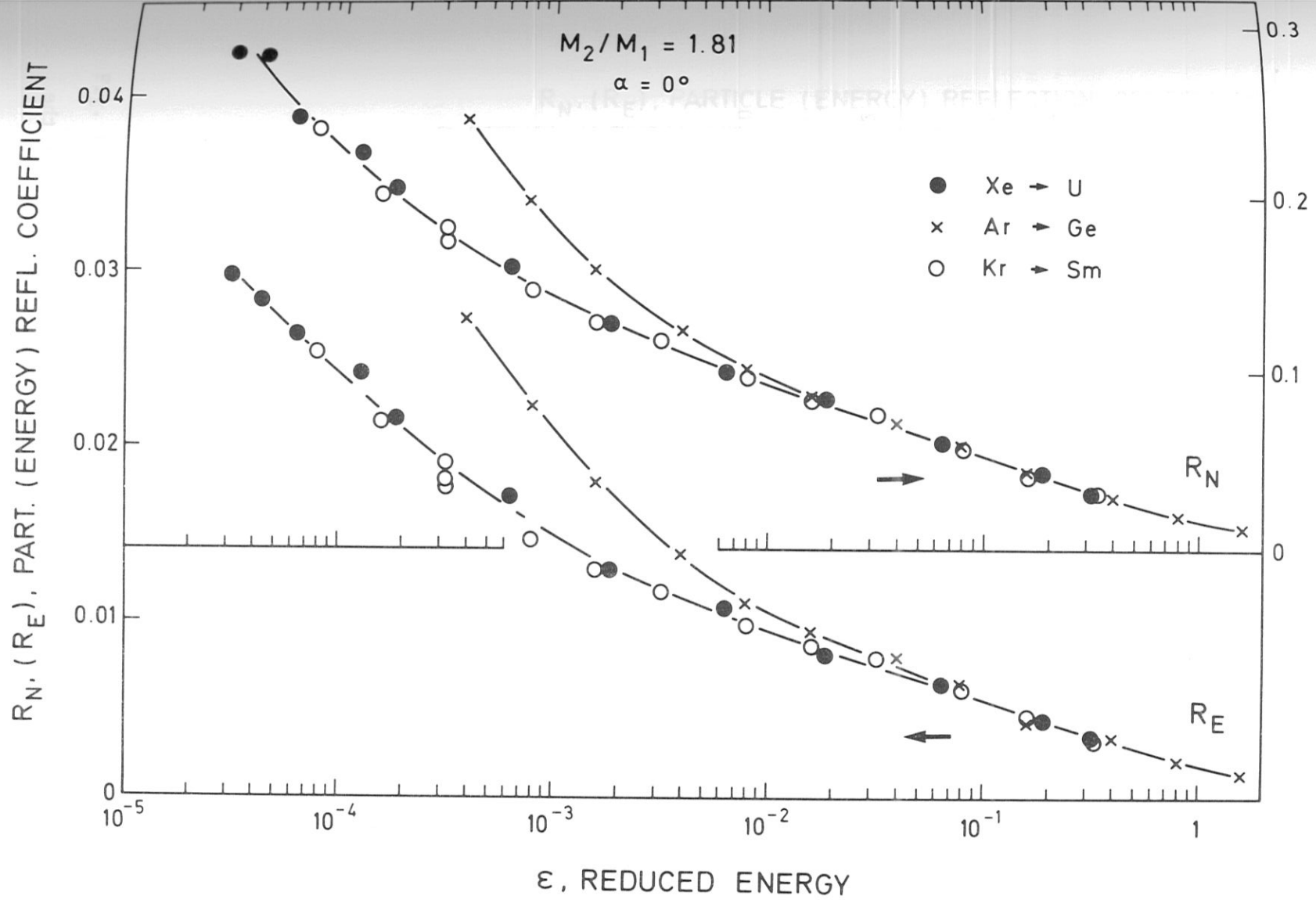

Fig. 10b Particle (R_N) and energy (R_E) reflection coefficients versus the reduced energy, ε, for a mass ratio, $M_2/M_1 = 1.81$ and normal incidence, $\alpha = 0^\circ$. The three examples chosen are the bombardment of Ge by Ar, Sm by Kr and U by Xe.

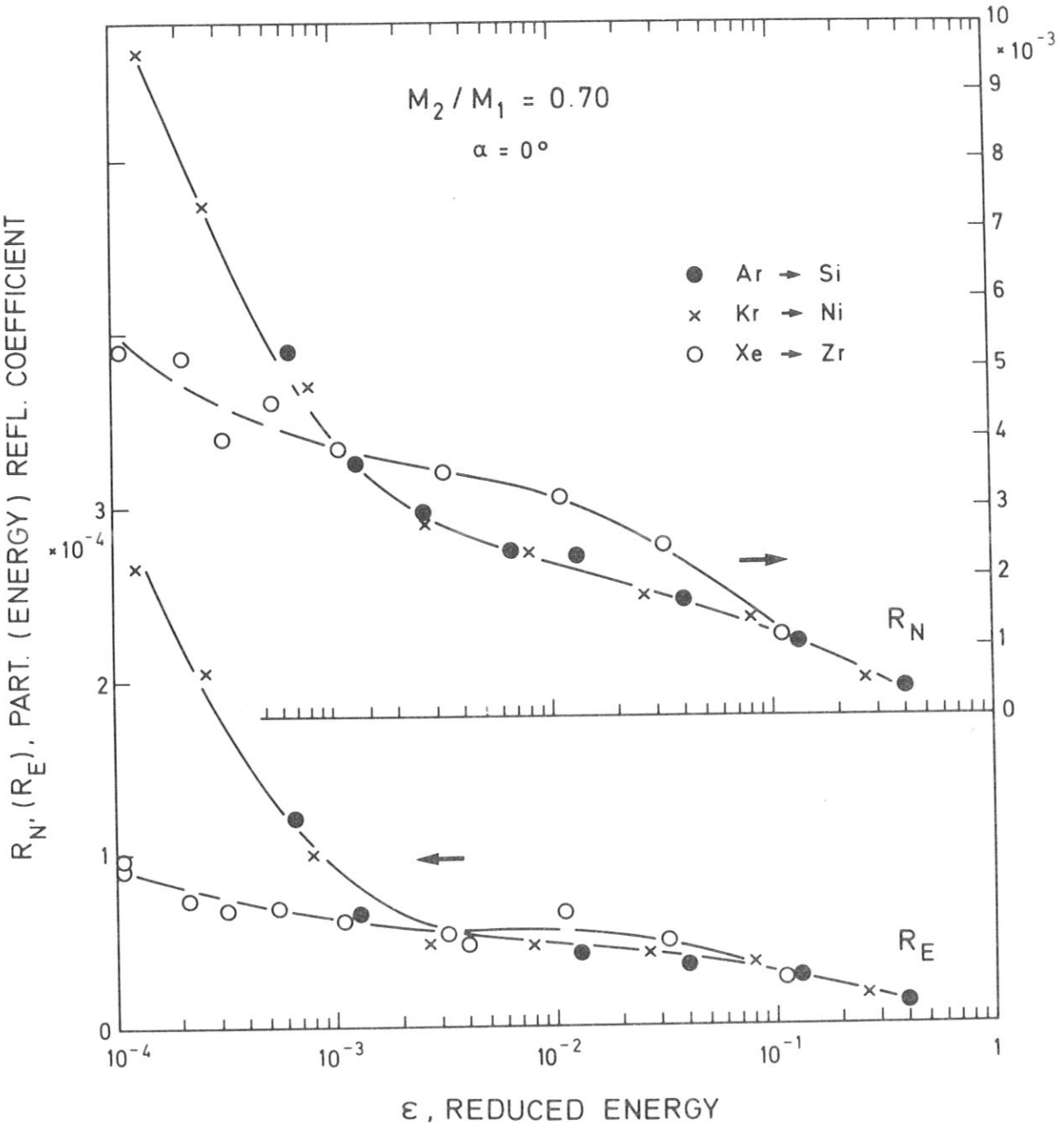

Fig. 10c Particle (R_N) and energy (R_E) reflection coefficients versus the reduced energy, ε, for a mass ratio, $M_2/M_1 = 0.70$ and normal incidence, $\alpha = 0^o$. The three examples chosen are the bombardment of Si by Ar, Ni by Kr and Zr by Xe.

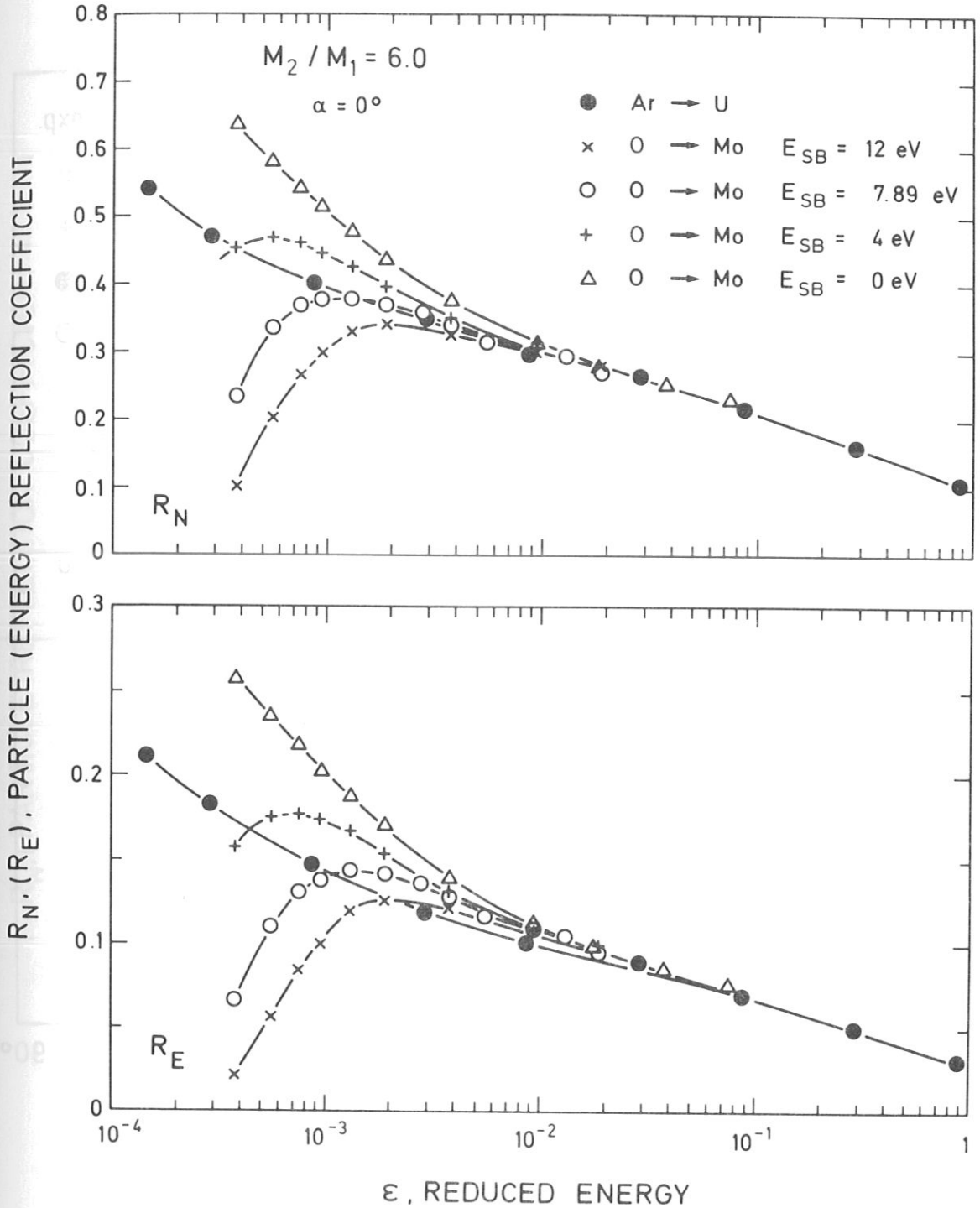

Fig. 11 Particle (R_N) and energy (R_E) reflection coefficients versus the reduced energy, ε, for a mass ratio, $M_2/M_1 = 6$ and normal incidence, $\alpha = 0^o$. The bombardment of U by Ar and Mo by O is investigated. The influence of a binding of O to the Mo-surface is shown for different binding energies (planar surface binding potential), E_s = 0, 4, 7.89, 12 eV.

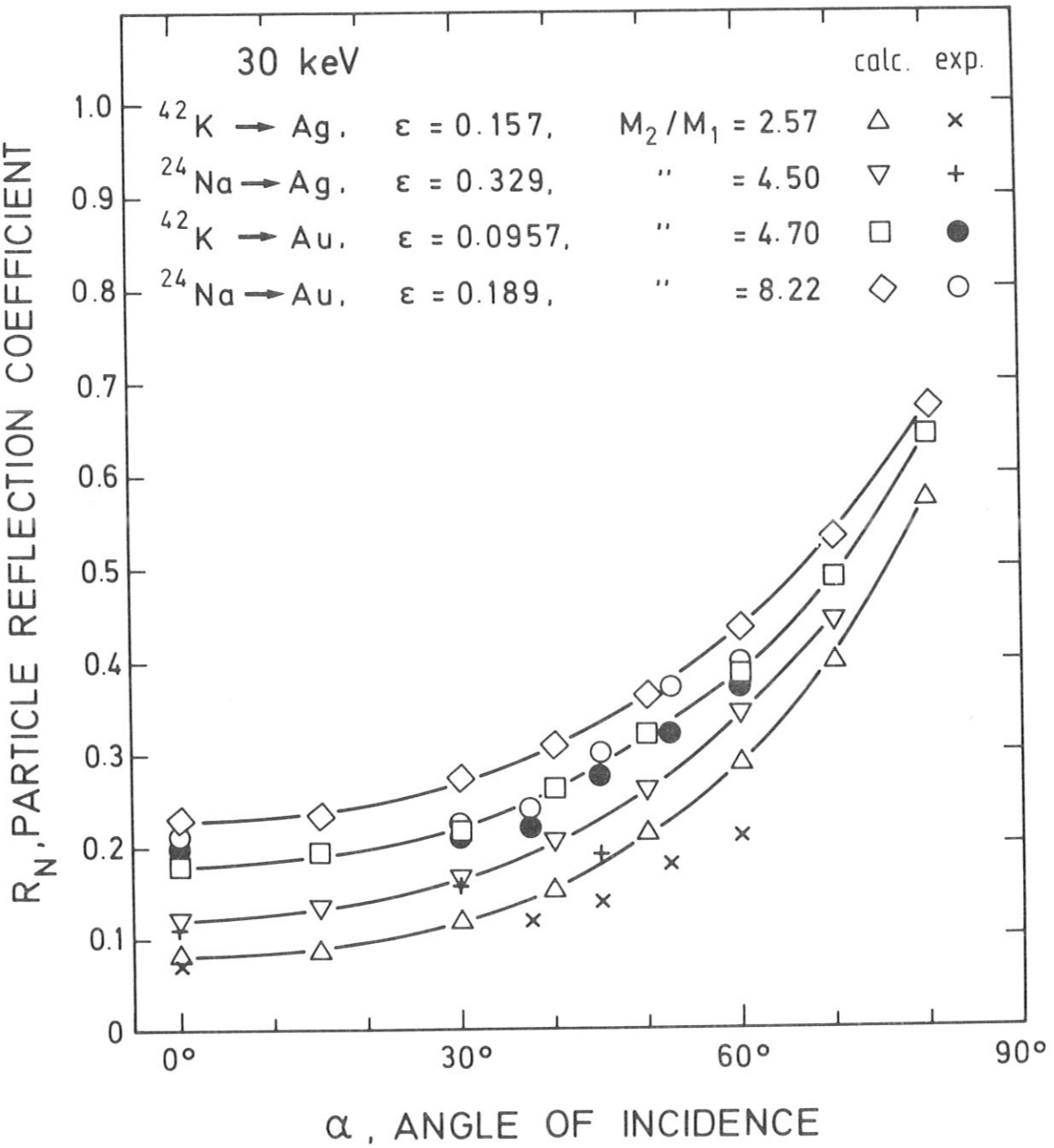

Fig. 12 Comparison of calculated and experimental /5/ data of the particle reflection coefficient, R_N, versus the angle of incidence, α, for 30 keV ^{24}Na and ^{42}K bombardment of Ag and Au.

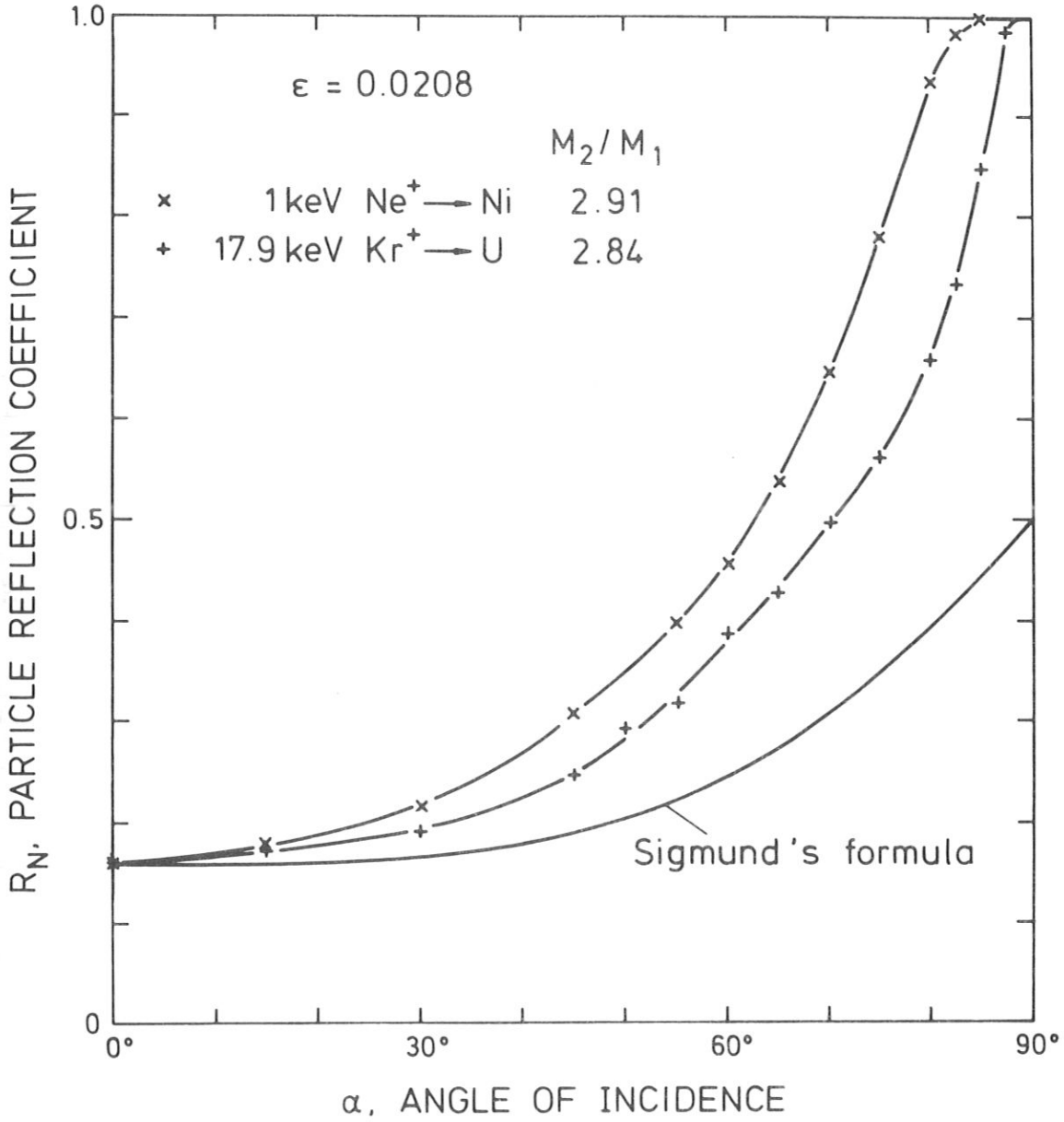

Fig. 13 Comparison of calculated and theoretical /6/ data of the particle reflection coefficient, R_N, versus the angle of incidence, α, for a reduced energy, ε = 0.0208. Ni is bombarded by 1 keV Ne, U by 17.93 keV Kr.

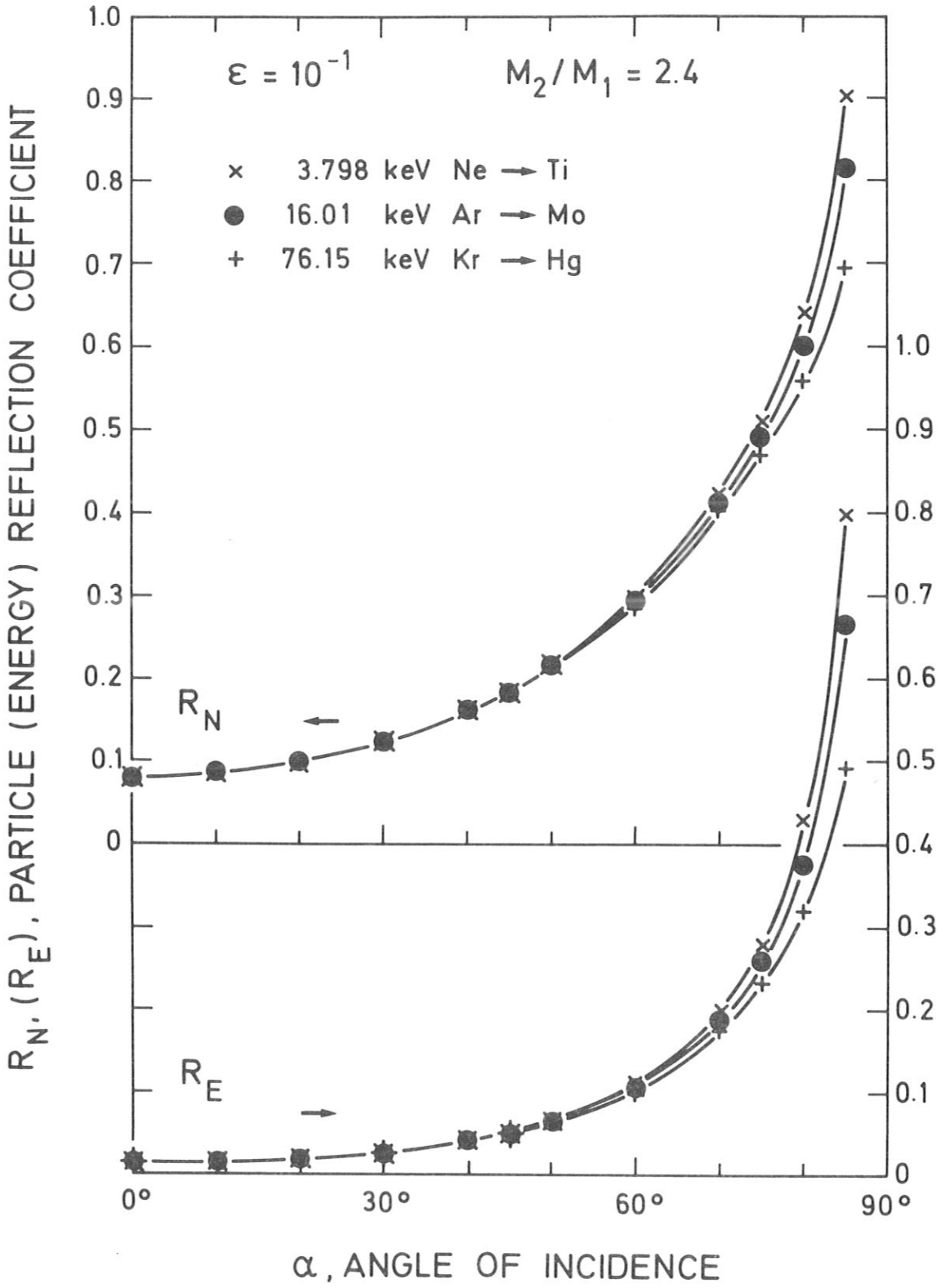

Fig. 14a Particle (R_N) and energy (R_E) reflection coefficients versus the angle of incidence, α, at a fixed reduced energy, $\varepsilon = 0.1$, and mass ratio, $M_2/M_1 = 2.4$. The three examples chosen are the bombardment of Ti by Ne, Mo by Ar, and Hg by Kr.

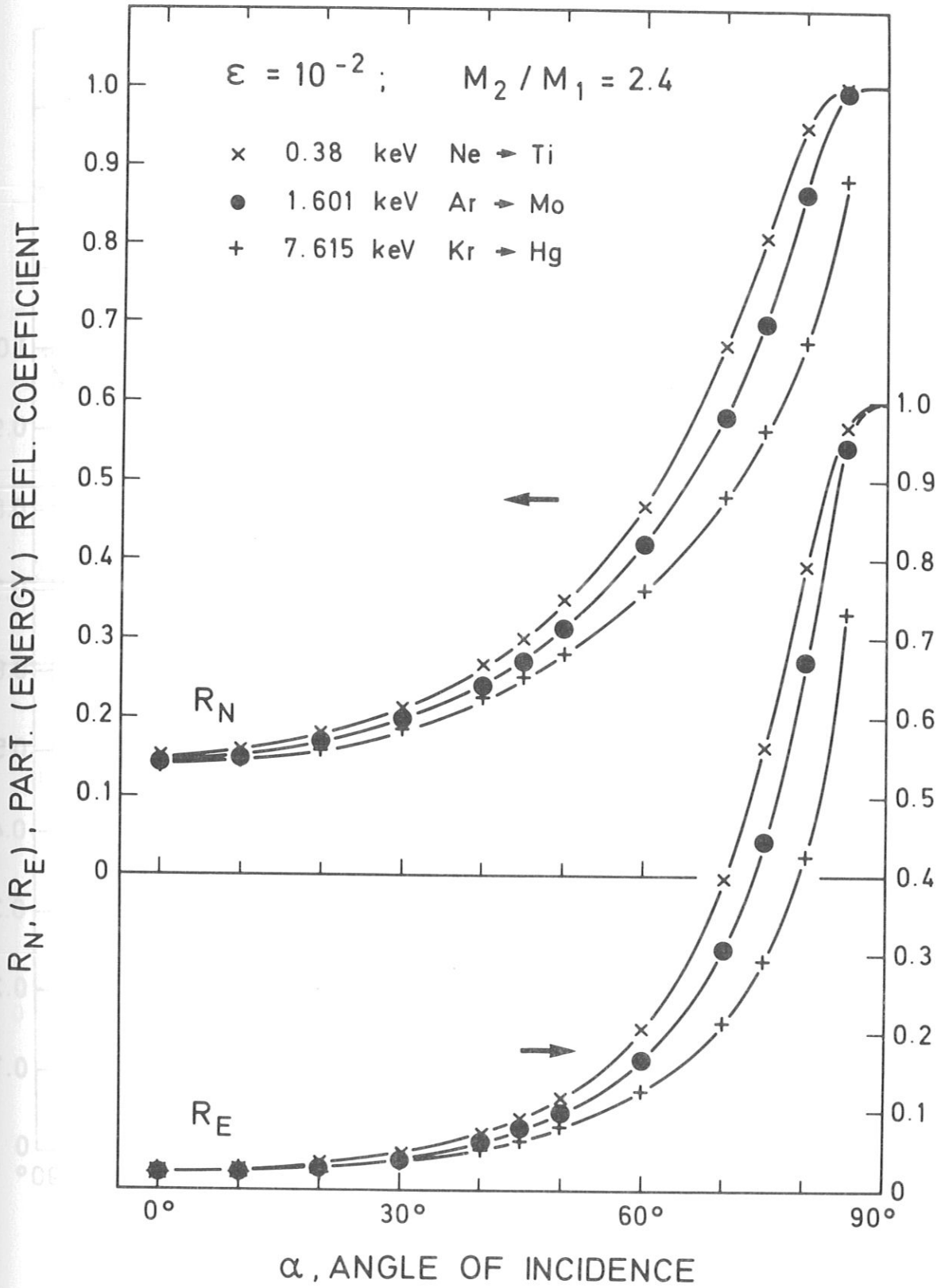

Fig. 14b Particle (R_N) and energy (R_E) reflection coefficients versus the angle of incidence, α, at a fixed reduced energy, $\varepsilon = 10^{-2}$, and mass ratio, $M_2/M_1 = 2.4$. The three examples chosen are the bombardment of Ti by Ne, Mo by Ar, and Hg by Kr.

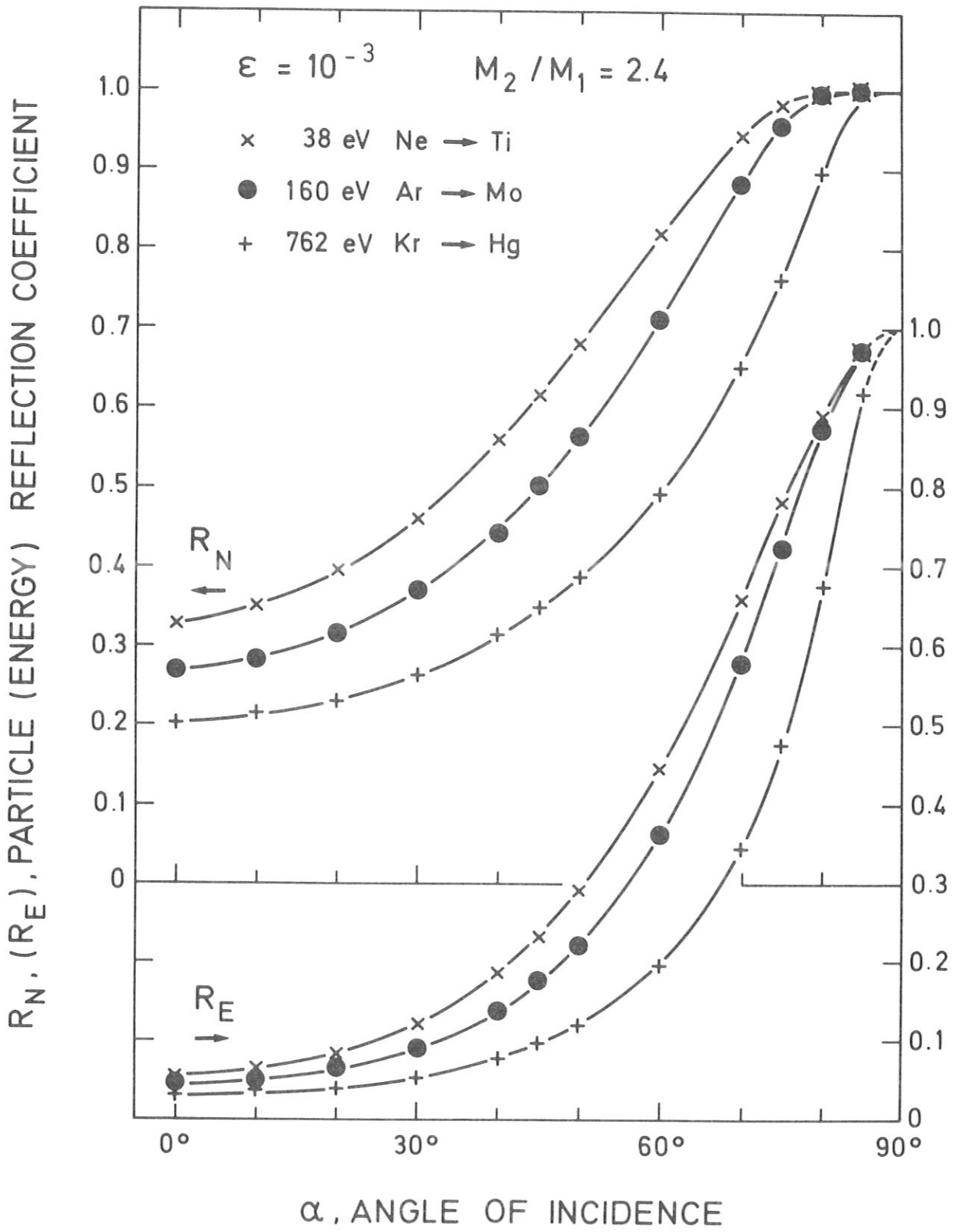

Fig. 14c Particle (R_N) and energy (R_E) reflection coefficients versus the angle of incidence, α, at a fixed reduced energy, $\varepsilon = 10^{-3}$, and mass ratio, $M_2/M_1 = 2.4$. The three examples chosen are the bombardment of Ti by Ne, Mo by Ar, and Hg by Kr.

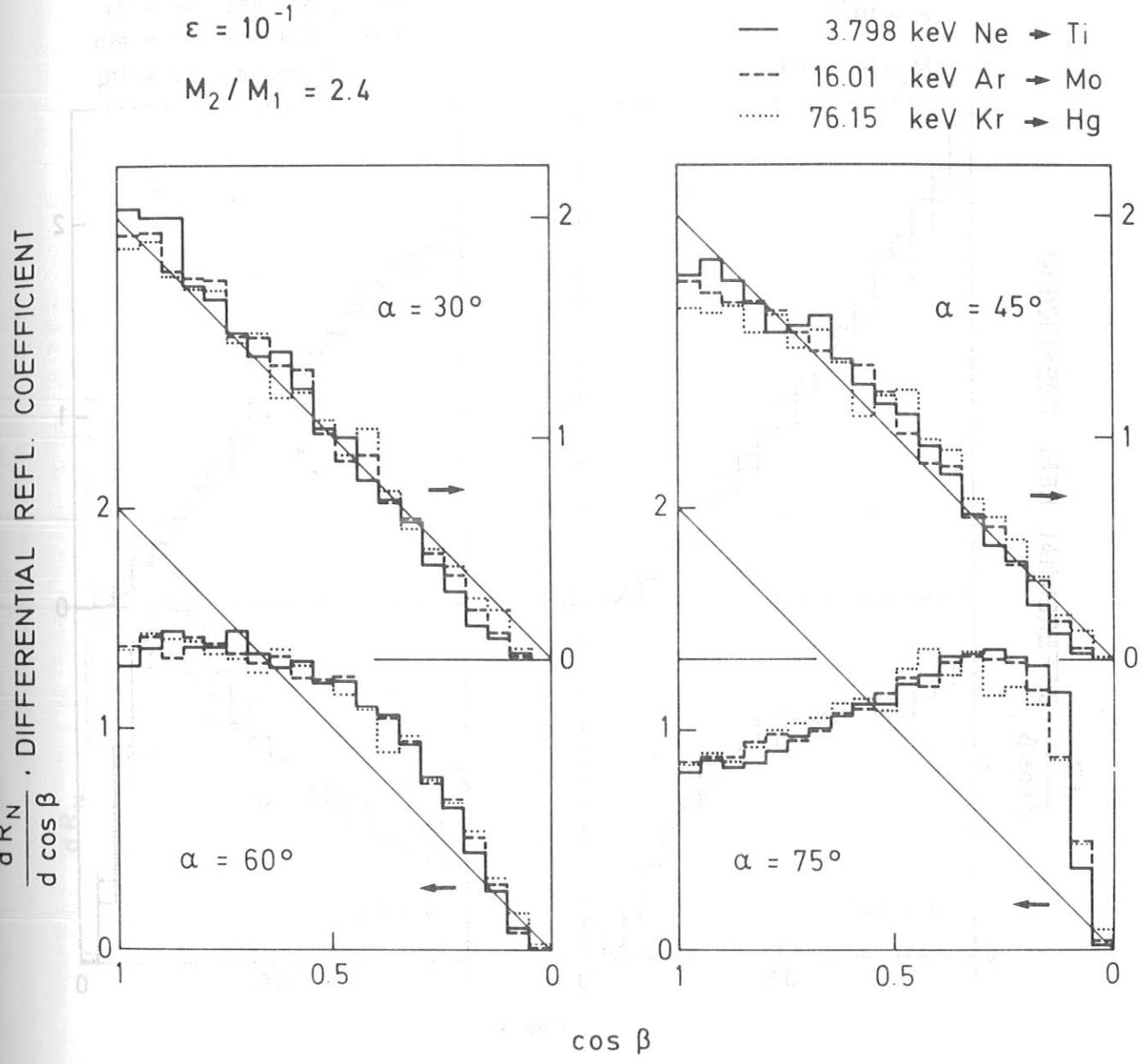

Fig. 15a Angular distributions of backscattered particles versus the cosine of the polar emission angle, ß, at a fixed reduced energy, $\varepsilon = 0.1$, a mass ratio, $M_2/M_1 = 2.4$, and four angles of incidence, $\alpha = 30^\circ, 45^\circ, 60^\circ, 75^\circ$ (integrated over the azimuthal angle, φ). The three examples chosen are the bombardment of Ti by Ne, Mo by Ar, and Hg by Kr. The straight line indicates a cosine distribution.

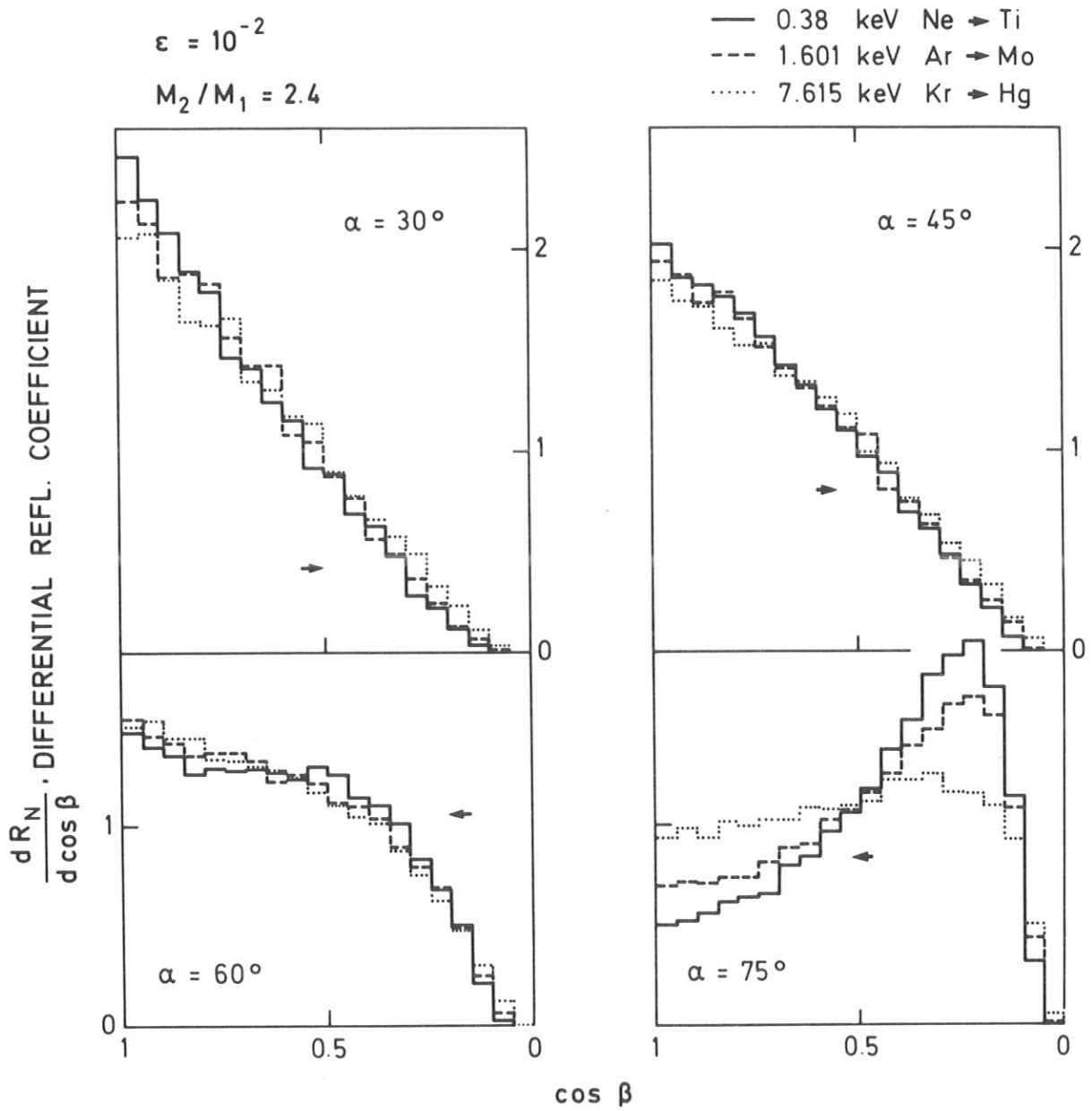

Fig. 15b Angular distributions of backscattered particles versus the cosine of the polar emission angle, ß, at a fixed reduced energy, $\varepsilon = 10^{-2}$, a mass ratio, $M_2/M_1 = 2.4$, and four angles of incidence, $\alpha = 30^{\circ}, 45^{\circ}, 60^{\circ}, 75^{\circ}$ (integrated over the azimuthal angle, φ). The three examples chosen are the bombardment of Ti by Ne, Mo by Ar, and Hg by Kr. The straight line indicates a cosine distribution.

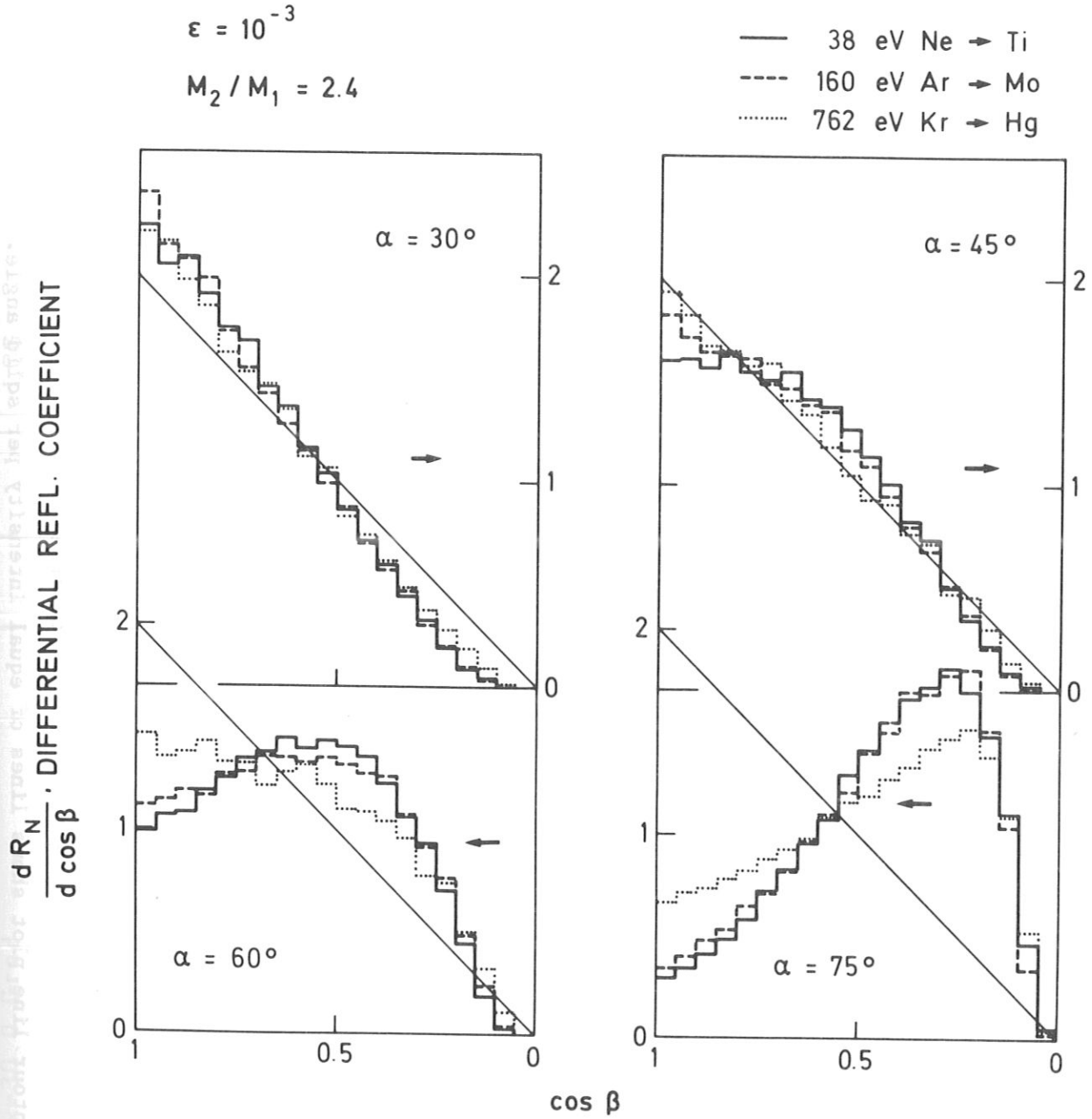

Fig. 15c Angular distributions of backscattered particles versus the cosine of the polar emission angle, ß, at a fixed reduced energy, $\varepsilon = 10^{-3}$, a mass ratio, $M_2/M_1 = 2.4$, and four angles of incidence, $\alpha = 30^{\circ}, 45^{\circ}, 60^{\circ}, 75^{\circ}$ (integrated over the azimuthal angle, φ). The three examples chosen are the bombardment of Ti by Ne, Mo by Ar, and Hg by Kr. The straight line indicates a cosine distribution.

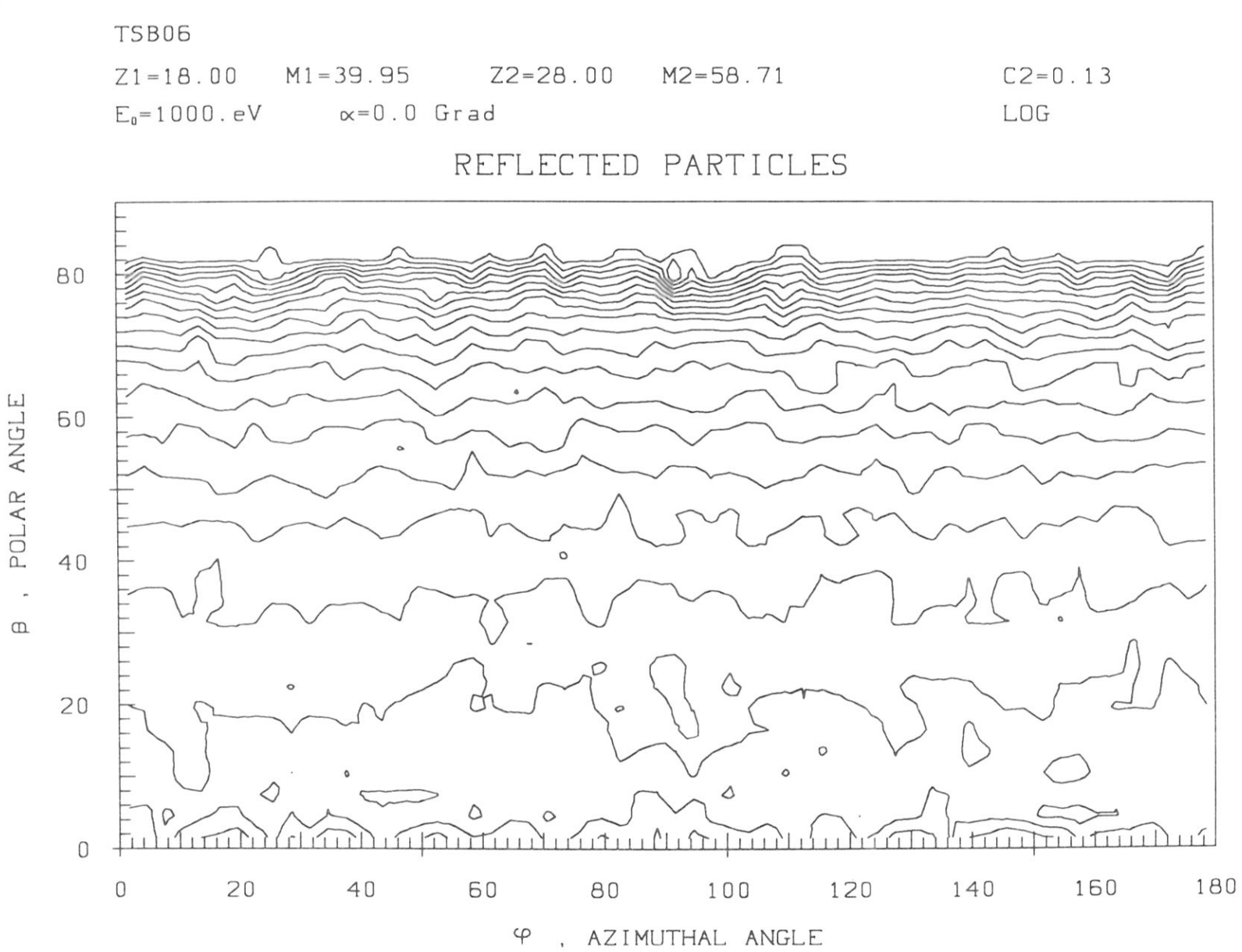

Fig. 16a Complete angular distributions of backscattered particles for an angle of incidence, $\alpha = 0^{\circ}$. Ni was bombarded by 1 keV Ar. The contour line plot shows lines of equal intensity per solid angle. The distance, c = 0.13 between adjacent contour-lines is logarithmic.

Z1=18.00 M1=39.95 Z2=28.00 M2=58.71 C2=0.13

E_0=1000.eV ∝=30.0 Grad LOG

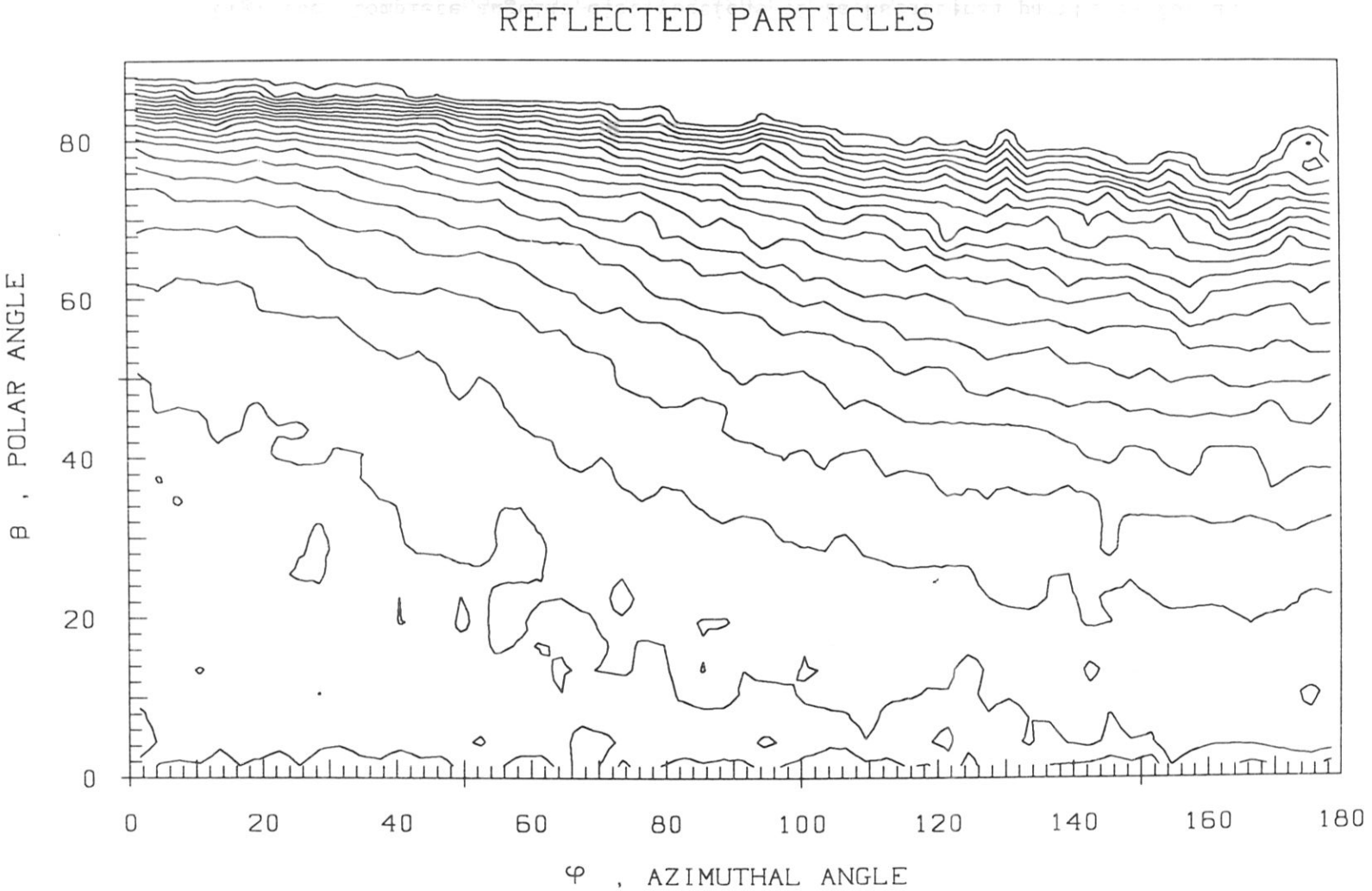

Fig. 16b Complete angular distributions of backscattered particles for an angle of incidence, $\alpha = 30^{\circ}$. Ni was bombarded by 1 keV Ar. The contour line plot shows lines of equal intensity per solid angle. The distance, c = 0.13 between adjacent contour-lines is logarithmic.

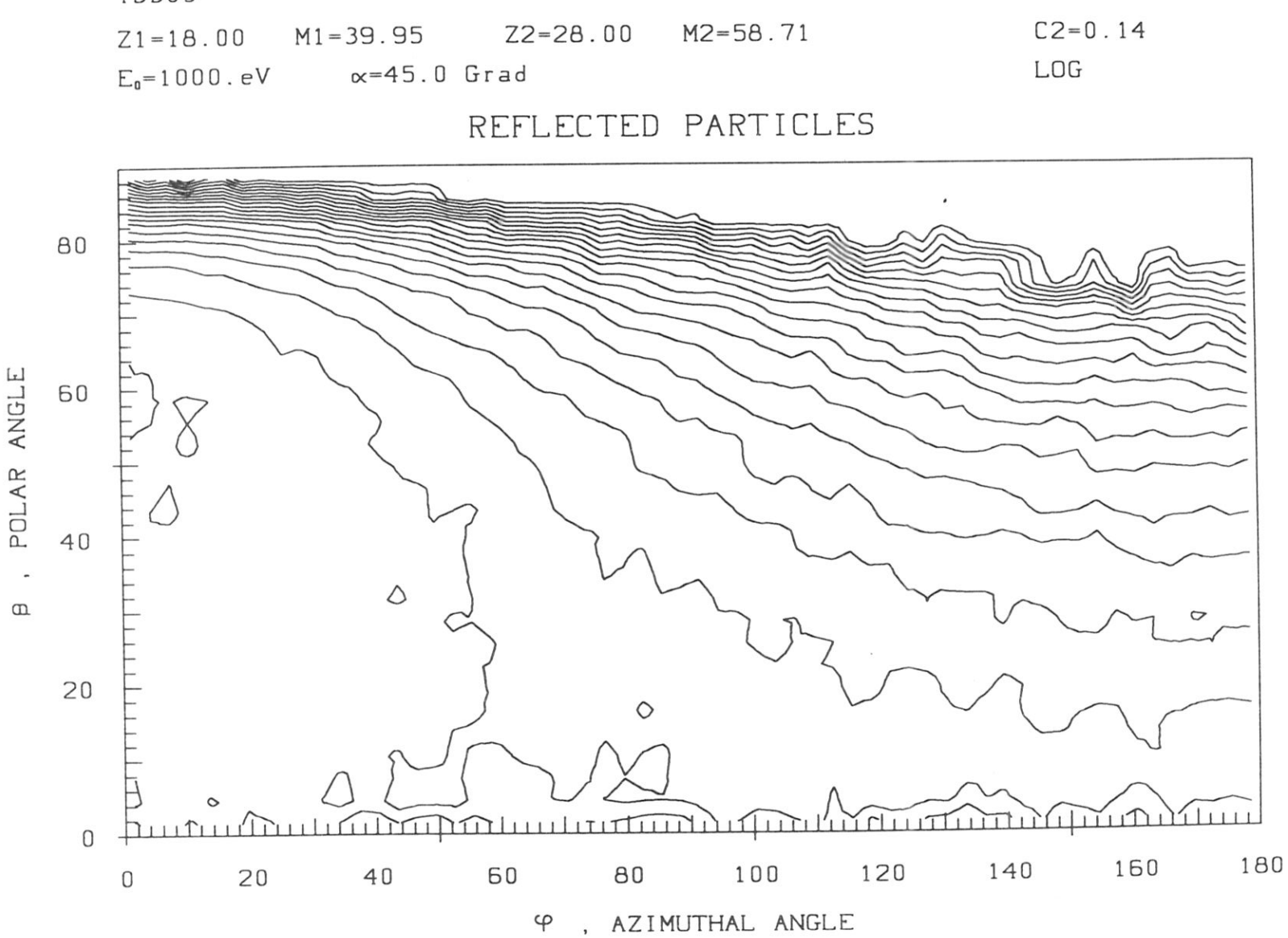

Fig. 16c Complete angular distributions of backscattered particles for an angle of incidence, $\alpha = 45^{\circ}$. Ni was bombarded by 1 keV Ar. The contour line plot shows lines of equal intensity per solid angle.

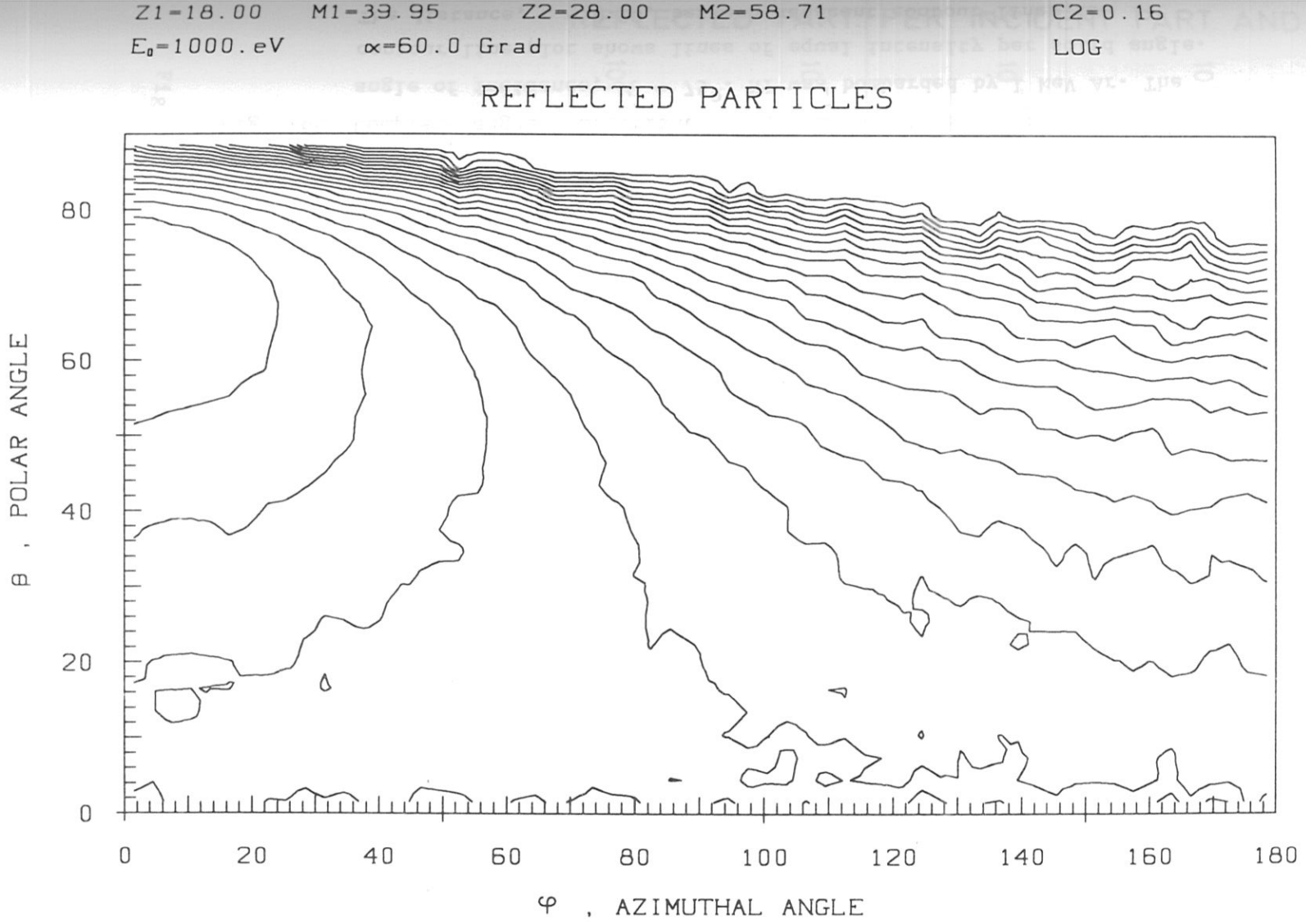

Fig. 16d Complete angular distributions of backscattered particles for an angle of incidence, $\alpha = 60^{\circ}$. Ni was bombarded by 1 keV Ar. The contour line plot shows lines of equal intensity per solid angle. The distance, c = 0.16, between adjacent contour-lines is logarithmic.

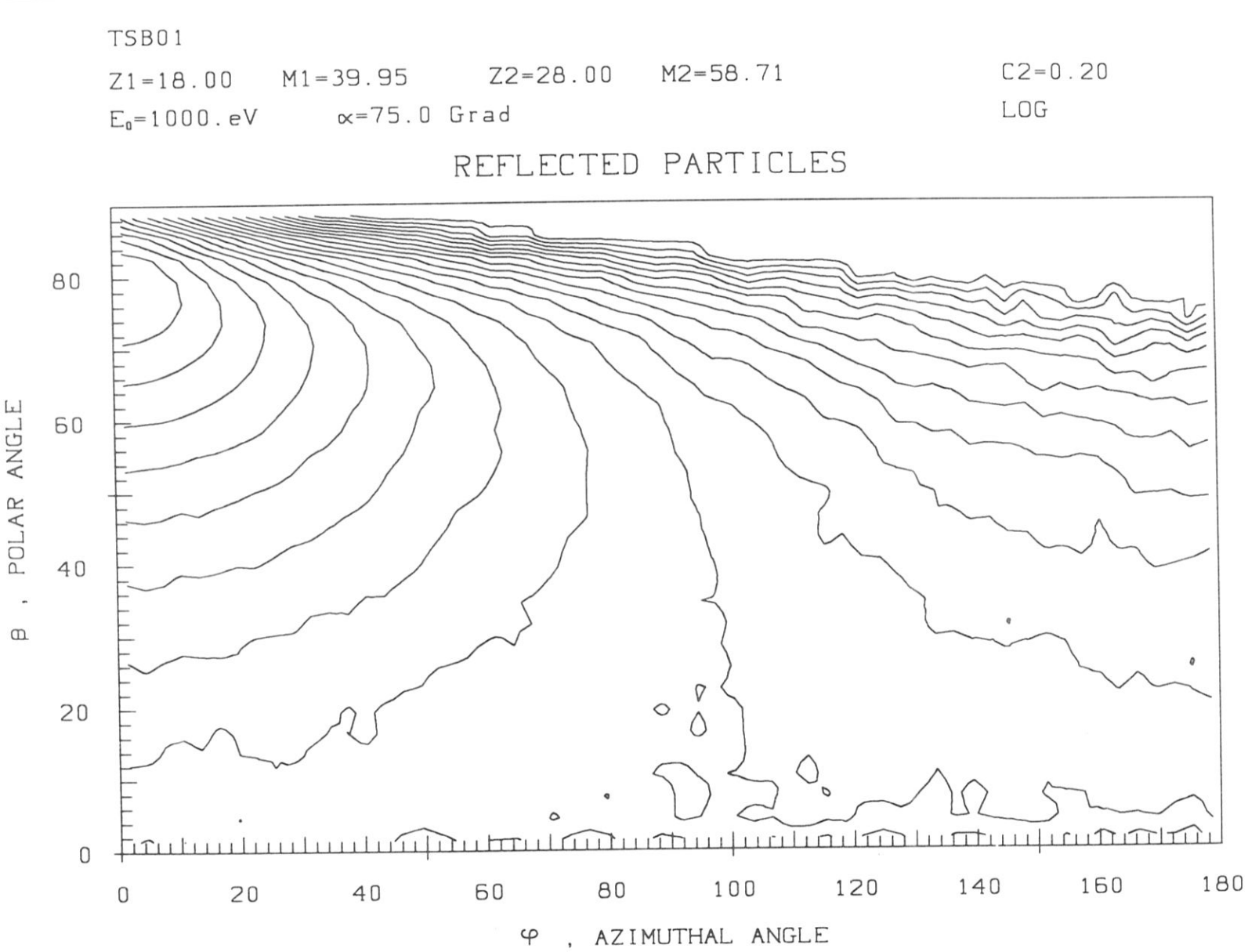

Fig. 16e Complete angular distributions of backscattered particles for an angle of incidence, $\alpha = 75^{\circ}$. Ni was bombarded by 1 keV Ar. The contour line plot shows lines of equal intensity per solid angle. The distance, c = 0.20, between adjacent contour-lines is

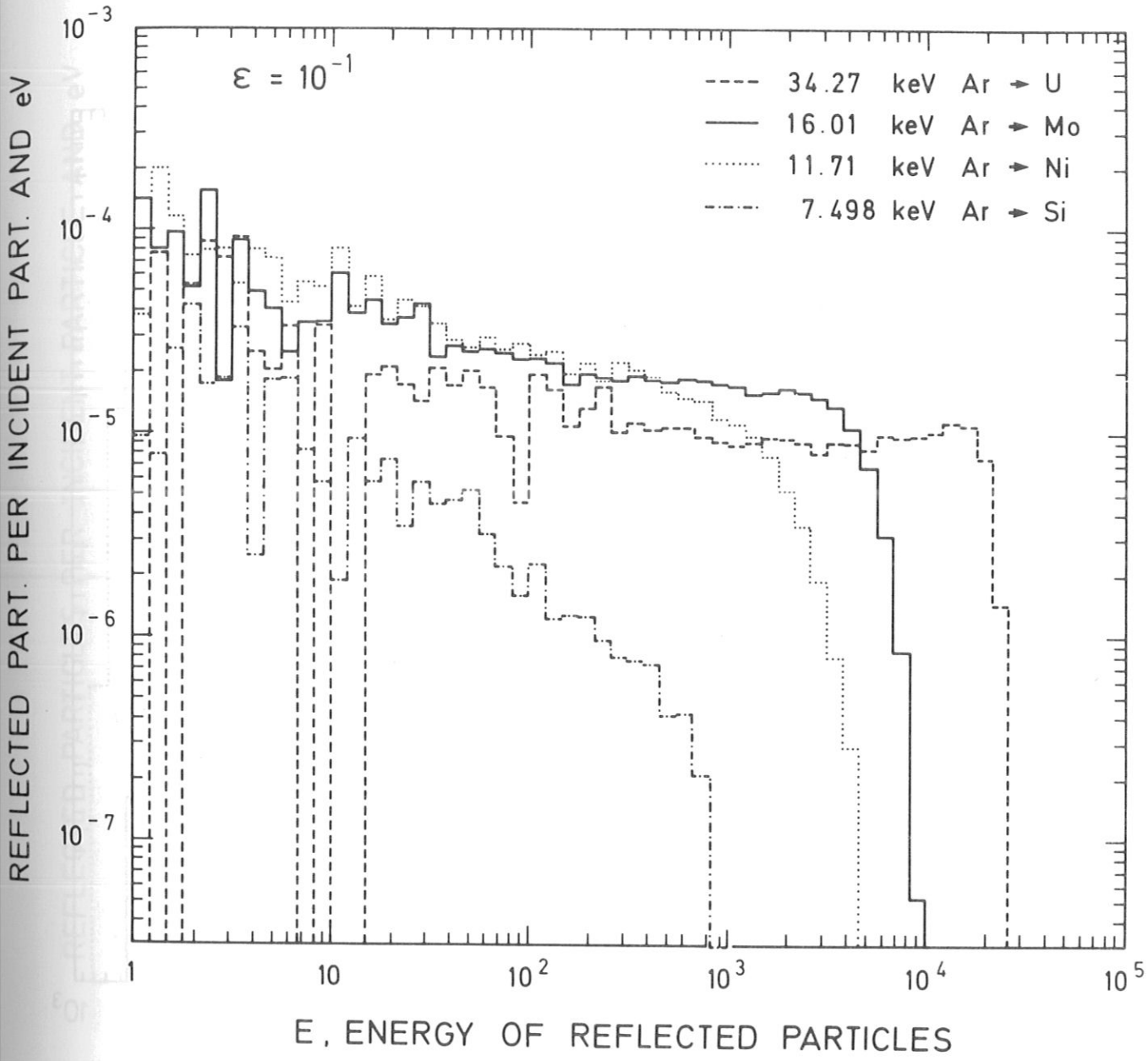

Fig. 17 Energy distributions of backscattered particles for a fixed reduced energy, $\mathcal{E} = 0.1$, and normal incidence, $\alpha = 0^{\circ}$. The four examples are

7.498	keV	Ar → Si,	M_2/M_1	= 0.703
11.71	keV	Ar → Ni,	M_2/M_1	= 1.47
16.01	keV	Ar → Mo,	M_2/M_1	= 2.40
34.27	keV	Ar → U,	M_2/M_1	= 5.96

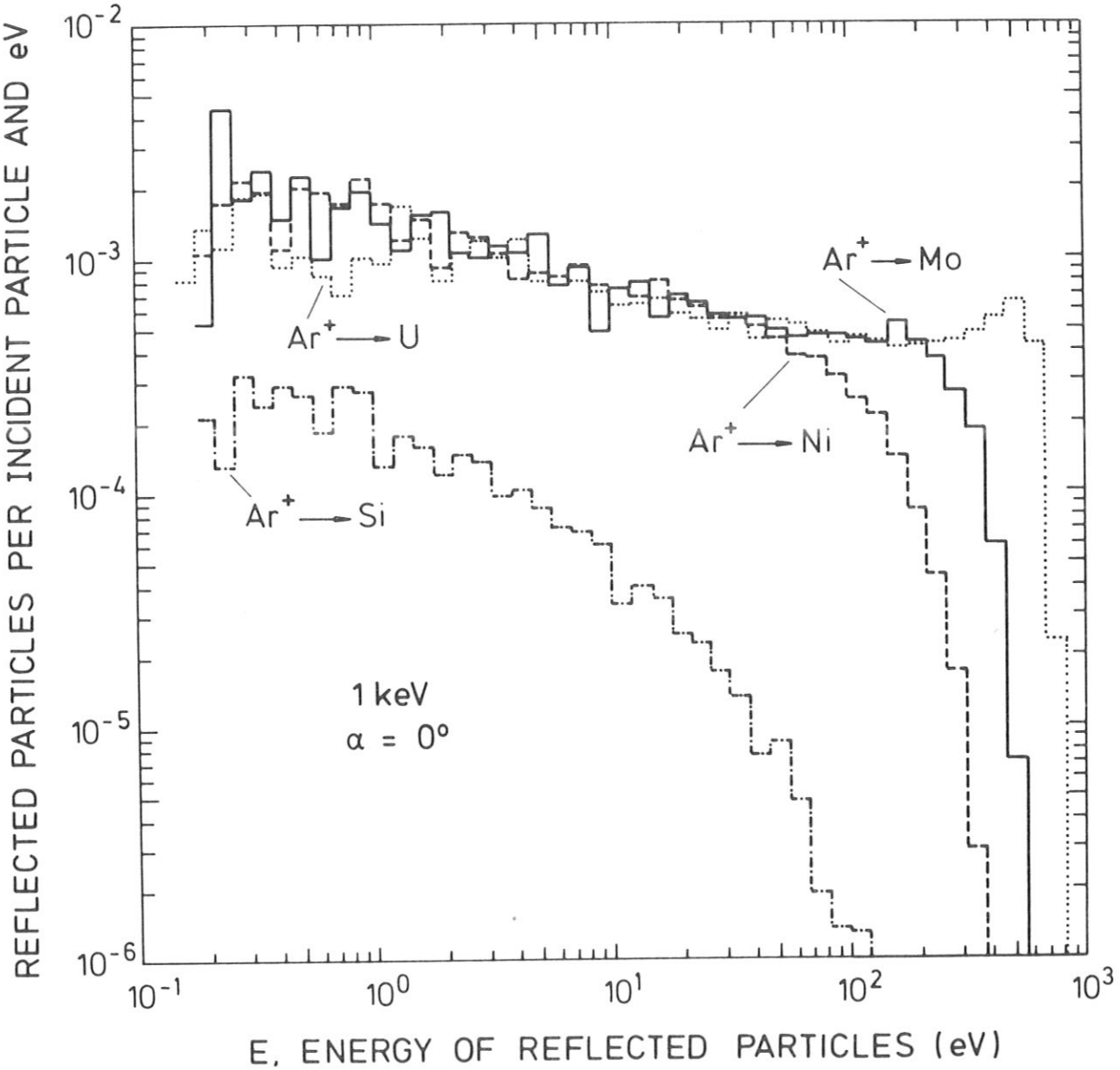

Fig. 18 Energy distributons of backscattered particles for a fixed incident energy, E_o = 1 keV, and normal incidence, $\alpha = 0^o$. The four examples are

Ar → Si	$M_2/M_1 = 0.703$
Ar → Ni	$M_2/M_1 = 1.47$
Ar → Mo	$M_2/M_1 = 2.40$
Ar → U	$M_2/M_1 = 5.96$

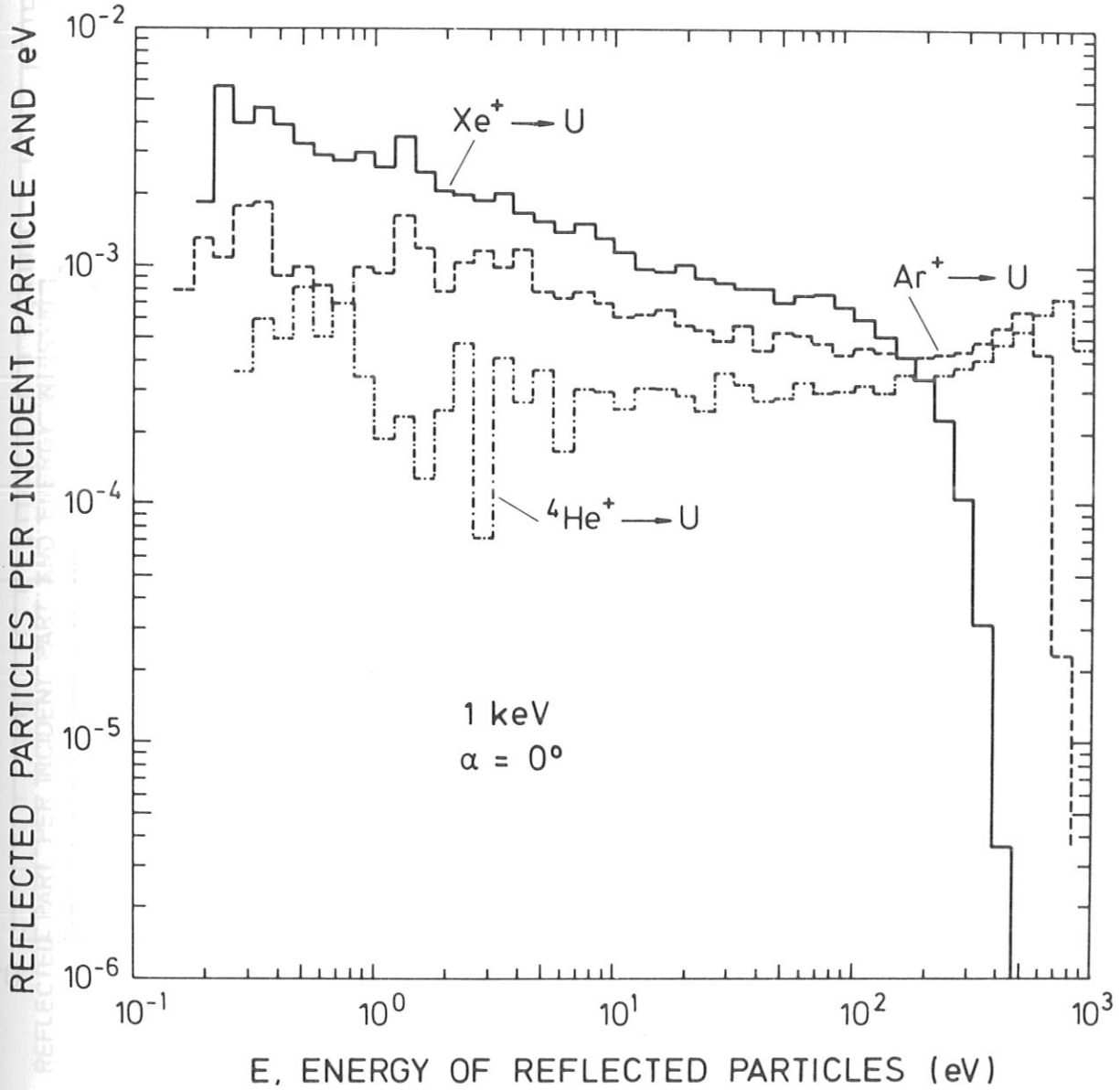

Fig. 19a Energy distributions of backscattered particles for a fixed incident energy, E_o = 1 keV, and normal incidence, α = 0°. The three examples are

He → U	M_2/M_1 = 59.52
Ar → U	M_2/M_1 = 5.96
Xe → U	M_2/M_1 = 1.81

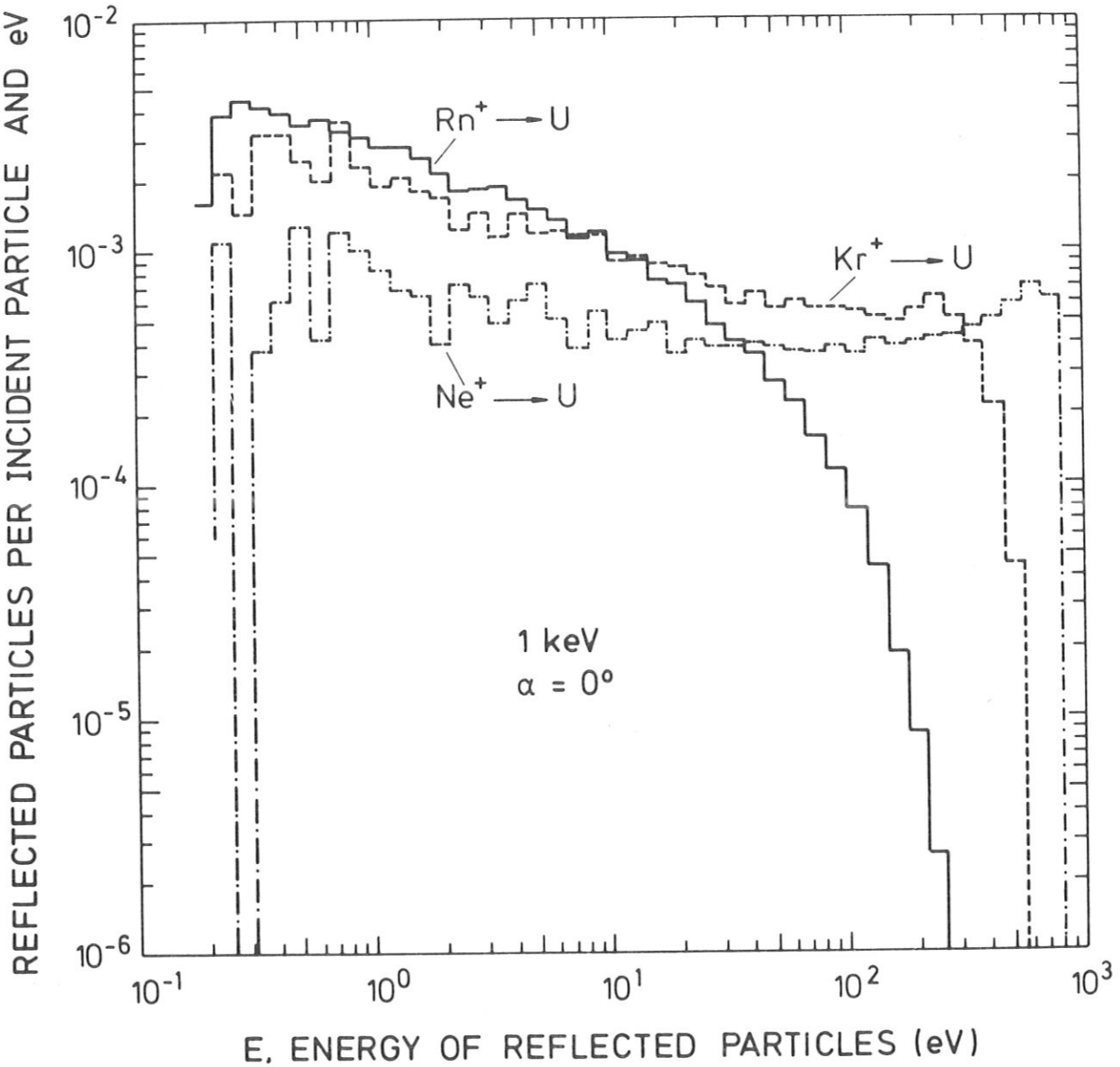

Fig. 19b Energy distributions of backscattered particles for a fixed incident energy, E_o = 1 keV, and normal incidence, $\alpha = 0^o$. The three examples are

Ne → U	M_2/M_1 = 11.80
Kr → U	M_2/M_1 = 2.84
Rn → U	M_2/M_1 = 1.07

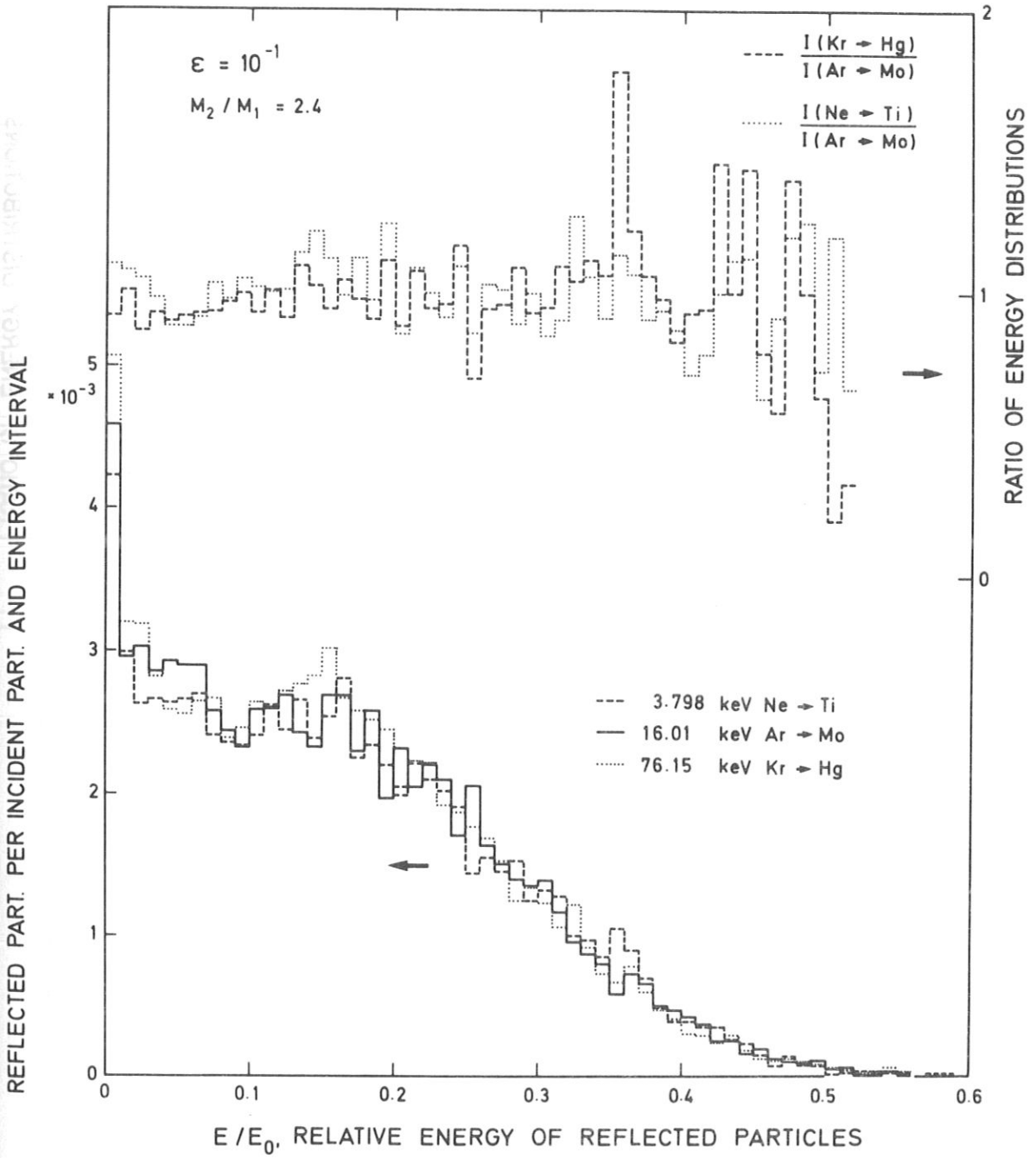

Fig. 20a Energy distributions of backscattered particles for a fixed reduced energy, $\varepsilon = 0.1$, a mass ratio, $M_2/M_1 = 2.4$ and normal incidence, $\alpha = 0^{\circ}$. The three examples are the bombardment of Ti by Ne, Mo by Ar, and Hg by Kr. The upper histograms represent ratios of the energy distributions (bottom), where the Ar/Mo example was used for normalization.

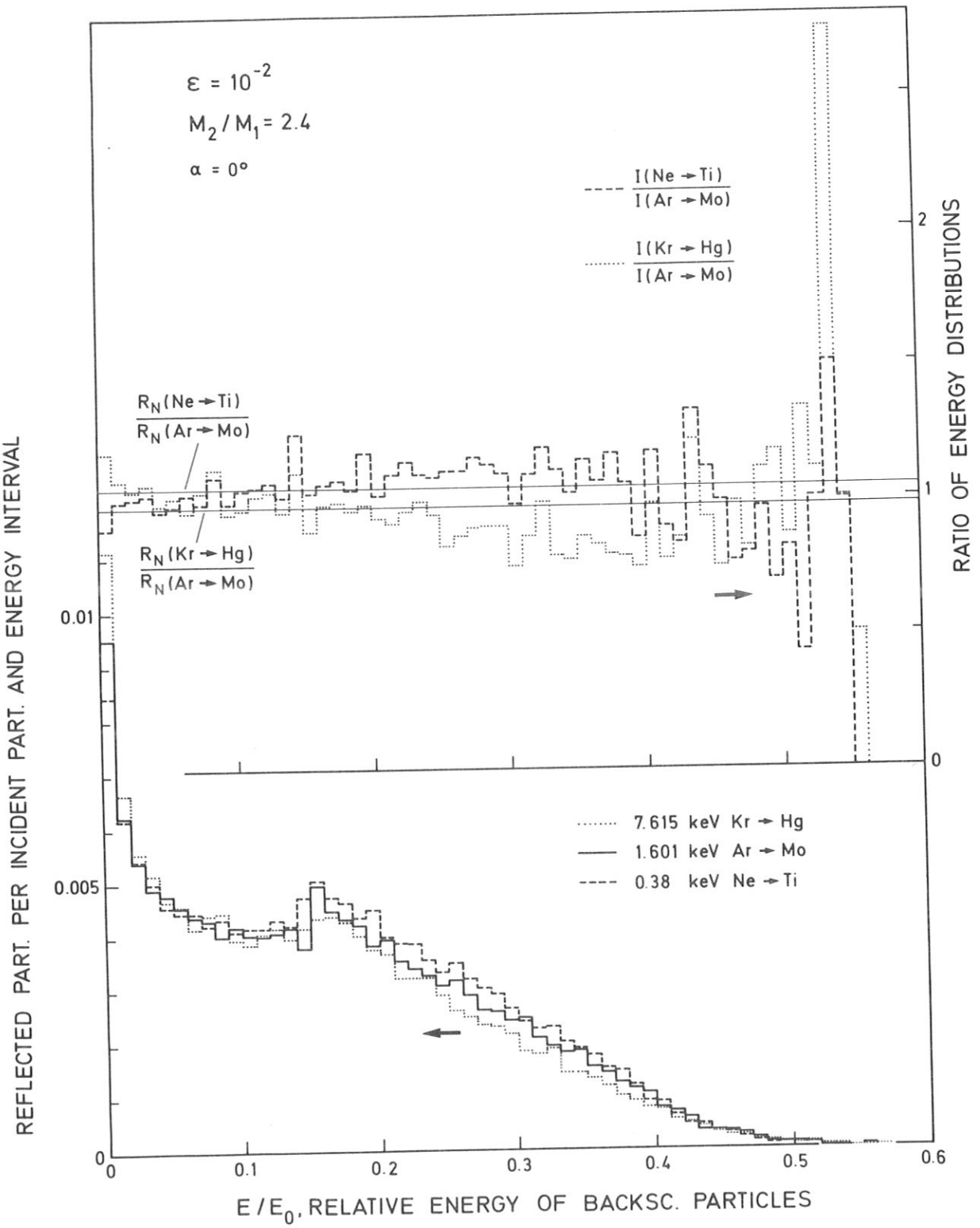

Fig. 20b Energy distributions of backscattered particles for a fixed reduced energy, $\varepsilon = 10^{-2}$, a mass ratio, $M_2/M_1 = 2.4$ and normal incidence, $\alpha = 0^{\circ}$. The three examples are the bombardment of Ti by Ne, Mo by Ar, and Hg by Kr. The upper histograms represent ratios of the energy distributions (bottom), where the Ar/Mo example was used for normalization.

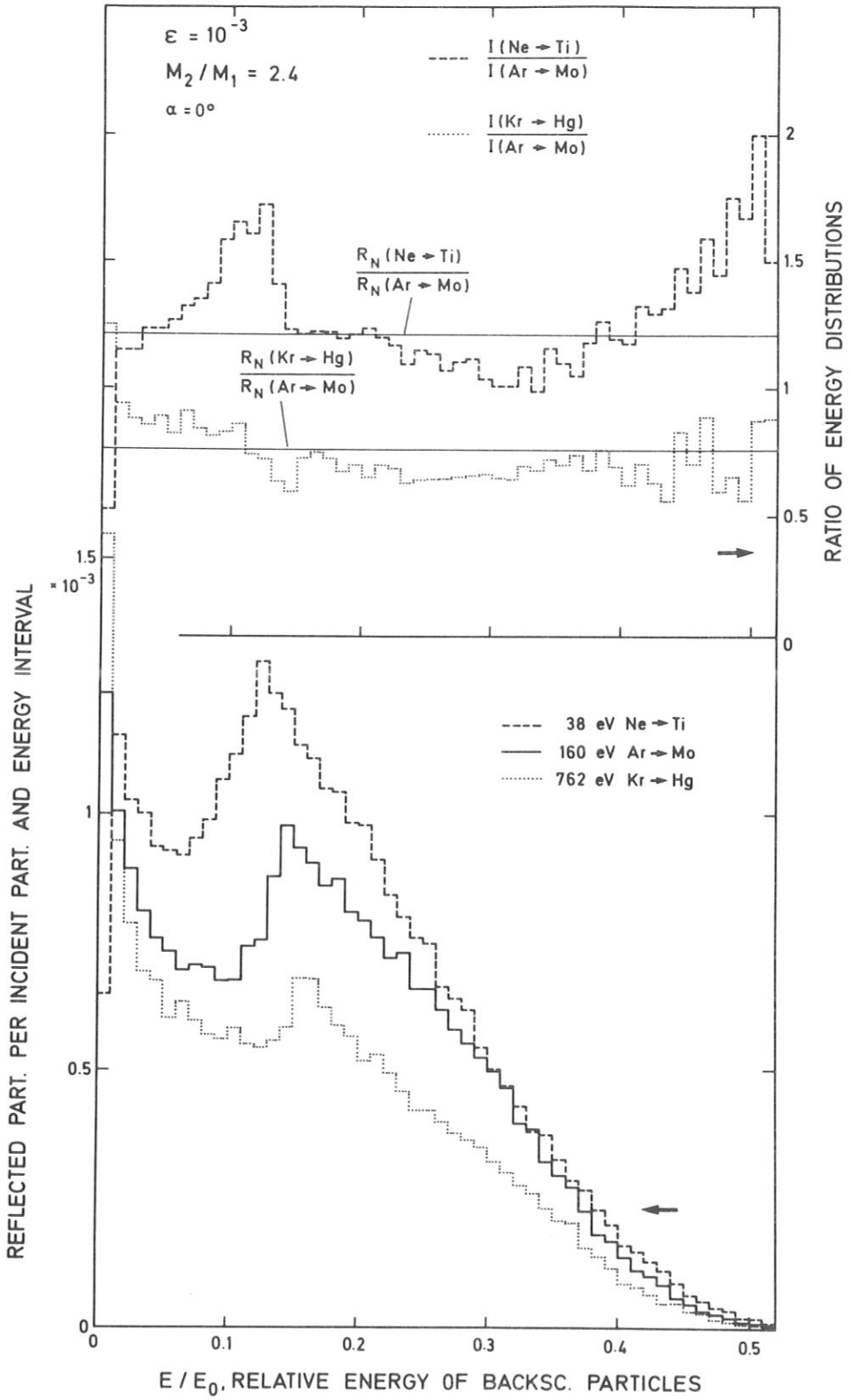

Fig. 20c Energy distributions of backscattered particles for a fixed reduced energy, $\varepsilon = 10^{-3}$, a mass ratio, $M_2/M_1 = 2.4$ and normal incidence, $\alpha = 0^{o}$. The three examples are the bombardment of Ti by Ne, Mo by Ar, and Hg by Kr. The upper histrograms represent ratios of the energy distributions (bottom), where the Ar/Mo example was used for normalization.

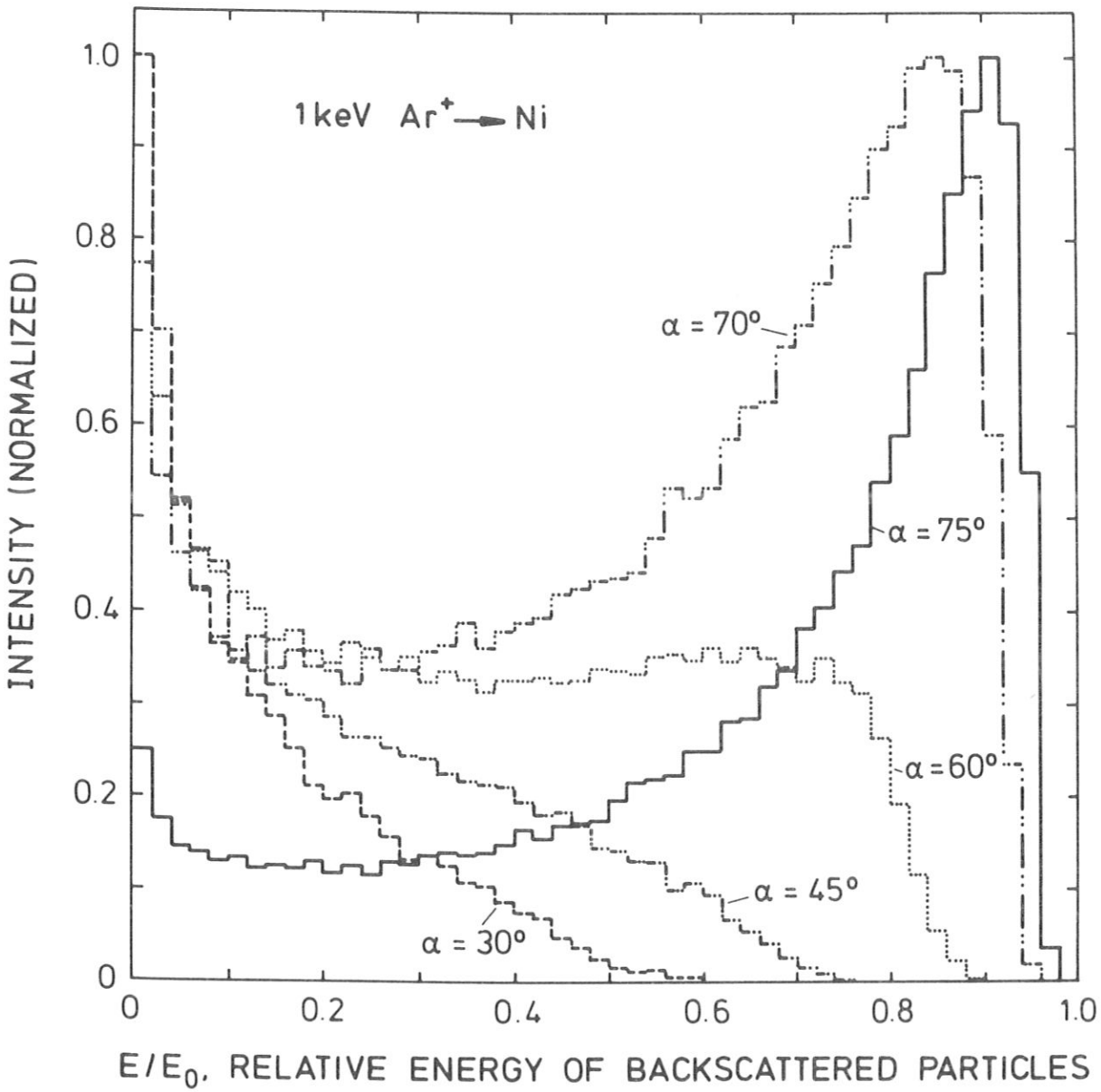

Fig. 21 Normalized energy distributions of backscattered particles for Ni bombarded by 1 keV Ar. The dependence of the energy distributions on the angle of incidence, α, is shown for $\alpha = 30^{\circ}$, 45°, 60°, 70°, 75°. For normal incidence, $\alpha = 0^{\circ}$, the energy distribution is similar to the distribution at $\alpha = 30^{\circ}$.

Z1=18.00 M1=39.95 Z2=28.00 M2=58.71 C1=0.11

E_0=1000.eV ∝=0.0 Grad 0.<|φ|<15.0 LOG

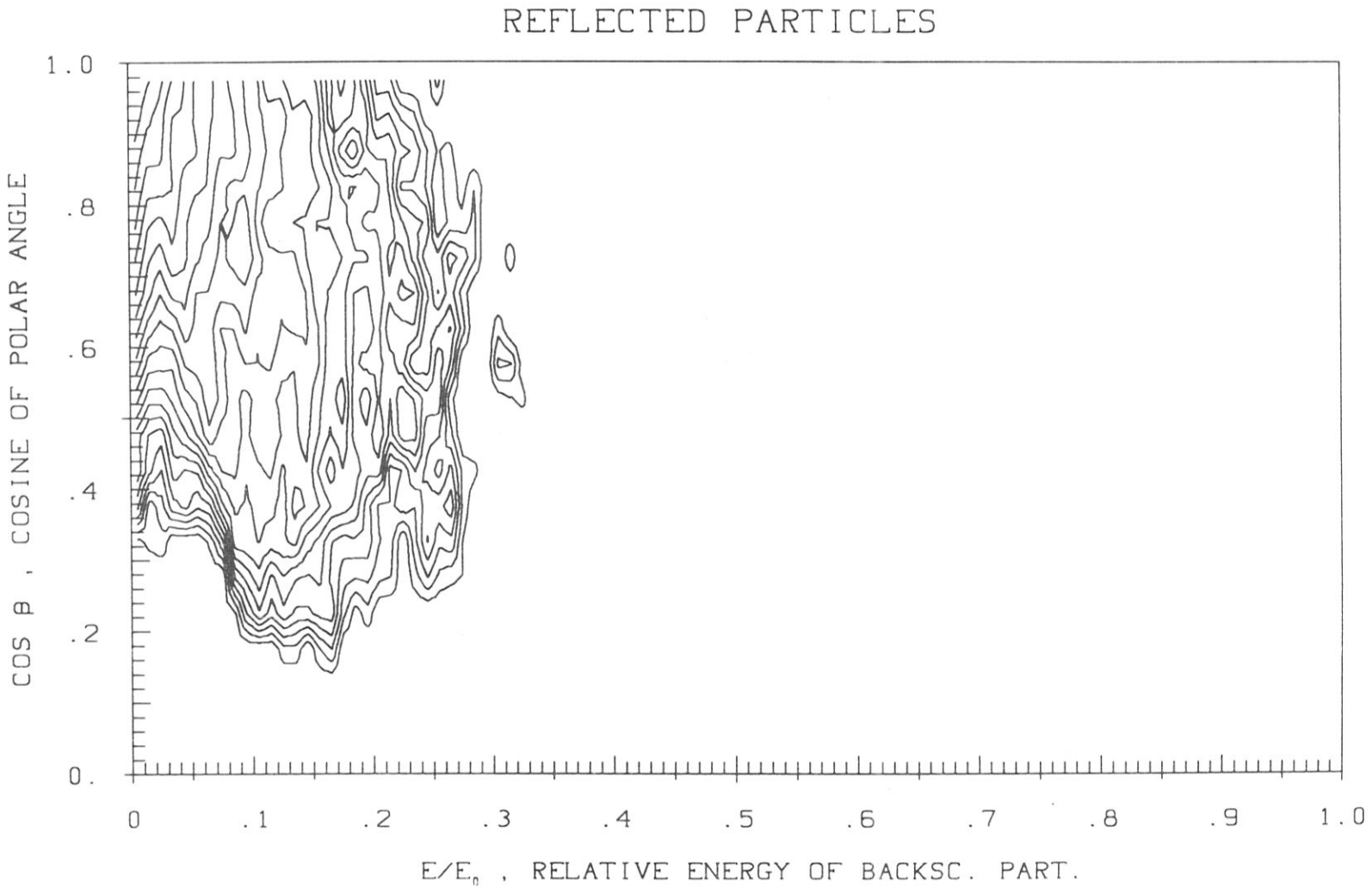

Fig. 22a Intensity distributions of backscattered particles versus the energy of the backscattered particles and the cosine of the polar emission angle, ß, in the forward direction ($-15^{\circ} < \varphi < 15^{\circ}$). Ni is bombarded by 1 keV ar at an angle of incidence, $\alpha = 0^{\circ}$. The contour plot shows lines of equal intensity per solid angle. The distance, c = 0.11, between adjacent contour lines is logarithmic.

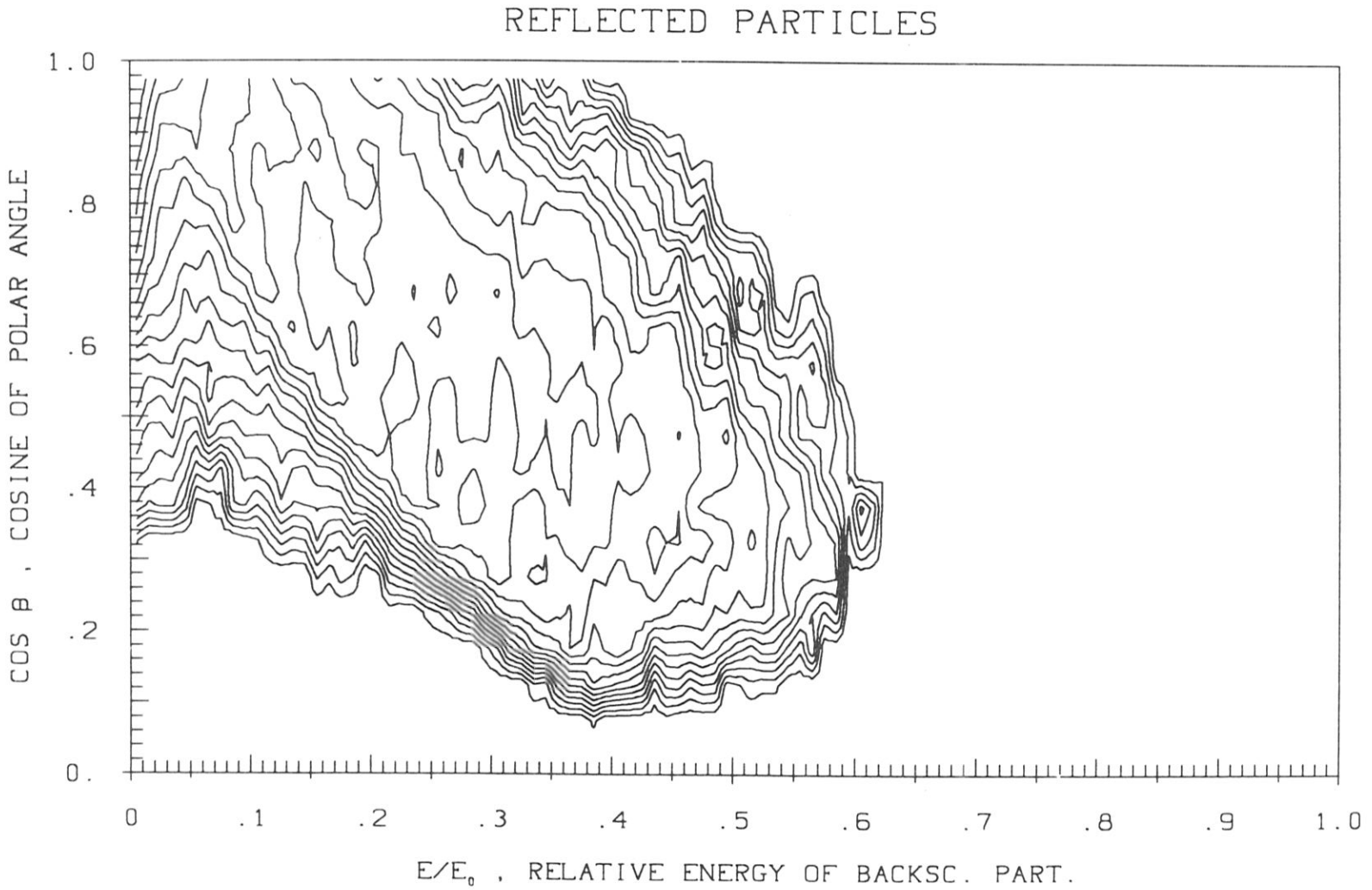

Fig. 22b Intensity distributions of backscattered particles versus the energy of the backscattered particles and the cosine of the polar emission angle, ß, in the forward direction ($-15^{\circ} < \varphi < 15^{\circ}$). Ni is bombarded by 1 keV ar at an angle of incidence, $\alpha = 30^{\circ}$. The contour plot shows lines of equal intensity per solid angle. The

Z1=18.00 M1=39.95 Z2=28.00 M2=58.71 C1=0.12

E_0=1000.eV α=45.0 Grad $0. < |\varphi| < 15.0$ LOG

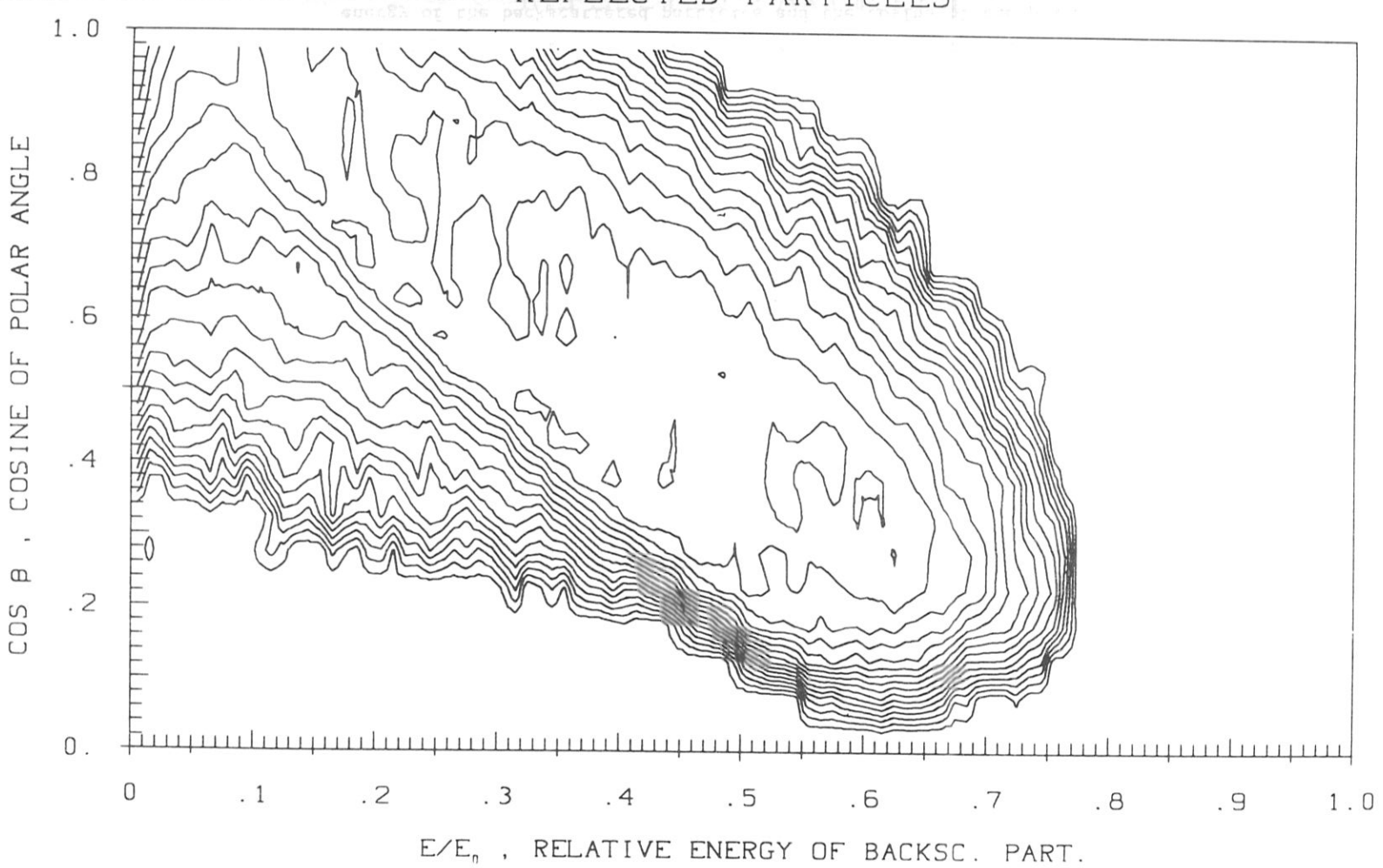

Fig. 22c Intensity distributions of backscattered particles versus the energy of the backscattered particles and the cosine of the polar emission angle, ß, in the forward direction ($-15^{\circ} < \varphi < 15^{\circ}$). Ni is bombarded by 1 keV ar at an angle of incidence, α = 45°. The contour plot shows lines of equal intensity per solid angle. The distance, c = 0.12, between adjacent contour lines is logarithmic.

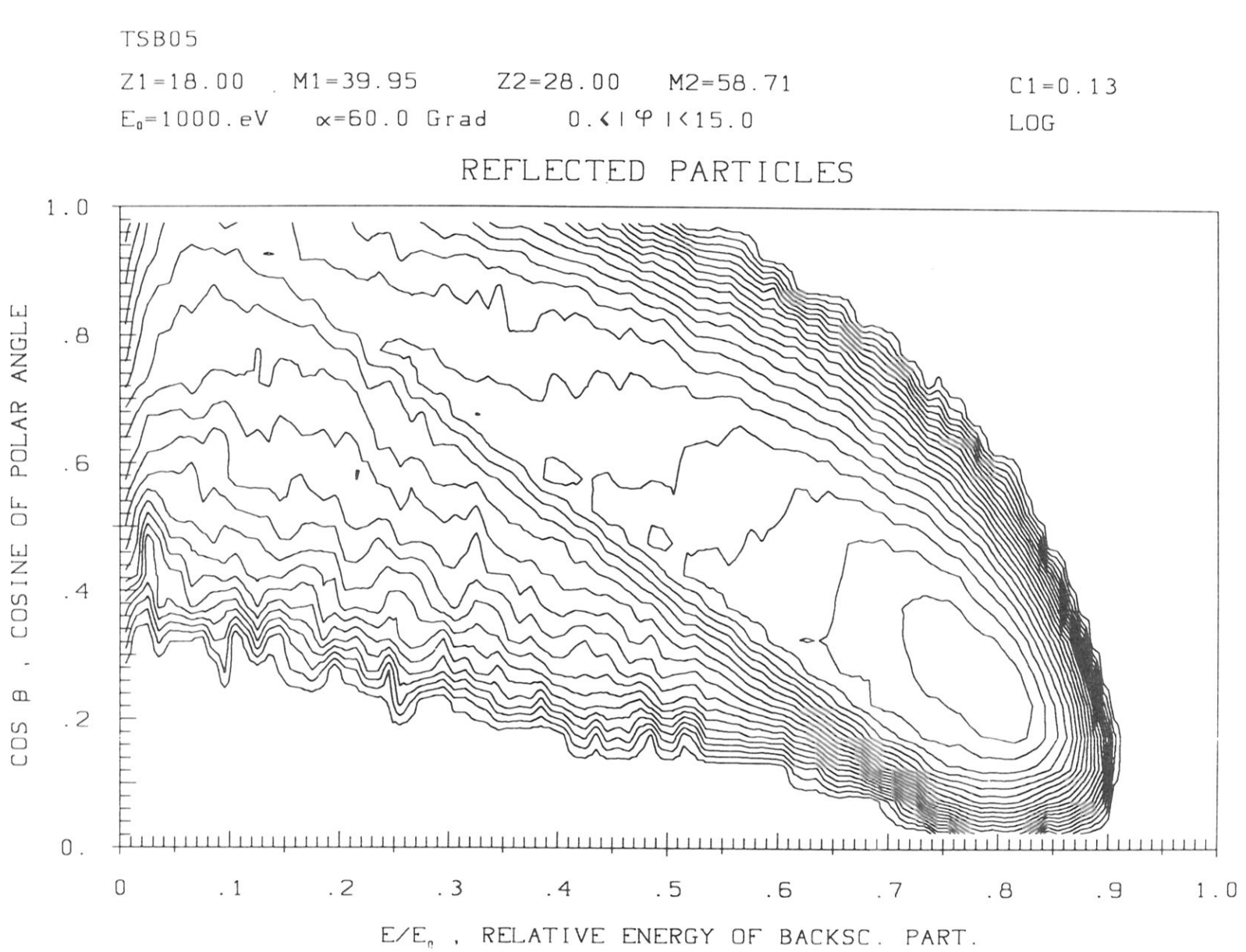

Fig. 22d Intensity distributions of backscattered particles versus the energy of the backscattered particles and the cosine of the polar emission angle, ß, in the forward direction ($-15^{o}<\varphi<15^{o}$). Ni is bombarded by 1 keV Ar at an angle of incidence, α = 60^{o}. The contour plot shows lines of equal intensity per solid angle. The distance, c = 0.13, between adjacent contour lines is

Z1=18.00 M1=39.95 Z2=28.00 M2=58.71 C1=0.18

E_0=1000.eV α=75.0 Grad $0. < |\varphi| < 15.0$ LOG

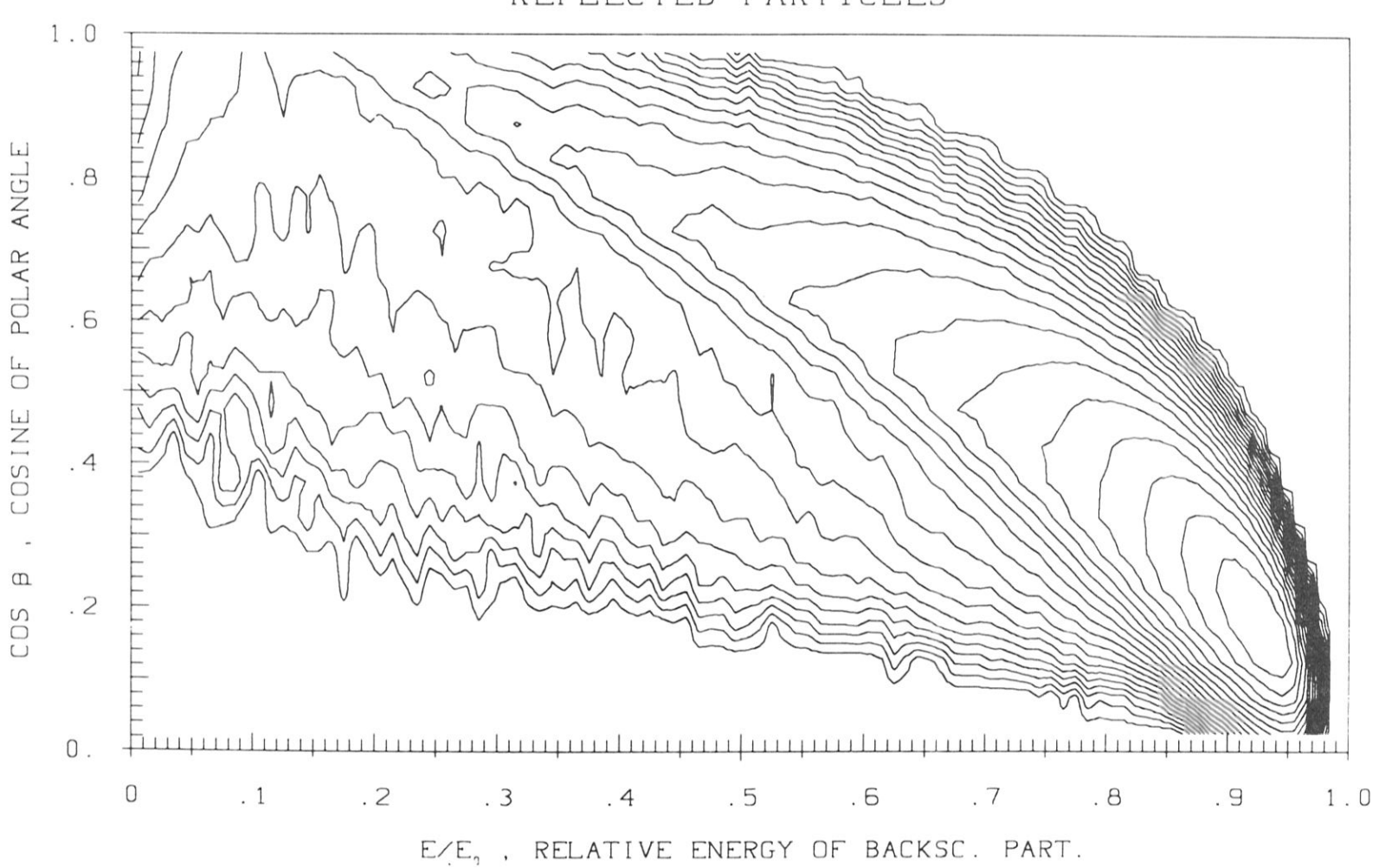

Fig. 22e Intensity distributions of backscattered particles versus the energy of the backscattered particles and the cosine of the polar emission angle, ß, in the forward direction ($-15^{\circ} < \varphi < 15^{\circ}$). Ni is bombarded by 1 keV ar at an angle of incidence, $\alpha = 75^{\circ}$. The contour plot shows lines of equal intensity per solid angle. The distance, c = 0.18, between adjacent contour lines is logarithmic.

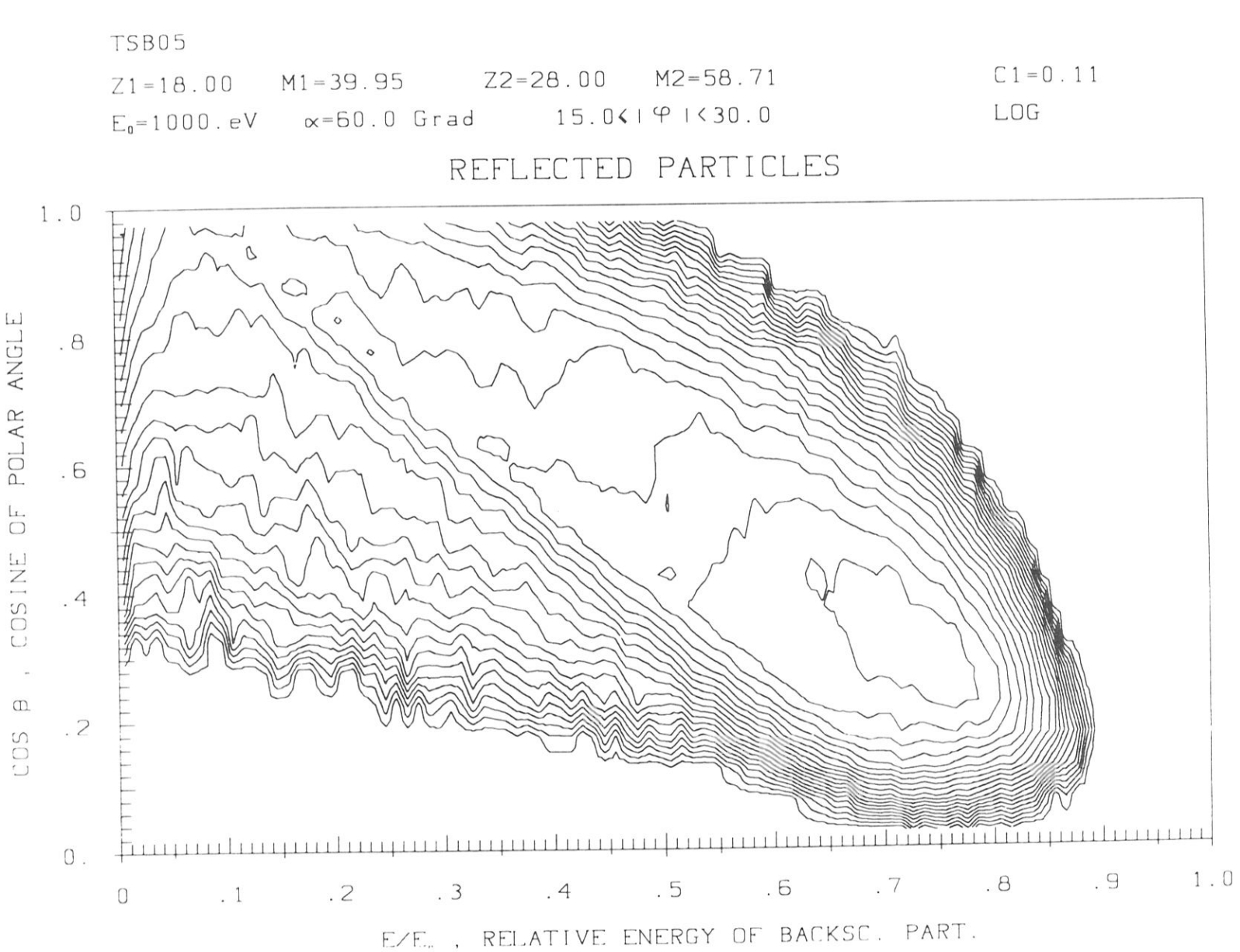

Fig. 23a Intensity distributions of backscattered particles versus the relative energy of the backscattered particles and the cosine of the polar emission angle, ß, in an azimuthal direction, $15^{o} < |\varphi| < 30^{o}$. Ni is bombarded by 1 keV Ar at an angle of incidence, $\alpha = 60^{o}$. The contour plot shows lines of equal intensity per solid angle. The distance C = 0.11 between adjacent contour lines is

Z1=18.00 M1=39.95 Z2=28.00 M2=58.71 C1=0.12

E_0=1000.eV α=60.0 Grad 45.0<|φ|<60.0 LOG

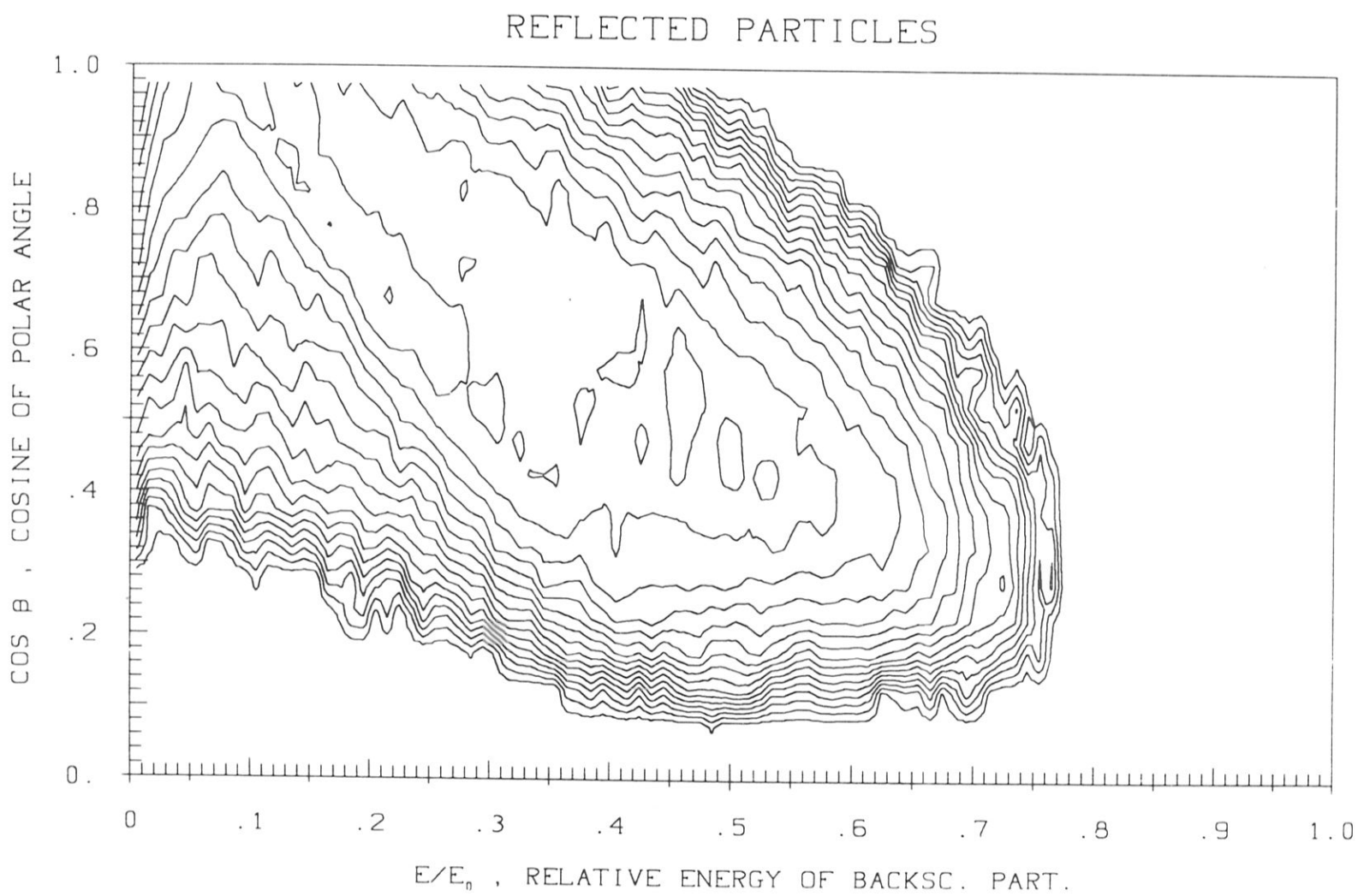

Fig. 23b Intensity distributions of backscattered particles versus the relative energy of the backscattered particles and the cosine of the polar emission angle, ß, in an azimuthal direction, $45^\circ < |\varphi| < 60^\circ$. Ni is bombarded by 1 keV Ar at an angle of incidence, $\alpha = 60^\circ$. The contour plot shows lines of equal intensity per solid angle. The distance, c = 0.12, between adjacent contour lines is logarithmic.

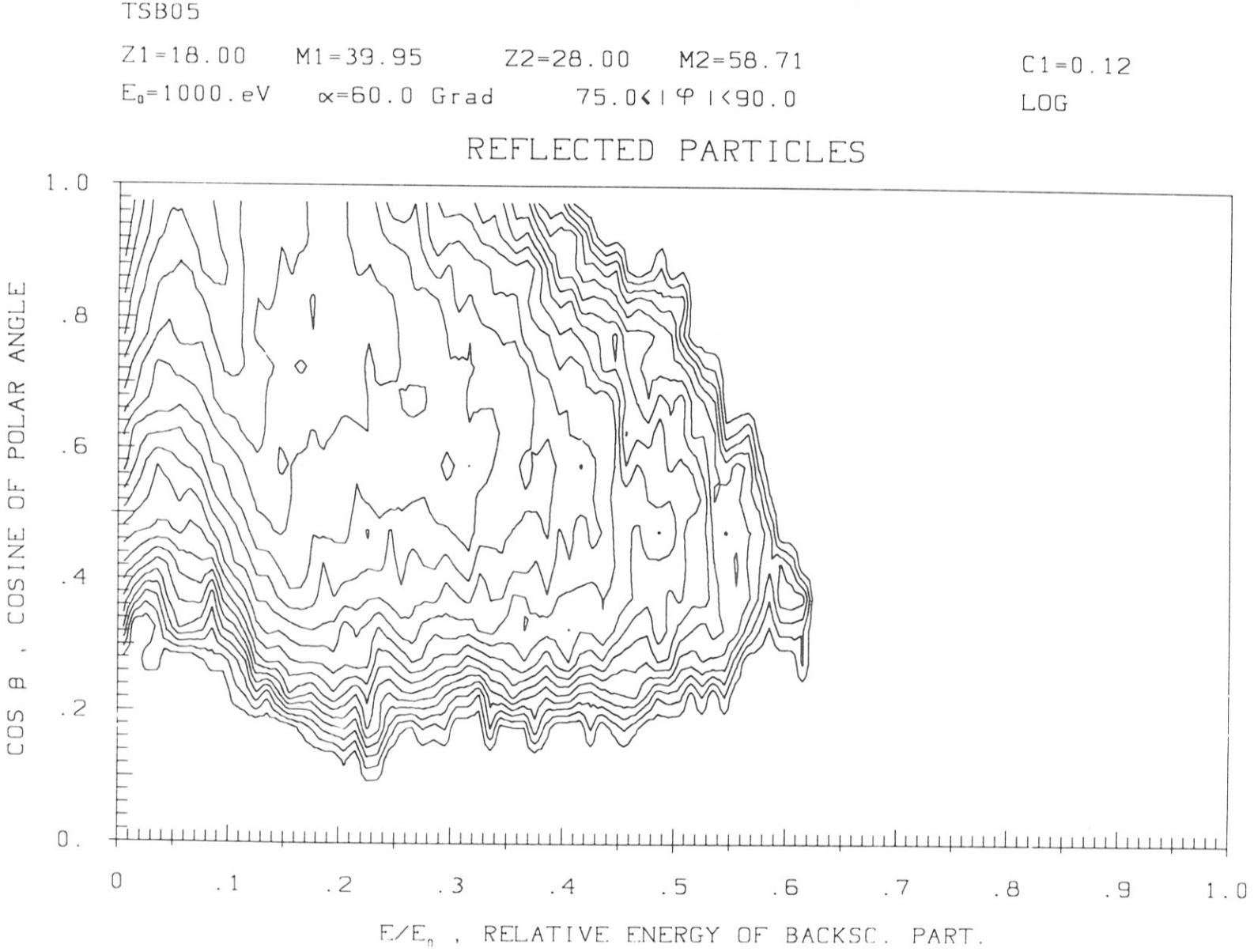

Fig. 23c Intensity distributions of backscattered particles versus the relative energy of the backscattered particles and the cosine of the polar emission angle, β, in an azimuthal direction, $75^{\circ} < |\varphi| < 90^{\circ}$. Ni is bombarded by 1 keV Ar at an angle of incidence, $\alpha = 60^{\circ}$. The contour plot shows lines of equal intensity per solid angle.

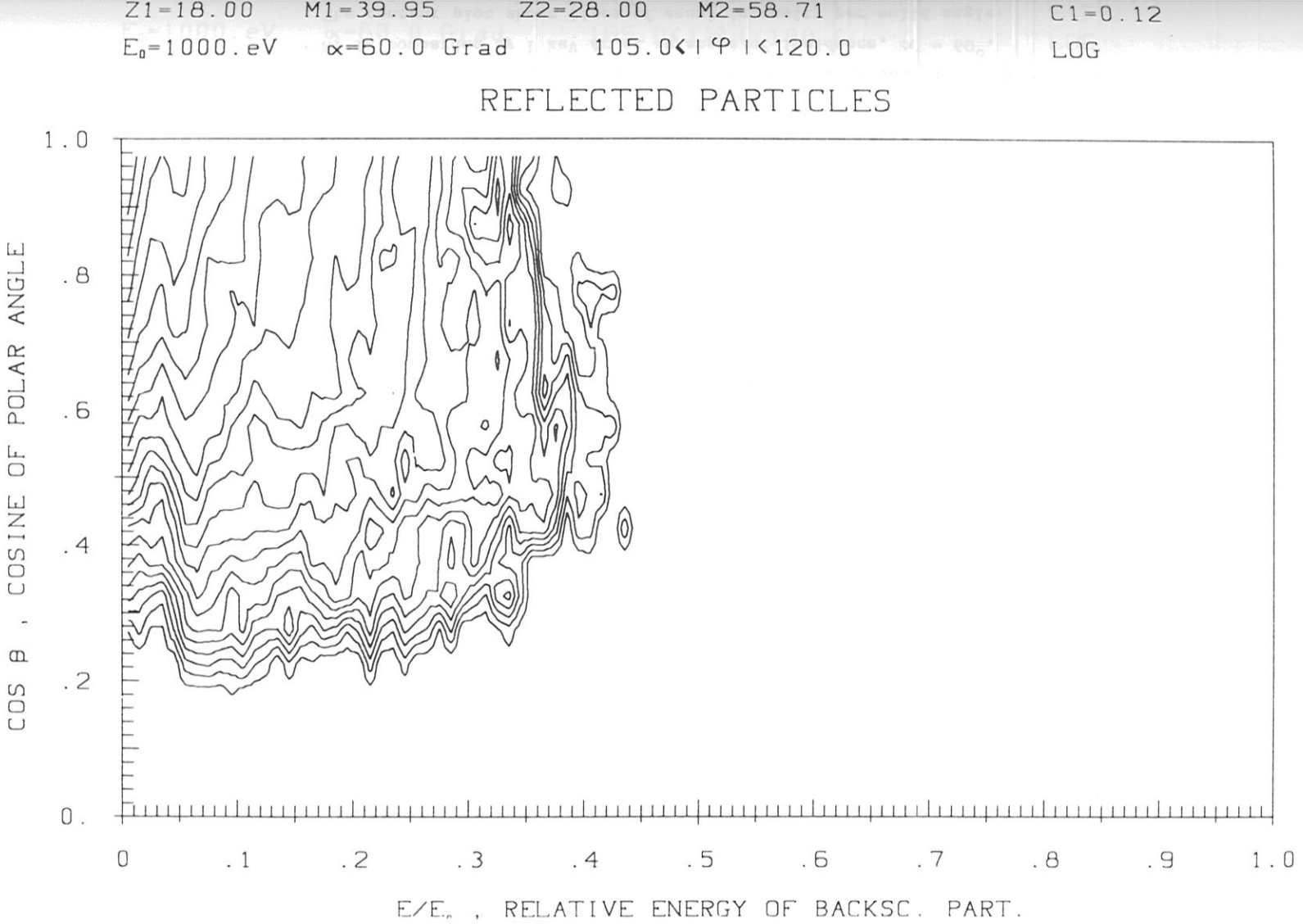

Fig. 23d Intensity distributions of backscattered particles versus the relative energy of the backscattered particles and the cosine of the polar emission angle, ß, in an azimuthal direction, $105^{\circ} < |\varphi| < 120^{\circ}$. Ni is bombarded by 1 keV Ar at an angle of incidence, $\alpha = 60^{\circ}$. The contour plot shows lines of equal intensity per solid angle. The distance, c = 0.12, between adjacent contour lines is logarithmic.

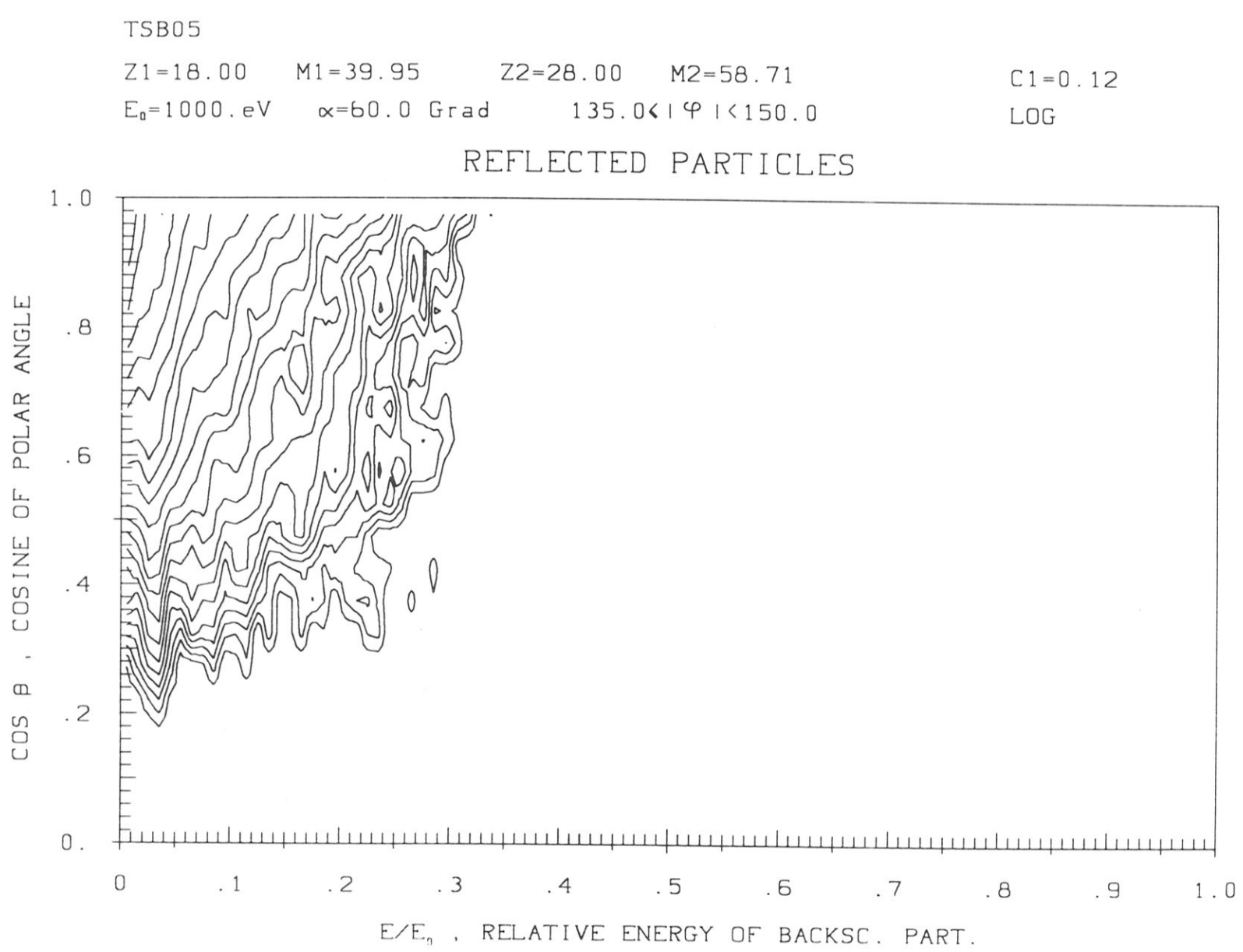

Fig. 23e Intensity distributions of backscattered particles versus the relative energy of the backscattered particles and the cosine of the polar emission angle, ß, in an azimuthal direction, $135^{o} < |\varphi| < 150^{o}$. Ni is bombarded by 1 keV Ar at an angle of incidence, $\alpha = 60^{o}$. The contour plot shows lines of equal intensity per solid angle.

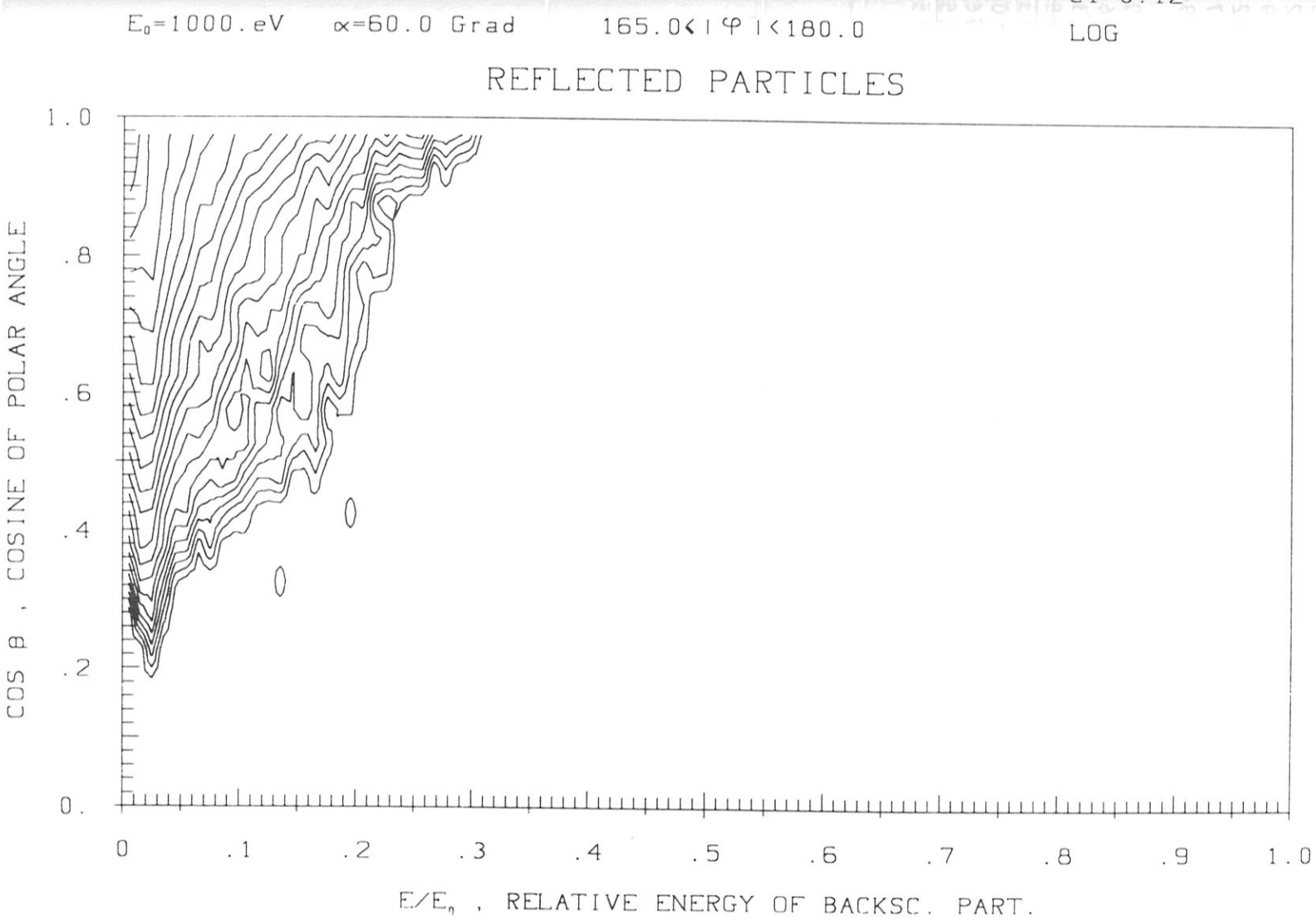

Fig. 23f Intensity distributions of backscattered particles versus the relative energy of the backscattered particles and the cosine of the polar emission angle, ß, in an azimuthal direction, $135^{\circ} < |\varphi| < 180^{\circ}$. Ni is bombarded by 1 keV Ar at an angle of incidence, $\alpha = 60^{\circ}$. The contour plot shows lines of equal intensity per solid angle. The distance, c = 0.12, between adjacent contour lines is logarithmic.

REFLECTION DATA FROM TRIM CALCULATIONS

	E0 (KEV)	EPS	ALPHA (DEGREE)	RN	RE	RE/RN
HE4 -> LI	0.035	5.61E-2	0	6.41E-2	7.71E-3	0.120
	0.05	8.00E-2	0	5.27E-2	6.61E-3	0.126
	0.1	1.60E-1	0	3.88E-2	4.85E-2	0.125
	0.3	4.80E-1	0	2.53E-2	3.09E-3	0.122
	1.0	1.60E+0	0	1.30E-2	1.68E-3	0.129
	3.0	4.80E+0	0	4.65E-3	5.20E-4	0.112
	10.0	1.60E+1	0	1.40E-3	1.78E-4	0.127
	30.0	4.80E+2	0	1.52E-4	1.40E-5	0.0894
LI -> LI	0.025	1.97E-2	0	1.26E-3	7.66E-5	0.0608
	0.03	2.37E-2	0	1.61E-3	1.08E-4	0.0668
	0.04	3.16E-2	0	2.52E-3	1.59E-4	0.0631
	0.05	3.95E-2	0	2.90E-3	1.70E-4	0.0587
	0.1	7.89E-2	0	5.30E-3	2.84E-4	0.0535
	0.3	2.37E-1	0	3.15E-3	1.57E-4	0.0500
	1.0	7.89E-1	0	2.26E-3	1.74E-4	0.0769
	3.0	2.37E+0	0	9.20E-4	5.97E-5	0.0650
	10.0	7.89E+0	0	6.00E-5	3.31E-6	0.055
	30.0	2.37E+1	0	0.	0.	0.

REFLECTION DATA FROM TRIM CALCULATIONS

	E0 (KEV)	EPS	ALPHA (DEGREE)	RN	RE	RE/RN
HE4 -> BE	0.024	2.98E-2	0	1.78E-1	2.99E-2	0.168
	0.03	3.73E-2	0	1.55E-1	2.61E-2	0.169
	0.05	6.21E-2	0	1.17E-1	2.00E-2	0.171
	0.07	8.69E-2	0	9.45E-2	1.57E-2	0.166
	0.1	1.24E-1	0	7.94E-2	1.36E-2	0.172
	0.15	1.86E-1	0	6.47E-2	1.09E-2	0.169
	0.2	2.48E-1	0	5.53E-2	9.48E-3	0.171
	0.3	3.73E-1	0	4.56E-2	7.65E-3	0.168
	0.5	6.21E-1	0	3.38E-2	5.78E-3	0.171
	1.0	1.24E+0	0	2.56E-2	4.13E-3	0.161
BE -> BE	0.05	2.02E-2	0	1.45E-3	8.75E-5	0.0597
	0.07	2.82E-2	0	1.75E-3	9.34E-5	0.0540
	0.1	4.03E-2	0	3.00E-3	1.63E-4	0.0540
	0.15	6.05E-2	0	4.27E-3	2.23E-4	0.0506
	0.2	8.07E-2	0	3.60E-3	1.77E-4	0.0500
	0.3	1.21E-1	0	3.90E-3	2.28E-4	0.0603
	0.5	2.02E-1	0	3.80E-3	1.81E-4	0.0489
	0.7	2.82E-1	0	2.90E-3	1.86E-4	0.0624
	1.0	4.03E-1	0	2.60E-3	1.41E-4	0.0554
	2.0	8.07E-1	0	1.55E-3	7.08E-5	0.0457
	5.0	2.02E+0	0	9.50E-4	7.07E-5	0.0744
NE -> BE	0.05	4.20E-3	0	5.00E-5	1.96E-6	0.0420

REFLECTION DATA FROM TRIM CALCULATIONS

	E0 (KEV)	EPS	ALPHA (DEGREE)	RN	RE	RE/RN
HE4 -> C	0.05	4.13E-2	0	1.42E-1	2.82E-2	0.198
	0.07	5.78E-2	0	1.26E-1	2.52E-2	0.201
	0.1	8.26E-1	0	1.04E-1	2.11E-2	0.204
	0.3	2.48E-1	0	6.60E-2	1.32E-2	0.200
	1.0	8.26E-1	0	3.60E-2	6.84E-3	0.190
	3.0	2.48E+0	0	1.71E-2	2.99E-3	0.175
	10.0	8.26E+0	0	4.60E-3	7.69E-4	0.167
	30.0	2.48E+1	0	1.20E-3	1.75E-4	0.146
	100.0	8.26E+1	0	3.00E-4	4.83E-5	0.161
C -> C	0.1	1.57E-2	0	1.29E-3	8.25E-5	0.0643
	0.3	4.70E-2	0	3.81E-3	2.07E-4	0.0541
	1.0	1.57E-1	0	3.73E-3	1.94E-4	0.0526
	3.0	4.70E-1	0	2.54E-3	1.47E-4	0.0587
	30.0	4.70E+0	0	1.80E-4	9.99E-6	0.0555
	100.0	1.57E+1	0	4.10E-5	1.27E-6	0.0310
NE -> C	0.05	3.20E-3	0	1.20E-3	3.74E-5	0.0320
	0.07	4.48E-3	0	1.14E-3	2.26E-5	0.0198
	0.1	6.40E-3	0	4.70E-4	1.21E-5	0.0258
	0.2	1.28E-2	0	3.20E-4	7.30E-6	0.0228
	0.3	1.92E-2	0	1.90E-4	2.84E-6	0.0150
	0.5	3.20E-2	0	1.60E-4	3.66E-6	0.0229
	1.0	6.40E-2	0	1.60E-4	2.23E-6	0.0139
	3.0	1.92E-1	0	1.10E-4	2.15E-6	0.0205
C -> C	0.1	1.57E-2	0	1.19E-3	8.01E-5	0.0673
	0.1	1.57E-2	10	2.90E-3	2.39E-4	0.0822
	0.1	1.57E-2	20	9.24E-3	1.08E-3	0.117
	0.1	1.57E-2	30	2.94E-2	4.56E-3	0.155
	0.1	1.57E-2	40	7.64E-2	1.62E-2	0.212
	0.1	1.57E-2	50	1.81E-1	5.21E-2	0.287
	0.1	1.57E-2	55	2.60E-1	8.66E-2	0.333
	0.1	1.57E-2	57.5	3.04E-1	1.09E-1	0.360
	0.1	1.57E-2	60	3.60E-1	1.38E-1	0.384
	0.1	1.57E-2	62.5	4.18E-1	1.72E-1	0.412
	0.1	1.57E-2	65	4.77E-1	2.08E-1	0.436
	0.1	1.57E-2	67.5	5.40E-1	2.53E-1	0.469
	0.1	1.57E-2	70	6.11E-1	3.00E-1	0.491
	0.1	1.57E-2	75	7.33E-1	4.01E-1	0.548
	0.1	1.57E-2	80	8.27E-1	4.94E-1	0.597
	0.1	1.57E-2	82.5	8.57E-1	5.16E-1	0.602
	0.1	1.57E-2	85	8.77E-1	5.50E-1	0.628
	0.1	1.57E-2	87.5	8.91E-1	5.58E-1	0.627

C -> C	1.0	1.57E-1	0	5.30E-3	3.33E-4	0.0629
	1.0	1.57E-1	10	5.17E-3	3.23E-4	0.0630
	1.0	1.57E-1	15	6.32E-3	4.76E-4	0.0753
	1.0	1.57E-1	20	9.20E-3	7.46E-4	0.0810
	1.0	1.57E-1	30	1.66E-2	1.74E-3	0.105
	1.0	1.57E-1	40	3.92E-2	5.94E-3	0.152
	1.0	1.57E-1	45	5.49E-2	9.87E-3	0.180
	1.0	1.57E-1	50	8.09E-2	1.66E-2	0.205
	1.0	1.57E-1	55	1.25E-1	3.16E-2	0.253
	1.0	1.57E-1	60	1.72E-1	5.04E-2	0.294
	1.0	1.57E-1	65	2.34E-1	8.27E-2	0.354
	1.0	1.57E-1	67.5	2.82E-1	1.13E-1	0.399
	1.0	1.57E-1	70	3.28E-1	1.43E-1	0.437
	1.0	1.57E-1	72.5	4.03E-1	1.99E-1	0.493
	1.0	1.57E-1	75	4.79E-1	2.64E-1	0.552
	1.0	1.57E-1	77.5	5.96E-1	3.71E-1	0.623
	1.0	1.57E-1	80	7.21E-1	5.14E-1	0.713
	1.0	1.57E-1	82.5	8.53E-1	6.87E-1	0.806
	1.0	1.57E-1	85	9.60E-1	8.51E-1	0.887
	1.0	1.57E-1	87.5	9.93E-1	9.23E-1	0.930

REFLECTION DATA FROM TRIM CALCULATIONS

	E0 (KEV)	EPS	ALPHA (DEGREE)	RN	RE	RE/RN
HE4 -> SI	0.03	1.02E-2	0	4.08E-1	1.78E-1	0.437
	0.035	1.19E-2	0	3.91E-1	1.71E-1	0.437
	0.05	1.70E-2	0	3.59E-1	1.55E-1	0.431
	0.07	2.38E-2	0	3.41E-1	1.44E-1	0.422
	0.1	3.41E-2	0	3.22E-1	1.33E-1	0.413
	0.25	8.52E-2	0	2.76E-1	1.13E-1	0.408
	0.3	1.02E-1	0	2.59E-1	1.04E-1	0.403
	0.5	1.70E-1	0	2.40E-1	9.38E-2	0.391
	1.0	3.41E-1	0	2.06E-1	7.71E-2	0.375
	2.0	6.82E-1	0	1.68E-1	5.98E-2	0.356
	3.0	1.02E+0	0	1.37E-1	4.68E-2	0.342
	4.0	1.36E+0	0	1.16E-1	3.71E-2	0.319
	8.0	2.72E+0	0	7.39E-2	2.10E-2	0.285
	10.0	3.41E+0	0	5.69E-2	1.51E-2	0.266
	12.0	4.09E+0	0	5.00E-2	1.31E-2	0.262
	24.0	8.18E+0	0	2.24E-2	4.91E-3	0.219
	30.0	1.02E+1	0	1.43E-2	2.93E-3	0.205
	40.0	1.36E+1	0	7.80E-3	1.68E-3	0.215
	80.0	2.73E+1	0	4.10E-3	7.67E-4	0.187
	100.0	3.41E+1	0	2.35E-3	4.88E-4	0.208
	300.0	1.02E+2	0	4.50E-4	7.43E-5	0.165
NE -> SI	0.04	1.49E-3	0	1.21E-1	8.88E-3	0.0737
	0.05	1.86E-3	0	1.08E-1	8.40E-3	0.0776
	0.07	2.61E-3	0	1.04E-1	7.15E-3	0.0690
	0.1	3.73E-3	0	8.78E-2	6.38E-3	0.0726
	0.3	1.12E-2	0	5.79E-2	4.20E-3	0.0725
	1.0	3.73E-2	0	3.76E-2	2.76E-3	0.0735
	3.0	1.12E-1	0	2.50E-2	1.99E-3	0.0797
	10.0	3.73E-1	0	1.46E-2	1.25E-3	0.0861
	30.0	1.12E+0	0	7.00E-3	5.40E-4	0.0772
	100.0	3.73E+0	0	2.00E-3	1.66E-4	0.0830
	300.0	1.12E+1	0	5.00E-4	4.67E-5	0.0933
SI -> SI	0.04	8.67E-4	0	8.50E-4	7.08E-5	0.0833
	0.05	1.08E-3	0	2.02E-3	1.47E-4	0.0730
	0.07	1.52E-3	0	3.70E-3	2.60E-4	0.0703
	0.1	2.17E-3	0	3.56E-3	2.15E-4	0.0604
	0.3	6.51E-3	0	9.28E-3	4.57E-4	0.0492
	1.0	2.17E-2	0	1.07E-2	4.82E-4	0.0451
	3.0	6.51E-2	0	8.00E-3	3.64E-4	0.0456
	10.0	2.17E-1	0	4.70E-3	2.39E-4	0.0508
	30.0	6.51E-1	0	2.30E-3	1.25E-4	0.0543
	100.0	2.17E+0	0	5.20E-4	2.47E-5	0.0475
AR -> SI	0.05	6.67E-4	0	5.50E-3	1.24E-4	0.0227
	0.07	9.34E-4	0	4.15E-3	8.44E-5	0.0203
	0.1	1.33E-3	0	3.66E-3	7.15E-5	0.0195
	0.2	2.67E-3	0	2.94E-3	4.73E-5	0.0161
	0.3	4.00E-3	0	2.12E-3	4.74E-5	0.0224
	0.5	6.67E-3	0	2.37E-3	3.66E-5	0.0154
	1.0	1.33E-2	0	2.02E-3	3.75E-5	0.0185
	3.0	4.00E-2	0	1.66E-3	3.40E-5	0.0205
	10.0	1.33E-1	0	1.04E-3	2.70E-5	0.0260
	30.0	4.00E-1	0	3.90E-4	1.23E-5	0.0315

REFLECTION DATA FROM TRIM CALCULATIONS

	E0 (KEV)	EPS	ALPHA (DEGREE)	RN	RE	RE/RN
NE -> TI	0.05	1.32E-3	0	3.07E-1	5.21E-2	0.170
	0.1	2.63E-3	0	2.34E-1	3.98E-2	0.170
	0.2	5.27E-3	0	1.81E-1	2.97E-2	0.165
	0.5	1.32E-2	0	1.40E-1	2.32E-2	0.166
	1.0	2.63E-2	0	1.15E-1	1.85E-2	0.161
	2.0	5.27E-2	0	9.90E-2	1.60E-2	0.162
	5.0	1.32E-1	0	7.45E-2	1.24E-2	0.166
	10.0	2.63E-1	0	5.89E-2	9.68E-3	0.164
	20.0	5.27E-1	0	4.35E-2	7.12E-3	0.164
	50.0	1.32E+0	0	2.39E-2	3.89E-3	0.163
	100.0	2.63E+0	0	1.42E-2	2.07E-3	0.146
	200.0	5.27E+0	0	7.56E-3	1.10E-3	0.146
NE -> TI	0.038	1.00E-3	0	3.27E-1	5.58E-2	0.170
	0.038	1.00E-3	10	3.49E-1	6.46E-2	0.185
	0.038	1.00E-3	20	3.95E-1	8.59E-2	0.217
	0.038	1.00E-3	30	4.60E-1	1.23E-1	0.268
	0.038	1.00E-3	40	5.60E-1	1.88E-1	0.336
	0.038	1.00E-3	45	6.14E-1	2.34E-1	0.381
	0.038	1.00E-3	50	6.79E-1	2.90E-1	0.428
	0.038	1.00E-3	60	8.17E-1	4.43E-1	0.542
	0.038	1.00E-3	70	9.43E-1	6.56E-1	0.695
	0.038	1.00E-3	75	9.83E-1	7.81E-1	0.795
	0.038	1.00E-3	80	9.98E-1	8.92E-1	0.894
	0.038	1.00E-3	85	1.00E+0	9.68E-1	0.968
NE -> TI	0.380	1.00E-2	0	1.50E-1	2.48E-2	0.166
	0.380	1.00E-2	10	1.58E-1	2.74E-2	0.173
	0.380	1.00E-2	20	1.79E-1	3.41E-2	0.191
	0.380	1.00E-2	30	2.11E-1	4.70E-2	0.223
	0.380	1.00E-2	40	2.67E-1	7.24E-2	0.271
	0.380	1.00E-2	45	3.00E-1	9.01E-2	0.301
	0.380	1.00E-2	50	3.49E-1	1.18E-1	0.337
	0.380	1.00E-2	60	4.67E-1	2.04E-1	0.437
	0.380	1.00E-2	70	6.71E-1	3.97E-1	0.592
	0.380	1.00E-2	75	8.07E-1	5.64E-1	0.699
	0.380	1.00E-2	80	9.47E-1	7.93E-1	0.837
	0.380	1.00E-2	85	1.00E+0	9.68E-1	0.968
NE -> TI	3.798	1.00E-1	0	8.05E-2	1.32E-2	0.164
	3.798	1.00E-1	10	8.54E-2	1.46E-2	0.171
	3.798	1.00E-1	20	9.52E-2	1.76E-2	0.184
	3.798	1.00E-1	30	1.23E-1	2.63E-2	0.213
	3.798	1.00E-1	40	1.60E-1	4.04E-2	0.253
	3.798	1.00E-1	45	1.82E-1	4.95E-2	0.272
	3.798	1.00E-1	50	2.14E-1	6.41E-2	0.300
	3.798	1.00E-1	60	2.96E-1	1.09E-1	0.368
	3.798	1.00E-1	70	4.24E-1	2.01E-1	0.474
	3.798	1.00E-1	75	5.06E-1	2.80E-1	0.550
	3.798	1.00E-1	80	6.40E-1	4.27E-1	0.668
	3.798	1.00E-1	85	9.02E-1	7.95E-1	0.881

REFLECTION DATA FROM TRIM CALCULATIONS

	E0 (KEV)	EPS	ALPHA (DEGREE)	RN	RE	RE/RN
HE4 -> NI	0.05	7.64E-3	0	4.49E-1	2.38E-1	0.531
	0.07	1.07E-2	0	4.27E-1	2.21E-1	0.518
	0.10	1.53E-2	0	4.08E-1	2.06E-1	0.506
	0.15	2.29E-2	0	3.83E-1	1.87E-1	0.488
	0.20	3.06E-2	0	3.66E-1	1.77E-1	0.482
	0.30	4.59E-2	0	3.48E-1	1.63E-1	0.469
	0.50	7.65E-2	0	3.25E-1	1.48E-1	0.455
	0.70	1.07E-1	0	3.03E-1	1.37E-1	0.451
	1.0	1.53E-1	0	2.84E-1	1.25E-1	0.440
	1.5	2.29E-1	0	2.63E-1	1.11E-1	0.423
	2.0	3.06E-1	0	2.39E-1	9.85E-2	0.413
	3.0	4.59E-1	0	2.08E-1	8.42E-2	0.406
	5.0	7.65E-1	0	1.73E-1	6.60E-2	0.382
	10.0	1.53E+0	0	1.15E-1	3.99E-2	0.347
	20.0	3.06E+0	0	6.84E-2	2.06E-2	0.301
	50.0	7.65E+0	0	2.41E-2	6.45E-3	0.268
	100.0	1.53E+1	0	1.02E-2	2.53E-3	0.249
NE -> NI	0.03	6.25E-4	0	4.28E-1	1.00E-1	0.234
	0.04	8.33E-4	0	4.19E-1	9.76E-2	0.233
	0.05	1.04E-3	0	3.93E-1	9.17E-2	0.233
	0.07	1.46E-3	0	3.60E-1	8.55E-2	0.238
	0.10	2.08E-3	0	3.25E-1	7.46E-2	0.223
	0.15	3.12E-3	0	2.79E-1	6.39E-2	0.229
	0.2	4.17E-3	0	2.55E-1	5.63E-2	0.223
	0.3	6.25E-3	0	2.18E-1	4.87E-2	0.223
	0.5	1.04E-2	0	1.89E-1	4.13E-2	0.219
	0.7	1.46E-2	0	1.83E-1	3.86E-2	0.183
	1.0	2.08E-2	0	1.63E-1	3.36E-2	0.207
	1.5	3.12E-2	0	1.47E-1	3.06E-2	0.209
	2.0	4.17E-2	0	1.37E-1	2.80E-2	0.205
	3.0	6.25E-2	0	1.19E-1	2.43E-2	0.204
	5.0	1.04E-1	0	1.07E-1	2.10E-2	0.197
	7.0	1.46E-1	0	8.98E-2	1.81E-2	0.201
	10.0	2.08E-1	0	8.14E-2	1.66E-2	0.204
	15.0	3.12E-1	0	7.05E-2	1.42E-2	0.202
	20.0	4.17E-1	0	6.23E-2	1.23E-2	0.197
	30.0	6.25E-1	0	4.80E-2	9.65E-3	0.201
	50.0	1.04E+0	0	3.65E-2	7.16E-3	0.197
	100.0	2.08E+0	0	2.38E-2	4.01E-3	0.169
	200.0	4.17E+0	0	9.50E-3	1.73E-3	0.184
	300.0	6.25E+0	0	8.10E-3	1.21E-3	0.150

AR -> NI	0.04	3.42E-4	0	1.73E-1	1.45E-2	0.0839
	0.05	4.27E-4	0	1.59E-1	1.41E-2	0.0880
	0.07	5.98E-4	0	1.65E-1	1.40E-2	0.0846
	0.1	8.54E-4	0	1.61E-1	1.30E-2	0.0811
	0.15	1.28E-3	0	1.50E-1	1.18E-2	0.0784
	0.2	1.71E-3	0	1.38E-1	1.08E-3	0.0782
	0.3	2.56E-3	0	1.20E-1	8.83E-3	0.0735
	0.5	4.27E-3	0	1.01E-1	7.23E-3	0.0721
	0.7	5.98E-3	0	8.56E-1	6.69E-3	0.0786
	1.0	8.54E-3	0	7.40E-2	5.45E-3	0.0740
	2.0	1.71E-2	0	5.52E-2	4.26E-3	0.0784
	3.0	2.56E-2	0	4.60E-2	3.59E-3	0.0775
	5.0	4.27E-2	0	4.24E-2	3.15E-3	0.0751
	10.0	8.54E-2	0	3.25E-2	2.81E-3	0.0860
	11.71	1.00E-1	0	3.15E-2	2.65E-3	0.0842
	20.0	1.71E-1	0	2.75E-2	2.54E-3	0.0933
	30.0	2.56E-1	0	1.94E-2	1.71E-3	0.0880
	50.0	4.27E-1	0	1.60E-2	1.23E-3	0.0762
	100.0	8.54E-1	0	9.40E-3	7.94E-4	0.0845
	200.0	1.71E+0	0	5.50E-3	9.89E-4	0.181
	300.0	2.56E+0	0	3.00E-3	2.20E-4	0.0740
NI -> NI	0.03	1.29E-4	0	3.00E-5	2.89E-6	0.0962
	0.04	1.72E-4	0	3.20E-4	2.57E-5	0.0804
	0.05	2.15E-4	0	1.46E-3	1.14E-4	0.0777
	0.07	3.01E-4	0	4.18E-3	3.35E-4	0.0801
	0.1	4.30E-4	0	8.54E-3	5.16E-4	0.0608
	0.15	6.45E-4	0	1.38E-2	8.56E-4	0.0619
	0.2	8.61E-4	0	1.56E-2	8.40E-4	0.0537
	0.3	1.29E-3	0	1.79E-2	8.55E-4	0.0477
	0.5	2.15E-3	0	1.94E-2	8.22E-4	0.0423
	1.0	4.30E-3	0	1.78E-2	7.00E-4	0.0393
	2.0	8.61E-3	0	1.56E-2	6.13E-4	0.0393
	5.0	2.15E-2	0	1.17E-2	4.69E-4	0.0400
	10.0	4.30E-2	0	9.77E-3	4.20E-4	0.0430
	30.0	1.29E-1	0	6.35E-3	2.99E-4	0.0472
	100.0	4.30E-1	0	3.38E-3	1.65E-4	0.0489
	300.0	1.29E+0	0	1.26E-3	6.99E-5	0.0555
KR -> NI	0.05	1.32E-4	0	9.56E-3	2.65E-4	0.0277
	0.07	1.85E-4	0	9.60E-3	2.41E-4	0.0251
	0.1	2.64E-4	0	7.34E-3	2.05E-4	0.0280
	0.3	7.92E-4	0	4.74E-3	9.95E-5	0.0210
	1.0	2.64E-3	0	2.78E-3	4.75E-5	0.0171
	3.0	7.92E-3	0	2.36E-3	4.61E-5	0.0200
	10.0	2.64E-2	0	1.73E-3	4.15E-5	0.0240
	30.0	7.92E-2	0	1.41E-3	3.56E-5	0.0253
	100.0	2.64E-1	0	5.30E-4	1.64E-5	0.0309
XE -> NI	0.1	1.22E-4	0	1.60E-4	2.25E-6	0.0140
	0.3	3.67E-4	0	3.00E-5	3.63E-7	0.0121

NE -> NI	1.0	2.08E-2	0	1.59E-1	3.35E-2	0.210
	1.0	2.08E-2	5	1.68E-1	3.52E-2	0.210
	1.0	2.08E-2	10	1.70E-1	3.61E-2	0.212
	1.0	2.08E-2	15	1.79E-1	3.93E-2	0.219
	1.0	2.08E-2	20	1.90E-1	4.26E-2	0.224
	1.0	2.08E-2	25	2.01E-1	4.91E-2	0.245
	1.0	2.08E-2	30	2.15E-1	5.58E-2	0.260
	1.0	2.08E-2	40	2.66E-1	8.05E-2	0.302
	1.0	2.08E-2	45	3.08E-1	1.02E-1	0.332
	1.0	2.08E-2	50	3.37E-1	1.23E-1	0.367
	1.0	2.08E-2	55	3.97E-1	1.62E-1	0.408
	1.0	2.08E-2	60	4.55E-1	2.08E-1	0.457
	1.0	2.08E-2	65	5.37E-1	2.78E-1	0.519
	1.0	2.08E-2	70	6.46E-1	3.89E-1	0.602
	1.0	2.08E-2	75	7.79E-1	5.57E-1	0.715
	1.0	2.08E-2	80	9.35E-1	7.93E-1	0.848
	1.0	2.08E-2	82.5	9.83E-1	9.02E-1	0.917
	1.0	2.08E-2	85	1.00E+0	9.70E-1	0.970
AR -> NI	1.0	8.54E-3	0	7.44E-2	5.58E-3	0.0750
	1.0	8.54E-3	30	1.30E-1	1.84E-2	0.141
	1.0	8.54E-3	45	2.20E-1	4.97E-2	0.226
	1.0	8.54E-3	60	4.11E-1	1.53E-1	0.372
	1.0	8.54E-3	70	6.41E-1	3.47E-1	0.541
	1.0	8.54E-3	75	8.01E-1	5.29E-1	0.660
	1.0	8.54E-3	80	9.52E-1	7.72E-1	0.881
	1.0	8.54E-3	85	1.00E+0	9.62E-1	0.962
NI -> NI	1.0	4.30E-3	0	1.78E-2	7.16E-4	0.0409
	1.0	4.30E-3	10	2.23E-2	9.66E-4	0.0442
	1.0	4.30E-3	20	3.49E-2	2.34E-3	0.0674
	1.0	4.30E-3	30	6.71E-2	7.14E-3	0.107
	1.0	4.30E-3	40	1.13E-1	1.73E-2	0.153
	1.0	4.30E-3	45	1.51E-1	2.79E-2	0.185
	1.0	4.30E-3	50	2.06E-1	4.66E-2	0.226
	1.0	4.30E-3	55	2.82E-1	7.74E-2	0.275
	1.0	4.30E-3	60	3.61E-1	1.20E-1	0.334
	1.0	4.30E-3	65	4.80E-1	1.96E-1	0.410
	1.0	4.30E-3	70	6.16E-1	3.13E-1	0.508
	1.0	4.30E-3	75	7.92E-1	4.91E-1	0.620
	1.0	4.30E-3	80	9.44E-1	7.32E-1	0.775
	1.0	4.30E-3	82.5	9.86E-1	8.45E-1	0.856
	1.0	4.30E-3	85	9.98E-1	9.23E-1	0.925
	1.0	4.30E-3	87.5	9.99E-1	9.64E-1	0.965

REFLECTION DATA FROM TRIM CALCULATIONS

	E0 (KEV)	EPS	ALPHA (DEGREE)	RN	RE	RE/RN
AR -> GE	0.05	3.95E-4	0	2.44E-1	2.72E-2	0.111
	0.1	7.90E-4	0	1.93E-1	2.22E-2	0.115
	0.2	1.58E-3	0	1.58E-1	1.80E-2	0.114
	0.5	3.95E-3	0	1.23E-1	1.38E-2	0.112
	1.0	7.90E-3	0	1.02E-1	1.10E-2	0.107
	2.0	1.58E-2	0	8.56E-2	9.52E-3	0.111
	5.0	3.95E-2	0	7.11E-2	7.99E-3	0.112
	10.0	7.90E-2	0	5.83E-2	6.38E-3	0.110
	20.0	1.58E-1	0	4.29E-2	4.86E-3	0.113
	50.0	3.95E-1	0	2.92E-2	3.42E-3	0.117
	100.0	7.90E-1	0	1.91E-2	2.09E-3	0.110
	200.0	1.58E+0	0	1.17E-2	1.29E-3	0.110

REFLECTION DATA FROM TRIM CALCULATIONS

	E0 (KEV)	EPS	ALPHA (DEGREE)	RN	RE	RE/RN
XE -> ZR	0.1	1.08E-4	0	4.21E-3	9.03E-5	0.0214
	0.3	3.24E-4	0	4.00E-3	6.77E-5	0.0169
	1.0	1.08E-3	0	3.85E-3	6.05E-5	0.0157
	3.0	3.24E-3	0	3.50E-3	5.25E-5	0.0150
	10.0	1.08E-2	0	3.15E-3	6.50E-5	0.0206
	30.0	3.24E-2	0	2.45E-3	4.77E-5	0.0195
	100.0	1.08E-1	0	1.14E-3	2.56E-5	0.0225

REFLECTION DATA FROM TRIM CALCULATIONS

	E0 (KEV)	EPS	ALPHA (DEGREE)	RN	RE	RE/RN
HE4 -> MO	0.1	9.37E-3	0	3.67E-1	1.74E-1	0.475
	0.2	1.88E-2	0	3.38E-1	1.57E-1	0.465
	0.3	2.81E-2	0	3.25E-1	1.47E-1	0.454
	1.0	9.37E-2	0	2.71E-1	1.16E-1	0.430
	3.0	2.81E-1	0	2.10E-1	8.17E-2	0.389
	10.0	9.37E-1	0	1.25E-1	4.34E-2	0.347
	30.0	2.81E+0	0	5.25E-2	1.53E-2	0.292
	100.0	9.37E+0	0	1.34E-2	3.51E-3	0.262
	300.0	2.81E+1	0	3.60E-3	8.04E-4	0.223
NE -> MO	0.04	5.65E-4	0	5.28E-1	1.81E-1	0.344
	0.05	7.06E-4	0	4.90E-1	1.71E-1	0.348
	0.1	1.41E-3	0	4.08E-1	1.38E-1	0.339
	0.3	4.23E-3	0	3.09E-1	9.89E-2	0.320
	1.0	1.41E-2	0	2.51E-1	7.50E-2	0.299
	3.0	4.24E-2	0	2.20E-1	6.59E-2	0.299
	10.0	1.41E-1	0	1.61E-1	4.66E-2	0.290
	30.0	4.24E-1	0	1.14E-1	2.99E-2	0.262
	100.0	1.41E+0	0	6.00E-2	1.48E-2	0.246
	300.0	4.24E+0	0	2.40E-2	5.59E-3	0.233
AR -> MO	0.05	3.12E-4	0	3.72E-1	6.36E-2	0.171
	0.1	6.25E-4	0	3.07E-1	5.36E-2	0.175
	0.3	1.87E-3	0	2.31E-1	3.88E-2	0.168
	1.0	6.25E-3	0	1.63E-1	2.67E-2	0.163
	3.0	1.87E-2	0	1.18E-1	1.90E-2	0.162
	10.0	6.25E-2	0	9.90E-2	1.64E-2	0.166
	30.0	1.87E-1	0	6.98E-2	1.14E-2	0.164
	100.0	6.25E-1	0	4.00E-2	6.51E-3	0.162
	300.0	1.87E+0	0	1.89E-2	2.65E-3	0.140
KR -> MO	0.05	1.07E-4	0	8.20E-2	4.53E-3	0.0560
	0.07	1.49E-4	0	9.00E-2	4.54E-3	0.0504
	0.1	2.13E-4	0	7.70E-2	4.23E-3	0.0550
	0.15	3.20E-4	0	8.51E-2	3.92E-3	0.0461
	0.2	4.27E-4	0	7.99E-2	3.69E-3	0.0461
	0.3	6.40E-4	0	6.20E-2	2.87E-3	0.0460
	1.0	2.13E-3	0	4.70E-2	1.91E-3	0.0410
	3.0	6.40E-3	0	3.60E-2	1.65E-3	0.0460
	10.0	2.13E-2	0	2.20E-2	1.06E-3	0.0490
	30.0	6.40E-2	0	1.70E-2	8.59E-4	0.0510
	100.0	2.13E-1	0	1.04E-2	7.32E-4	0.0704
	300.0	6.40E-1	0	3.60E-3	1.99E-4	0.0552
	500.0	1.07E+0	0	2.80E-3	1.43E-4	0.0511
	999.99	2.13E+0	0	1.10E-3	5.13E-5	0.0466
MO -> MO	0.07	1.17E-4	0	5.80E-4	4.29E-5	0.0739
	0.085	1.42E-4	0	1.33E-3	8.94E-5	0.0672
	0.1	1.67E-4	0	1.84E-3	1.17E-4	0.0634
	0.2	3.34E-4	0	7.80E-3	4.29E-4	0.0550
	0.3	5.01E-4	0	1.21E-2	6.47E-4	0.0540
	1.0	1.67E-3	0	1.70E-2	7.27E-4	0.0430
	3.0	5.01E-3	0	1.70E-2	6.41E-4	0.0380
	10.0	1.67E-2	0	1.36E-2	4.89E-4	0.0360
	30.0	5.01E-2	0	7.50E-3	2.53E-4	0.0340
	100.0	1.67E-1	0	6.05E-3	2.65E-4	0.0440
	300.0	5.01E-1	0	3.20E-3	1.37E-4	0.0430

XE -> MO	0.05	5.25E-5	0	9.80E-3	2.39E-4	0.0244
	0.07	7.36E-5	0	1.08E-2	2.62E-4	0.0243
	0.1	1.05E-4	0	8.20E-3	2.19E-4	0.0267
	0.15	1.58E-4	0	8.80E-3	1.61E-4	0.0183
	0.2	2.10E-4	0	7.10E-3	1.54E-4	0.0220
	0.3	3.15E-4	0	7.10E-3	1.72E-4	0.0240
	1.0	1.05E-3	0	5.20E-3	9.55E-5	0.0185
	3.0	3.15E-3	0	5.00E-3	8.14E-5	0.0163
	10.0	1.05E-2	0	3.70E-3	7.70E-5	0.0208
	30.0	3.15E-2	0	2.47E-3	5.29E-5	0.0214
	100.0	1.05E-1	0	1.46E-3	5.47E-5	0.0375
	300.0	3.15E-1	0	8.24E-4	2.54E-5	0.0310
RN -> MO	0.1	4.32E-5	0	2.00E-5	1.75E-7	0.0088
AR -> MO	0.16	1.00E-3	0	2.69E-1	4.64E-2	0.173
	0.16	1.00E-3	10	2.83E-1	5.12E-2	0.181
	0.16	1.00E-3	20	3.16E-1	6.49E-2	0.206
	0.16	1.00E-3	30	3.68E-1	9.13E-2	0.248
	0.16	1.00E-3	40	4.42E-1	1.38E-1	0.311
	0.16	1.00E-3	45	5.02E-1	1.75E-1	0.349
	0.16	1.00E-3	50	5.63E-1	2.21E-1	0.392
	0.16	1.00E-3	60	7.09E-1	3.61E-1	0.508
	0.16	1.00E-3	70	8.82E-1	5.77E-1	0.654
	0.16	1.00E-3	75	9.54E-1	7.22E-1	0.757
	0.16	1.00E-3	80	9.94E-1	8.69E-1	0.874
	0.16	1.00E-3	85	1.00E+0	9.71E-1	0.971
AR -> MO	1.60	1.00E-2	0	1.45E-1	2.33E-2	0.161
	1.60	1.00E-2	10	1.50E-1	2.48E-2	0.165
	1.60	1.00E-2	20	1.69E-1	3.13E-2	0.185
	1.60	1.00E-2	30	1.99E-1	4.27E-2	0.215
	1.60	1.00E-2	40	2.41E-1	6.11E-2	0.253
	1.60	1.00E-2	45	2.72E-1	7.67E-2	0.282
	1.60	1.00E-2	50	3.12E-1	9.77E-2	0.313
	1.60	1.00E-2	60	4.19E-1	1.66E-1	0.397
	1.60	1.00E-2	70	5.80E-1	3.06E-1	0.527
	1.60	1.00E-2	75	7.00E-1	4.42E-1	0.632
	1.60	1.00E-2	80	8.65E-1	6.72E-1	0.776
	1.60	1.00E-2	85	9.96E-1	9.42E-1	0.946
AR -> MO	16.01	1.00E-1	0	8.10E-2	1.30E-2	0.160
	16.01	1.00E-1	10	8.90E-2	1.52E-2	0.169
	16.01	1.00E-1	20	9.96E-2	1.83E-2	0.184
	16.01	1.00E-1	30	1.23E-1	2.62E-2	0.213
	16.01	1.00E-1	40	1.60E-1	3.93E-2	0.245
	16.01	1.00E-1	45	1.82E-1	4.92E-2	0.270
	16.01	1.00E-1	50	2.15E-1	6.38E-2	0.296
	16.01	1.00E-1	60	2.93E-1	1.05E-1	0.360
	16.01	1.00E-1	70	4.10E-1	1.86E-1	0.454
	16.01	1.00E-1	75	4.90E-1	2.57E-1	0.524
	16.01	1.00E-1	80	5.98E-1	3.73E-1	0.625
	16.01	1.00E-1	85	8.13E-1	6.63E-1	0.816

0 -> MO	0.02	3.75E-4	0	6.37E-1	2.57E-1	0.404
	0.03	5.62E-4	0	5.83E-1	2.35E-1	0.404
ESB=0 EV	0.04	7.50E-4	0	5.43E-1	2.18E-1	0.401
	0.05	9.37E-4	0	5.14E-1	2.05E-1	0.398
	0.07	1.31E-3	0	4.77E-1	1.87E-1	0.391
	0.1	1.87E-3	0	4.37E-1	1.70E-1	0.388
	0.2	3.75E-3	0	3.77E-1	1.39E-1	0.369
	0.5	9.37E-3	0	3.12E-1	1.10E-1	0.354
	1.0	1.87E-2	0	2.81E-1	9.73E-2	0.346
	2.0	3.75E-2	0	2.52E-1	8.52E-2	0.339
	4.0	7.50E-2	0	2.30E-1	7.62E-2	0.331
0 -> MO	0.02	3.75E-4	0	4.52E-1	1.57E-1	0.347
	0.03	5.62E-4	0	4.68E-1	1.76E-1	0.375
ESB=4 EV	0.04	7.50E-4	0	4.59E-1	1.77E-1	0.385
	0.05	9.37E-4	0	4.46E-1	1.73E-1	0.388
	0.07	1.31E-3	0	4.26E-1	1.67E-1	0.393
	0.1	1.87E-3	0	3.96E-1	1.53E-1	0.386
	0.2	3.75E-3	0	3.48E-1	1.31E-1	0.378
	0.5	9.37E-3	0	3.05E-1	1.08E-1	0.353
	1.0	1.87E-2	0	2.79E-1	9.75E-2	0.349
0 -> MO	0.02	3.75E-4	0	2.36E-1	6.59E-2	0.279
	0.03	5.62E-4	0	3.35E-1	1.09E-1	0.327
ESB=7.89 EV	0.04	7.50E-4	0	3.69E-1	1.30E-1	0.353
	0.05	9.37E-4	0	3.77E-1	1.37E-1	0.364
	0.07	1.31E-3	0	3.78E-1	1.43E-1	0.379
	0.1	1.87E-3	0	3.71E-1	1.41E-1	0.380
	0.15	2.81E-3	0	3.60E-1	1.36E-1	0.379
	0.2	3.75E-3	0	3.41E-1	1.28E-1	0.375
	0.3	5.62E-3	0	3.16E-1	1.16E-1	0.368
	0.5	9.37E-3	0	3.09E-1	1.10E-1	0.355
	0.7	1.31E-2	0	2.95E-1	1.04E-1	0.352
	1.0	1.87E-2	0	2.69E-1	9.35E-2	0.348
0 -> MO	0.02	3.75E-4	0	1.02E-1	2.15E-2	0.211
	0.03	5.62E-4	0	2.02E-1	5.67E-2	0.281
ESB=12 EV	0.04	7.50E-4	0	2.66E-1	8.40E-2	0.316
	0.05	9.37E-4	0	2.97E-1	1.00E-1	0.338
	0.07	1.31E-3	0	3.31E-1	1.19E-1	0.361
	0.1	1.87E-3	0	3.40E-1	1.26E-1	0.370
	0.2	3.75E-3	0	3.25E-1	1.21E-1	0.371
	0.5	9.37E-3	0	2.99E-1	1.09E-1	0.363
	1.0	1.87E-2	0	2.80E-1	9.75E-2	0.348

REFLECTION DATA FROM TRIM CALCULATIONS

	E0 (KEV)	EPS	ALPHA (DEGREE)	RN	RE	RE/RN
NA24 -> AG	30.0	3.29E-1	0	1.21E-1	3.25E-2	0.269
	30.0	3.29E-1	15	1.35E-1	3.69E-2	0.274
	30.0	3.29E-1	30	1.64E-1	4.91E-2	0.300
	30.0	3.29E-1	40	2.05E-1	6.97E-2	0.339
	30.0	3.29E-1	50	2.57E-1	9.70E-2	0.378
	30.0	3.29E-1	60	3.40E-1	1.49E-1	0.437
	30.0	3.29E-1	70	4.41E-1	2.26E-1	0.512
K42 -> AG	30.0	1.57E-1	0	8.21E-2	1.43E-2	0.174
	30.0	1.57E-1	15	8.83E-2	1.63E-2	0.185
	30.0	1.57E-1	30	1.20E-1	2.74E-2	0.228
	30.0	1.57E-1	40	1.52E-1	3.83E-2	0.252
	30.0	1.57E-1	50	2.12E-1	6.59E-2	0.310
	30.0	1.57E-1	60	2.90E-1	1.06E-1	0.366
	30.0	1.57E-1	70	3.95E-1	1.80E-1	0.455
	30.0	1.57E-1	80	5.66E-1	3.41E-1	0.603

REFLECTION DATA FROM TRIM CALCULATIONS

	E0 (KEV)	EPS	ALPHA (DEGREE)	RN	RE	RE/RN
KR -> SM	0.05	8.10E-5	0	2.38E-1	2.53E-2	0.106
	0.1	1.62E-4	0	2.01E-1	2.13E-2	0.106
	0.2	3.24E-4	0	1.81E-1	1.92E-2	0.106
	0.5	8.10E-4	0	1.46E-1	1.46E-2	0.100
	1.0	1.62E-3	0	1.28E-1	1.29E-2	0.100
	2.0	3.24E-3	0	1.18E-1	1.16E-2	0.0987
	5.0	8.10E-3	0	9.66E-2	9.70E-3	0.100
	10.0	1.62E-2	0	8.41E-2	8.62E-3	0.103
	20.0	3.24E-2	0	7.55E-2	7.86E-3	0.104
	50.0	8.10E-2	0	5.72E-2	6.06E-3	0.106
	100.0	1.62E-1	0	4.02E-2	4.64E-3	0.115
	200.0	3.24E-1	0	3.09E-2	3.30E-3	0.107

REFLECTION DATA FROM TRIM CALCULATIONS

	E0 (KEV)	EPS	ALPHA (DEGREE)	RN	RE	RE/RN
W -> W	0.07	3.12E-5	0	5.00E-5	2.77E-6	0.0553
	0.1	4.46E-5	0	5.10E-4	3.19E-5	0.0610
	0.15	6.68E-5	0	2.20E-3	1.26E-4	0.0574
	0.2	8.91E-5	0	4.79E-3	2.68E-4	0.0558
	0.3	1.34E-4	0	9.22E-3	4.46E-4	0.0485
	0.5	2.23E-4	0	1.54E-2	6.97E-4	0.0455
	0.7	3.12E-4	0	1.77E-2	7.90E-4	0.0448
	1.0	4.46E-4	0	2.08E-2	8.82E-4	0.0428
	2.0	8.91E-4	0	2.22E-2	8.96E-4	0.0408
	5.0	2.23E-3	0	2.16E-2	7.70E-4	0.0356
	10.0	4.46E-3	0	1.87E-2	6.88E-4	0.0383
	30.0	1.34E-2	0	1.57E-2	6.20E-4	0.0394
W -> W	0.1	4.46E-5	0	2.70E-4	1.60E-5	0.056
	0.1	4.46E-5	10	6.54E-4	3.90E-5	0.061
	0.1	4.46E-5	20	4.00E-3	4.10E-4	0.099
	0.1	4.46E-5	30	1.40E-2	1.80E-3	0.129
	0.1	4.46E-5	40	4.00E-2	6.50E-3	0.163
	0.1	4.46E-5	50	9.50E-2	1.99E-2	0.209
	0.1	4.46E-5	60	1.86E-1	4.87E-2	0.262
	0.1	4.46E-5	70	3.13E-1	9.91E-2	0.317
	0.1	4.46E-5	75	3.72E-1	1.28E-1	0.344
	0.1	4.46E-5	80	4.34E-1	1.60E-1	0.370
	0.1	4.46E-5	82.5	4.63E-1	1.74E-1	0.377
	0.1	4.46E-5	85	4.77E-1	1.84E-1	0.386
	0.1	4.46E-5	87.5	4.87E-1	1.91E-1	0.392

REFLECTION DATA FROM TRIM CALCULATIONS

	E0 (KEV)	EPS	ALPHA (DEGREE)	RN	RE	RE/RN
NA24 -> AU	30.0	1.89E-1	0	2.29E-1	8.13E-2	0.356
	30.0	1.89E-1	15	2.33E-1	8.78E-2	0.377
	30.0	1.89E-1	30	2.74E-1	1.08E-1	0.395
	30.0	1.89E-1	40	3.06E-1	1.27E-1	0.416
	30.0	1.89E-1	50	3.61E-1	1.65E-1	0.457
	30.0	1.89E-1	60	4.32E-1	2.21E-1	0.513
	30.0	1.89E-1	70	5.32E-1	3.08E-1	0.580
	30.0	1.89E-1	80	6.71E-1	4.65E-1	0.694
K42 -> AU	30.0	9.57E-2	0	1.79E-1	4.94E-2	0.276
	30.0	9.57E-2	15	1.94E-1	5.55E-2	0.286
	30.0	9.57E-2	30	2.18E-1	6.83E-2	0.314
	30.0	9.57E-2	40	2.60E-1	9.13E-2	0.351
	30.0	9.57E-2	50	3.21E-1	1.27E-1	0.396
	30.0	9.57E-2	60	3.86E-1	1.75E-1	0.453
	30.0	9.57E-2	70	4.87E-1	2.56E-1	0.525
	30.0	9.57E-2	80	6.41E-1	4.24E-1	0.661

REFLECTION DATA FROM TRIM CALCULATIONS

	E0 (KEV)	EPS	ALPHA (DEGREE)	RN	RE	RE/RN
KR -> HG	0.05	6.56E-5	0	3.49E-1	5.76E-2	0.165
	0.1	1.31E-4	0	3.09E-1	5.17E-2	0.167
	0.2	2.63E-4	0	2.65E-1	4.41E-2	0.166
	0.5	6.56E-4	0	2.22E-1	3.60E-2	0.162
	1.0	1.31E-3	0	1.99E-1	3.14E-2	0.158
	2.0	2.63E-3	0	1.74E-1	2.66E-2	0.153
	5.0	6.56E-3	0	1.50E-1	2.28E-2	0.152
	10.0	1.31E-2	0	1.33E-1	2.03E-2	0.153
	20.0	2.63E-2	0	1.19E-1	1.83E-2	0.154
	50.0	6.56E-2	0	9.58E-2	1.49E-2	0.156
	100.0	1.31E-1	0	7.67E-2	1.17E-2	0.153
	200.0	2.63E-1	0	5.52E-2	8.72E-3	0.158
KR -> HG	0.762	1.00E-3	0	2.02E-1	3.15E-2	0.157
	0.762	1.00E-3	10	2.14E-1	3.49E-2	0.163
	0.762	1.00E-3	20	2.29E-1	4.14E-2	0.181
	0.762	1.00E-3	30	2.60E-1	5.38E-2	0.207
	0.762	1.00E-3	40	3.13E-1	7.82E-2	0.250
	0.762	1.00E-3	45	3.48E-1	9.71E-2	0.279
	0.762	1.00E-3	50	3.85E-1	1.19E-1	0.309
	0.762	1.00E-3	60	4.91E-1	1.96E-1	0.399
	0.762	1.00E-3	70	6.50E-1	3.43E-1	0.527
	0.762	1.00E-3	75	7.60E-1	4.74E-1	0.624
	0.762	1.00E-3	80	8.94E-1	6.73E-1	0.753
	0.762	1.00E-3	85	9.94E-1	9.15E-1	0.921
KR -> HG	7.615	1.00E-2	0	1.41E-1	2.15E-2	0.153
	7.615	1.00E-2	10	1.47E-1	2.31E-2	0.157
	7.615	1.00E-2	20	1.60E-1	2.67E-2	0.167
	7.615	1.00E-2	30	1.87E-1	3.67E-2	0.196
	7.615	1.00E-2	40	2.28E-1	5.26E-2	0.231
	7.615	1.00E-2	45	2.52E-1	6.39E-2	0.254
	7.615	1.00E-2	50	2.82E-1	7.95E-2	0.282
	7.615	1.00E-2	60	3.61E-1	1.25E-1	0.346
	7.615	1.00E-2	70	4.79E-1	2.13E-1	0.444
	7.615	1.00E-2	75	5.63E-1	2.91E-1	0.517
	7.615	1.00E-2	80	6.75E-1	4.24E-1	0.628
	7.615	1.00E-2	85	8.81E-1	7.29E-1	0.828
KR -> HG	76.15	1.00E-1	0	8.44E-2	1.34E-2	0.159
	76.15	1.00E-1	30	1.22E-1	2.45E-2	0.201
	76.15	1.00E-1	45	1.82E-1	4.83E-2	0.265
	76.15	1.00E-1	60	2.87E-1	9.88E-2	0.344
	76.15	1.00E-1	70	3.99E-1	1.72E-1	0.433
	76.15	1.00E-1	75	4.70E-1	2.31E-1	0.493
	76.15	1.00E-1	80	5.55E-1	3.16E-1	0.570
	76.15	1.00E-1	85	6.93E-1	4.91E-1	0.708

REFLECTION DATA FROM TRIM CALCULATIONS

	E0 (KEV)	EPS	ALPHA (DEGREE)	RN	RE	RE/RN
HE4 -> U	0.05	1.76E-3	0	6.13E-1	3.96E-1	0.645
	0.1	3.51E-3	0	5.91E-1	3.66E-1	0.620
	0.2	7.03E-3	0	5.64E-1	3.39E-1	0.601
	0.3	1.05E-2	0	5.39E-1	3.21E-1	0.595
	0.5	1.76E-2	0	5.23E-1	3.00E-1	0.573
	1.0	3.51E-2	0	4.87E-1	2.69E-1	0.553
	3.0	1.05E-1	0	4.13E-1	2.08E-1	0.504
	5.0	1.76E-1	0	3.73E-1	1.79E-1	0.480
	10.0	3.51E-1	0	2.94E-1	1.31E-1	0.445
	30.0	1.05E+0	0	1.78E-1	6.38E-2	0.358
	50.0	1.76E+0	0	1.21E-1	3.75E-2	0.309
	75.0	2.64E+0	0	8.42E-2	2.32E-2	0.275
	100.0	3.51E+0	0	6.10E-2	1.56E-2	0.256
	200.0	7.03E+0	0	2.57E-2	6.18E-3	0.241
	300.0	1.05E+1	0	1.42E-2	3.44E-3	0.242
NE -> U	0.02	1.19E-4	0	6.74E-1	3.63E-1	0.538
	0.05	2.98E-4	0	5.91E-1	3.08E-1	0.521
	0.1	5.97E-4	0	5.34E-1	2.71E-1	0.508
	0.3	1.79E-3	0	4.75E-1	2.25E-1	0.475
	0.5	2.98E-3	0	4.51E-1	2.13E-1	0.473
	1.0	5.97E-3	0	4.29E-1	1.95E-1	0.455
	2.0	1.19E-2	0	3.99E-1	1.77E-1	0.444
	3.0	1.79E-2	0	3.79E-1	1.68E-1	0.443
	5.0	2.98E-2	0	3.64E-1	1.59E-1	0.437
	10.0	5.97E-2	0	3.31E-1	1.40E-1	0.424
	30.0	1.79E-1	0	2.65E-1	1.06E-1	0.400
	100.0	5.97E-1	0	1.78E-1	6.24E-2	0.350
	300.0	1.79E+0	0	9.20E-2	2.93E-2	0.317
	500.0	2.99E+0	0	6.31E-2	1.88E-2	0.298
AR -> U	0.05	1.46E-4	0	5.37E-1	2.11E-1	0.392
	0.1	2.92E-4	0	4.71E-1	1.82E-1	0.387
	0.3	8.75E-4	0	4.02E-1	1.47E-1	0.367
	1.0	2.92E-3	0	3.44E-1	1.19E-1	0.345
	3.0	8.75E-3	0	2.98E-1	1.01E-1	0.340
	10.0	2.92E-2	0	2.66E-1	8.86E-2	0.333
	30.0	8.75E-2	0	2.15E-1	6.85E-2	0.319
	34.27	1.00E-1	0	2.13E-1	6.81E-2	0.320
	100.0	2.92E-1	0	1.61E-1	4.89E-2	0.304
	300.0	8.75E-1	0	1.06E-1	2.98E-2	0.281
	500.0	1.46E+0	0	6.74E-2	1.78E-2	0.264
KR -> U	0.05	5.82E-5	0	4.21E-1	8.73E-2	0.208
	0.1	1.16E-4	0	3.71E-1	7.89E-2	0.213
	0.3	3.49E-4	0	2.86E-1	5.88E-2	0.206
	1.0	1.16E-3	0	2.37E-1	4.61E-2	0.195
	3.0	3.49E-3	0	1.98E-1	3.72E-2	0.188
	10.0	1.16E-2	0	1.62E-1	2.84E-2	0.175
	17.93	2.09E-2	0	1.49E-1	2.84E-2	0.190
	30.0	3.49E-2	0	1.32E-1	2.55E-2	0.194
	100.0	1.16E-1	0	1.02E-1	1.91E-2	0.187
	300.0	3.49E-1	0	6.40E-2	1.15E-2	0.179
	500.0	5.82E-1	0	5.35E-2	9.72E-3	0.182

XE -> U	0.05	3.20E-5	0	2.85E-1	2.97E-2	0.104
	0.07	4.48E-5	0	2.83E-1	2.83E-2	0.100
	0.1	6.40E-5	0	2.45E-1	2.63E-2	0.107
	0.2	1.28E-4	0	2.25E-1	2.41E-2	0.107
	0.3	1.92E-4	0	2.04E-1	2.15E-2	0.105
	1.0	6.40E-4	0	1.59E-1	1.64E-2	0.103
	3.0	1.92E-3	0	1.28E-1	1.29E-2	0.100
	10.0	6.40E-3	0	1.00E-1	1.07E-2	0.107
	30.0	1.92E-2	0	8.50E-2	8.09E-3	0.0950
	100.0	6.40E-2	0	6.00E-2	6.50E-3	0.108
	300.0	1.92E-1	0	4.30E-2	4.39E-3	0.101
	500.0	3.20E-1	0	3.13E-2	3.47E-3	0.111
RN -> U	0.05	1.50E-5	0	4.89E-2	2.32E-3	0.0474
	0.07	2.10E-5	0	6.50E-2	2.46E-3	0.0378
	0.1	3.00E-5	0	5.90E-2	2.37E-3	0.0400
	0.15	4.50E-5	0	6.78E-2	2.46E-3	0.0363
	0.2	6.00E-5	0	6.97E-2	2.45E-3	0.0352
	0.3	9.00E-5	0	5.77E-2	2.14E-3	0.0370
	1.0	3.00E-4	0	4.80E-2	1.73E-3	0.0360
	3.0	9.00E-4	0	4.50E-2	1.57E-3	0.0351
	10.0	3.00E-3	0	3.60E-2	1.17E-3	0.0325
	30.0	9.00E-3	0	2.80E-2	1.06E-3	0.0380
	100.0	3.00E-2	0	2.12E-2	8.87E-4	0.0419
	300.0	9.00E-2	0	1.02E-2	5.86E-4	0.0557
U -> U	0.07	1.88E-5	0	4.40E-4	2.34E-5	0.0533
	0.1	2.68E-5	0	2.22E-3	1.13E-4	0.0510
	0.15	4.02E-5	0	5.26E-3	2.65E-4	0.0504
	0.2	5.36E-5	0	8.91E-3	4.26E-4	0.0478
	0.3	8.04E-5	0	1.30E-2	6.37E-4	0.0480
	0.5	1.34E-4	0	1.92E-2	8.12E-4	0.0424
	1.0	2.68E-4	0	2.52E-2	9.17E-4	0.0365
	3.0	8.04E-4	0	2.50E-2	9.06E-4	0.0370
	10.0	2.68E-3	0	2.40E-2	7.74E-4	0.0330
	30.0	8.04E-3	0	1.80E-2	6.64E-4	0.0370
	100.0	2.68E-2	0	1.36E-2	4.50E-4	0.0331
	300.0	8.04E-2	0	1.00E-2	3.92E-4	0.0392
KR -> U	17.9	2.08E-2	0	1.60E-1	3.09E-2	0.193
	17.9	2.08E-2	5	1.49E-1	2.74E-2	0.185
	17.9	2.08E-2	15	1.71E-1	3.13E-2	0.184
	17.9	2.08E-2	20	1.63E-1	3.25E-2	0.200
	17.9	2.08E-2	30	1.93E-1	4.23E-2	0.220
	17.9	2.08E-2	45	2.48E-1	6.88E-2	0.278
	17.9	2.08E-2	50	2.94E-1	8.80E-2	0.299
	17.9	2.08E-2	55	3.18E-1	1.07E-1	0.337
	17.9	2.08E-2	60	3.87E-1	1.42E-1	0.368
	17.9	2.08E-2	65	4.28E-1	1.79E-1	0.418
	17.9	2.08E-2	70	4.97E-1	2.27E-1	0.458
	17.9	2.08E-2	75	5.61E-1	2.96E-1	0.528
	17.9	2.08E-2	80	6.57E-1	4.07E-1	0.619
	17.9	2.08E-2	82.5	7.32E-1	5.12E-1	0.699
	17.9	2.08E-2	85	8.47E-1	6.81E-1	0.805
	17.9	2.08E-2	87.5	9.86E-1	9.34E-1	0.948
U -> U	0.1	2.68E-5	0	2.10E-3	1.20E-4	0.0571
	0.1	2.68E-5	20	1.15E-2	1.15E-3	0.0998
	0.1	2.68E-5	30	3.37E-2	4.69E-3	0.139
	0.1	2.68E-5	40	8.81E-2	1.56E-2	0.177
	0.1	2.68E-5	50	1.70E-1	4.04E-2	0.238
	0.1	2.68E-5	60	3.18E-1	1.01E-1	0.316
	0.1	2.68E-5	65	4.11E-1	1.47E-1	0.358
	0.1	2.68E-5	70	5.33E-1	2.14E-1	0.403
	0.1	2.68E-5	75	6.37E-1	2.87E-1	0.450
	0.1	2.68E-5	80	7.34E-1	3.66E-1	0.499
	0.1	2.68E-5	85	7.97E-1	4.30E-1	0.539
	0.1	2.68E-5	87.5	8.22E-1	4.56E-1	0.555